University of Genoa

Doctorate school of Science and Technology of Chemistry and Materials

Curriculum of Pharmaceutical, Nutritional and Cosmetic Sciences

XXXI Cycle

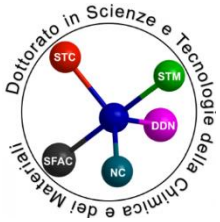

Formulation development of biopolymer based multilayer films for local treatment and wound repair of periodontitis

Tutor

Prof.Gabriele Caviglioli

PhD student

Karthik Neduri

A.A. 2018-2019

INDEX

CHAPTER 3

RESULTS AND DISCUSSION

CHAPTER 1

INTRODUCTION

1.1 Oral diseases

The oral cavity is the first section of the digestive system and consists of different anatomical structures, including teeth, gingiva and their supportive tissues, hard and soft palate, tongue, lips and a mucosal membrane lining the inner surface of the cheek. Currently oral diseases are considered as a serious threat to public health that challenges health systems around the world. They may possibly directly affect a limited locale of the human body, but their outcomes and impacts have an effect on the body as a whole (FDI World Dental Federation, 2015). Apart from trauma from injuries, there are many immune-mediated inflammatory mucocutaneous diseases that have an effect on the oral cavity, most of them presenting clinically with varied degrees of blistering, sloughing, erosions, ulcerations and pain (Perschbacher, 2018). But the most common acquired oral diseases worldwide are tooth decay and periodontal diseases.

1.2 Periodontitis

1.2.1 Aetiology and risk factors

Periodontal disease is one of the world's most prevalent chronic diseases, which is characterized by various degenerative and inflammatory states of gums, periodontal ligaments, alveolar bone and dental cementum (Jain et al., 2008). It is common in all groups, ethnicities, races, both genders and is mainly categorized into chronic periodontitis and aggressive periodontitis. Chronic periodontitis results from repeated attack from complex microbiota, whereas aggressive periodontitis involves rapid attachment loss and bone destruction, the destruction being non proportional to the microbial load. Further characterization depends on the magnitude of bone loss (localized or generalized) and the severity of the disease (slight, moderate or advanced).

The microbial growth of the pathogens, which occurs due to the accumulation of subgingival plaque is said to be the main cause of this disease (Zilberman and Elsner, 2008).The periodontal structures which support the gums and teeth are primarily damaged by harmful by-products and enzymes from periodontal bacteria, like leucotoxins, collagenases, fibrinolysins and other proteases (Pihlstrom et al., 2005), along with the triggered host immune response (Pihlstrom et al., 2005). The early stage of the disease the inflammation is limited to the gingiva and this condition is named as gingivitis and it can be reversed by

regularly maintaining good oral hygiene (Pihlstrom et al., 2005). However, if the plaque is not removed, it hardens to form tartar or calculus, which cannot be removable by daily brushing and flossing. Subsequently, the bacteria start invading deeper tissues, and the collagen and periodontal ligaments that support the teeth in place are degenerated (Singh et al., 2012b), inducing also resorption of the alveolar bone. Thus, a space is generated between the gingiva and the tooth due to the migration of gingival epithelium along the tooth surface known as "periodontal pocket" and the disease condition stemming from this is known as "periodontitis". This periodontal pocket serves microflora to reside effortlessly, thus contribute to worsening of the condition. If this condition is not treated, the tooth loosens and finally gets dislodged, causing edentulism.

According to WHO, 10–15 % of the worldwide population possesses severe periodontitis (Jacob, 2012), therefore the comprehension of the mechanisms leading to it is actively pursued. A microbiological cause is evident, but a massive count of microorganisms is normally present in the buccal cavity, as most of them live harmlessly in symbiosis with the healthy host (Ismail et al., 2013; Pihlstrom et al., 2005; Singh et al., 2012a). Evidence has been gathered showing that there is a shift in the type of microorganisms populating the oral cavity, from Gram-positive aerobic species in healthy individuals to Gram-negative anaerobic species in periodontitis patients (Ismail et al., 2013).

Actually, the organisms mainly responsible for periodontitis are Gram-negative anaerobic microflora like Bacteroides spp. (B. intermedius and B. gingivalis), fusiform organisms (Aggregatibacter actinomycetemcomitans, Wolinella recta, Eikenella spp., Porphyromonas gingivalis, Tannerella forsythensis), various bacilli and cocci and spirochetes. In addition to bacteria, even amoebas and trichomonads contribute to tissue damage (Jain et al., 2008) (Fig. 1).

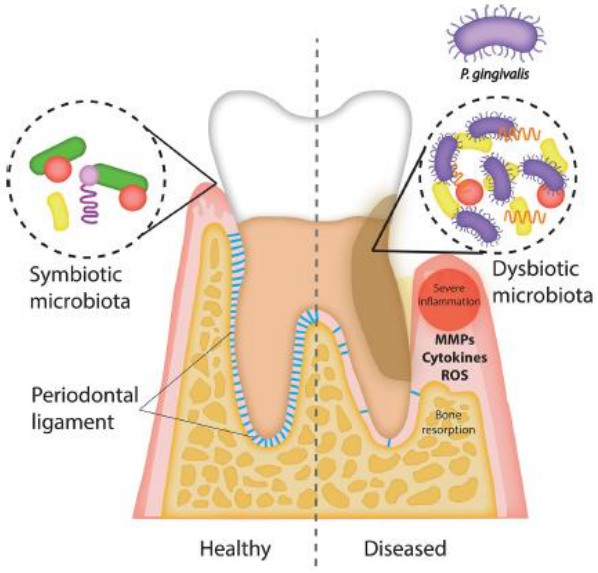

Figure 1. Aetiology and pathogenisis of periodontitis (Gross et al., 2017).

The inflammatory response in this disease condition involves activation of T lymphocytes, neutrophils, release of antibodies, chemical inflammatory mediators (cytokines, chemokines and C-reactive protein), and lipopolysaccharides present in the Gram-negative bacterial cell walls (Singh et al., 2015). Whereas, fibroblasts are stimulated by IL-1 and matrix metalloproteinases (MMPs) are secreted by neutrophil granulocytes, resulting in enhanced collagen degeneration, activation of cytokines and chemokines. Also osteoclast activity is augmented, due to TNF-α, by suppressing the production of collagen. Osteoclasts are activated by the release of antibodies and secretion of receptor activator of nuclear factor kappa-B (RANK) ligands by the lymphocytes (Parnami et al., 2013).

Furthermore, several researchers have proposed possible connections of periodontitis with common systemic diseases. The infection intiated by this disease causes bacteraemia, endotoxaemia and promotes systemic inflammatory response which play major role in systemic diseases. Diabetes mellitus (Lalla & Papapanou, 2011; Santos et al., 2012), psychological stress (Kaur et al., 2014b), genetic susceptibility (Kaur et al., 2016), host immune response, osteoporosis (Esfahanian et al., 2012; Guiglia et al., 2013) and ageing are the various well-established risk factors to periodontal disease (Van Dyke and Dave, 2005). Associations with respiratory (Saini et al., 2010), low birth weights and cardiovascular diseases (by expressing specific virulence factors) (Dhadse et al., 2010) are also being investigated.

1.2.2 Diagnosis and treatment

Clinical examination utilizing periodontal probe (Fig. 2) in combination with X-ray imaging are used to diagnose deeper pockets, and subsequently, microbiological techniques are done for the precise analysis of causative agents (Nair and Anoop, 2012). A reasonably accurate estimate of sulcus or pocket depth have been recorded with probe measurements. It is now obvious that probing depth measured from the gingival margin not often corresponds to sulcus or pocket depth. The difference is least in the absence of inflammatory changes and increases with increasing degrees of inflammation. In the presence of this disease condition the probe tip go by the inflamed tissues to stop at the level of the most intact coronal dento-gingival fibers, in the section of 0.3-0.5 mm above the apical termination of the junctional epithelium. Following periodontal therapy, decreased probing depth measurements may be due in part to reduced penetrability of the gingival tissues by the probe. Above all the interpretation of periodontal probing in the dental practice may need reassessment in relation to periodontal probing measurements to actual sulcus or pocket depth, (Listgarten, 1980).

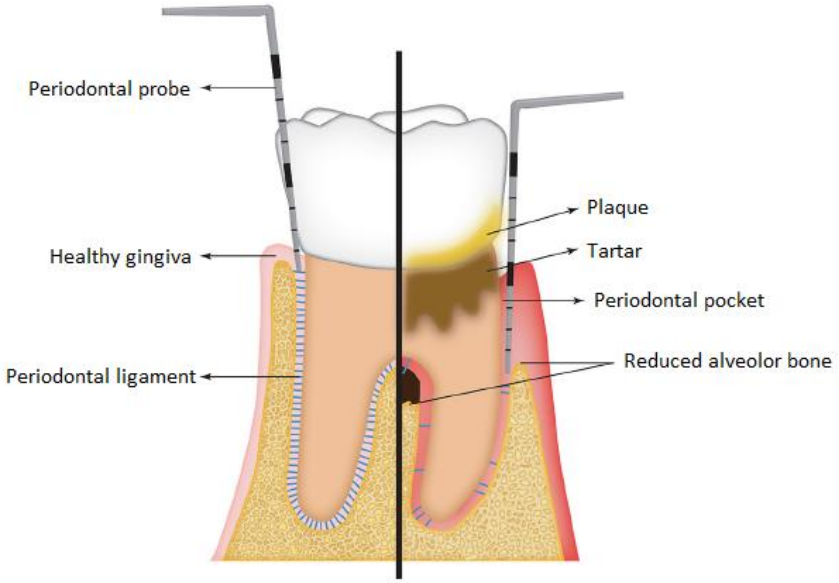

Figure 2. Clinical examination by a periodontal probe (Gross et al., 2017).

Depending on the severity of the disease a variety of surgical and nonsurgical treatments can be made available. Nevertheless, scaling and root planning is considered as the gold standard nonsurgical treatment given in periodontitis (Tariq et al., 2012): in this technique, the dentist uses various instruments to mechanically remove subgingival biofilm and calculus (Sanz et

al., 2012). These events have some drawbacks, like inability to reach the deep pockets and furcations (Herrera et al., 2012). Hence, antimicrobial drugs are administered as adjunct to these treatments for complete cure of the ailment, predominantly the aggressive periodontitis (Ahuja et al., 2012; Arweiler et al., 2014), but the infection caused by the bacterial aetiology should be considered for selecting the appropriate antibiotic and concurrently maintenance of daily oral hygiene by the patient is mandatory (Schwach-Abdellaoui et al., 2000).

The possible outcome of therapeutic success or failure is not only achieved by the antimicrobial action of the drug, but also by the site of infection, carrier system and route of drug delivery (Kaur et al., 2014a). Administration of oral antibiotics cause many systemic side effects like inadequate drug concentration reaching the pocket and decrease in the concentration rapidly to subtherapeutic level, requiring frequent dosing, causing patient incompliance and development of microbial resistance (Kataria et al., 2014). In view of the fact that the disease is confined to the periodontal cavity, local delivery of the drug in the pocket itself could be a probable choice (Garg et al., 2011d). The periodontal pocket simulates as a natural reservoir and provides easy admittance for the insertion of a medical device. Furthermore, the drug release and distribution in the whole pocket is provided by gingival crevicular fluid (GCF); in addition significant drug levels can be maintained in the GCF for extended duration. All these aforementioned characteristics make the intrapocket drug delivery a best choice (Jain et al., 2008). With the increased knowledge about the cause and pathogenesis of the disease, many types of dosage forms have been developed (Goyal et al., 2015; Garg et al., 2011c), as shown in the examples reported in Table I.

In addition, periodontal research in the past few decades has attempted to systematically establish successful clinical procedures (defined as guided tissue regeneration procedures) to regenerate periodontal tissues, and the consequent tooth support, with the use of biomaterials, such as hard- and soft-tissue grafts, or cell occlusive barrier membranes.

Table I. Various drug delivery approaches in the treatment of periodontitis.

Dosage form	Polymer	Drug	References
Films	HPMC, Carbopol 934	Metronidazole	Labib et al. (2014)
	Gelatin	Meloxicam	Cetin et al. (2005)
	PDLGA, chitosan	Ipriflavone	Perugini et al. (2003)
	Chitosan	Chlorhexidine gluconate	Ikinci et al. (2002)
	Collagen	Tetracycline	Minabe et al. (1991)
Strips	PCL	Tetracycline	Friesen et al. (2002)
	Ethylcellulose	Tetracycline, metronidazole	Somayaji et al. (1998)
	HPMC	Chlorhexidine, doxycycline	Ozcan et al. (1994)
	HPMC, methylcellulose	Doxycycline	Taner et al. (1994)
	Polyhydroxybutyric acid	Tetracycline hydrochloride	Deasy et al. (1989)
Gels	Chitosan	Simvastatin	Rao et al. (2013)
	Gellan gum	Azithromycin	Pradeep et al. (2013a)
	Xanthan	Alendronate	Pradeep et al. (2013b)
	Pluronic	Simvastatin	Pradeep et al. (2012a)
	Carboxymethylcellulose	Alendronate	Pradeep et al. (2012b)
Nanofibres	Polylactide (PLA)	Metronidazole	Reise et al. (2012)
	PCL	Doxycycline	Chaturvedi et al. (2013)
	Polytetrafluoroethylene (PTFE)	Human gingival fibroblasts cultured on substrates	Kearns et al. (2013)
	Gelatin	Periodontal ligament cells cultured on gelatin nanofibrous membrane	Zhang et al. (2009)

1.2.3 Periodontal wound healing

Periodontal treatment aims primarily at controlling the infection and inflammation caused by the oral bacterial biofilm and thereby arrest progressive attachment loss, and prevents further disease progression, which may eventually lead to tooth loss. Preferably, the aim of the treatment must include regeneration of the lost periodontal attachment apparatus. This means that wound healing after periodontal therapy is characterized by the formation of new cementum with functionally oriented collagen fibres on the previously exposed or affected portion of the root, and simultaneously with a new alveolar bone formation, and a periodontal ligament with physiologic width and composition (Laurell et al., 2006).

Recent studies suggest that the use of techniques like guided tissue regeneration (GTR) and the application of enamel matrix proteins (EMD) onto the exposed root result in true periodontal regeneration. Furthermore, the use of various growth factors and autologous blood concentrates for periodontal regeneration has also produced positive results, but more studies are needed. In general, both GTR and EMD, alone or in combination with bone grafts or substitutes, result in larger clinical improvements compared to conventional periodontal

treatment for deep intrabony and furcation Class II defects (i.e., bone loss between roots) (Stavropoulos et al., 2017).

1.3 Complications in dental implant surgery

The first introduction of dental implants dates back to 1970s, and is used in various regions of the mouth (Wheeler, 2009; Bornstein et al., 2008). Nowadays, implant surgery has become a routine therapy for the rehabilitation of completely or partly edentulous patients, but, despite its increasing popularity and high success rates, complications are still unavoidable and their management is becoming an important issue (Misch et al., 2008; Lamas Pelayo et al., 2008; Greenstein et al., 2008). Complications would happen either during intra-operative or post-operative period of the surgery.

Intra-operative complications, such as hematoma and ingestion or inhalation of mechanical components or instruments, can be serious as life-threatening. Other complications that take place during implant placements are typically associated with local damages such as nerve injury, adjacent teeth damage and perforations of the nasal cavity or maxillary sinus.

Peri-implantitis, sinusitis, peri-implant mucositis, and periapical implant lesions are the complications often encountered after surgery. Hence, implant therapy is a complex procedure and the management of these complications linked with this therapy requires special training and experience. Table II shows a planned classification taking into consideration the time of events occurring during the surgery and the circumstances that emerge postoperatively (Annibali et al., 2008).

Table II. Local complications in dental implant surgery.

Early-stage complications	Late-stage complications
• Infection • Edema • Ecchymoses and haematomas • Emphysema • Flap dehiscence • Sensory disorders	• Peri-implant mucositis • Maxillary sinusitis • Implant fractures • Failed osseointegration • Bony defects • Peri-implantitis

Moreover, postoperative pain after periodontal surgery is a common occurrence. According to a study, 70% of patients noticed some degree of pain following the periodontal surgery,

while most were only in the mild to moderate range; 44.1% of patients reported moderate pain; and 4.6% reported severe pain (Curtis et al., 1985). Pure mucogingival surgery was significantly related to pain and was 3.5 times more likely to cause pain than osseous surgery and 6 times more likely than plastic soft tissue surgery. The length of surgery was significantly linked to pain for osseous and soft tissue surgery.

Therefore, also complications following dental surgery might benefit from local treatment with an appropriate dosage form.

1.4 Biopolymers as wound healing materials

Wound healing is a physiological process involving many factors, whose complexity makes it prone to several abnormalities. Apart from cellular and biochemical components, several enzymatic pathways also happen to become active during repair and aid the tissue to heal.

The requirements of biomaterials for new therapies in regenerative medicine are vast. They must be biocompatible, allow vascularisation and should have good handling capabilities. The implant should stay at the intended site and adhere tightly to the tissue, and consequently can serve as excellent carrier for therapeutic agents or accelerate wound healing process.

The polymer scaffolds which are said to be biocompatible and biodegradable combined with cells or biological signals are being investigated as alternatives to conventional options for tissue reconstruction and transplantation.

The requirements like elasticity, tear-resistance and biodegradability can be quite different depending on the application.

The common feature of all these materials is the necessity of physical protection from external factors and conditions. The main characteristics that are required for ideal wound healing materials include ease of application, bioadhesiveness to the wound surface, inhibition of bacterial invasion, elasticity and high mechanical strength, biodegradability and finally being non-toxic and non-antigenic (Balasubramani et al., 2001; Jones et al., 2002).

A great deal of research is currently being undertaken to develop wound healing materials that can provide optimum healing conditions, taking into account all of these factors and healing mechanisms involving inflammation, tissue replacement, fibrosis, coagulation, etc. (Fig. 3) (Still et al., 2003; Stashak et al., 2004).

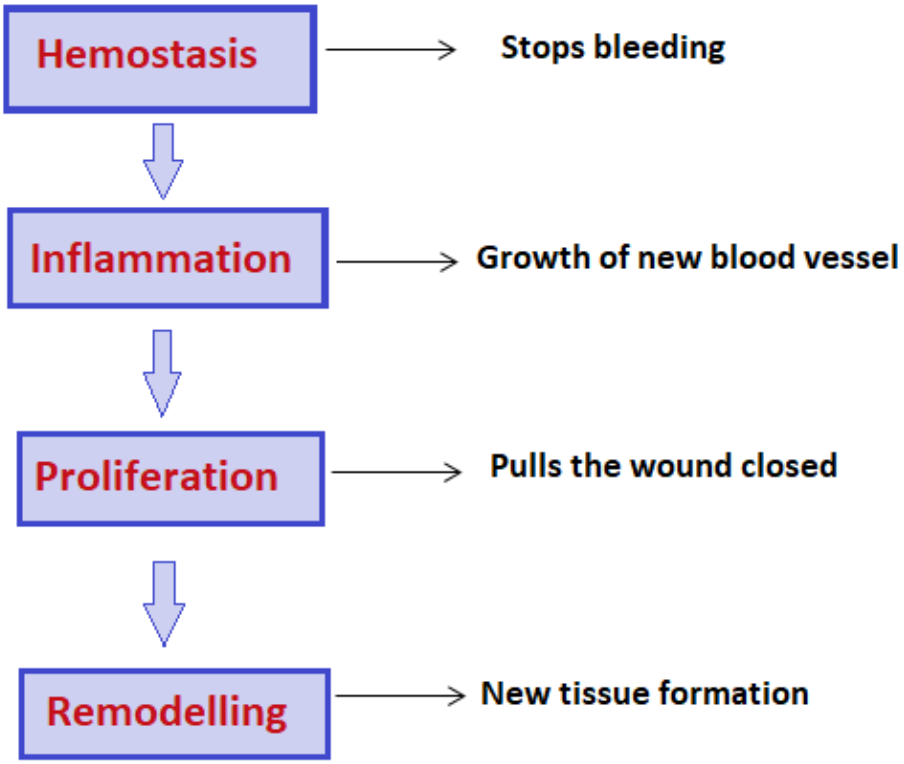

Figure 3. Wound healing mechanism.

Many natural and synthetic polymers like collagen, hyaluronic acid and its derivatives, alginic acid and its salts, and fucoidan and synthetic polymers, like polyurethane, Teflon, silicon and methylmethacrylate, are being widely used in the preparation of artificial wound dressing materials.

On the other hand, pharmaceutical formulations like natural and synthetic gel-like materials, composites, micro- or nanoparticulate systems, and films have been attributed profoundly in the development of biomaterials for wound healing and other tissue engineering purposes.

1.5 Multilayer films

A multilayer film can be defined as a film that contains two or more layers made of film-forming polymers with one or more active substances. Over the last few years, the release of active substances from multilayer films has become increasingly important due to their efficiency in administration for local therapy as well as systemic therapy (Rupprecht and Zinzen, 2004) and the advantages they possess over polymeric single-layered films or monolithic films, like increased drug loading and controlled drug delivery. However this

dosage form up to now encountered serious technological difficulties since these multilayer films are preferably produced by a casting process. Also considerable problems arise in the scaling-up of the production process from the laboratory to the mass production level.

1.5.1 Preparation methods of multilayer films

Over the years, the solvent casting method is said to be the manufacturing method of choice for both industrial and lab scale due to its simplicity and low cost. In this method, all the ingredients are dissolved in a suitable solvent, then cast on an inert substrate and subsequently dried. The drying step can be achieved either at room temperature or in hot air oven or by freeze or vacuum drying.

Alternative methods like double casting, crimping, compressing, coating and dropping have been used to prepare multilayer films (Preis M et al., 2014). The processes for preparation of the multilayer films are illustrated in Fig. 4.

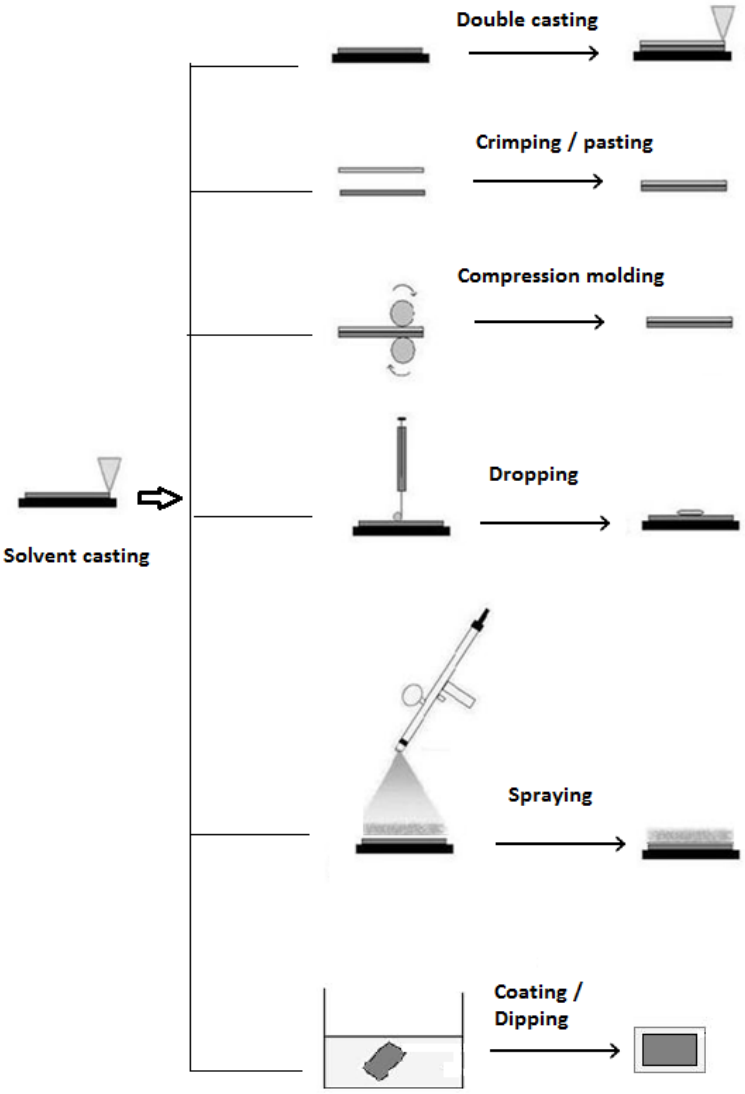

Figure 4. Preparation methods of multilayer films.

In the double casting method, initially a casting solution is prepared and cast on a suitable substrate and subsequently dried at room temperature or in hot air oven, then a second layer is casted above the first layer and dried.

Crimping method is also called as pasting or laminating. Two or three films of either similar or different thickness, either similar or different polymer composition, are prepared separately and then crimped.

In the compression method two films are prepared separately by solvent casting and superimposed, while one film still has a tacky surface, as the solvent has not evaporated yet or the film is not completely dry. A roll is used to compress the layers onto each other, then

the resulting double-layer is often weighed down by a metal plate to increase adhesion of the two layers.

In the dropping method, defined amounts of liquid of different aqueous and ethanol polymer solutions are dropped onto a film previously prepared using a computer-operated syringe.

In the coating method, a drug-free film or a film loaded with a drug prepared by casting is dipped into a polymer solution containing drug or without drug, using an appropriate solvent that does not disintegrate the film (Deadman, 1964). With an appropriate choice of interfacial tensions and evaporation rate, the second polymer will form a uniform layer upon the other. This process is adapted to yield multilayer films with specific drug-release properties.

Another method of preparing film is extrusion. Although hot-melt extrusion is comparatively a new technology in the pharmaceutical industry, it has been used in the production of many different dosage forms and its applicability in the production of films for both drug delivery and wound care applications has been demonstrated (Repka et al., 2000). When a multi-layered film is involved, the different layers can be coextruded and then laminated together, or else each layer can be separately extruded on the previous one, and then laminated together.

On the other hand, different types of printing methods like 3D printing, inkjet printing and flexographic printing, have recently attracted interest as emerging technologies for fabrication of drug delivery systems. Based on the selection of the technology, a very high precision in depositing a preferred ratio of active compound/s and excipients onto appropriate substrates can be achieved, which facilitates the preparation of single or multiple dosage forms with functional sophisticated features. The main ideas in the use of this type of technologies are to develop and fabricate pharmaceuticals in a tailored manner to meet some of the predicted personalization needs of patients.

Three-dimensional (3D) printing is described as process to make 3D objects by a computer-aided design 3D model. This method could be used for manufacturing polymeric thin films and multilayer films by depositing sequential layers of material. The objects that are created can be of virtually any shape or geometry. Many 3D printing technologies like stereolithography, sintering, melting, fused deposition modeling (FDM) or fused filament fabrication (FFF) are in existence (Maren et al.,2015).

Also inkjet technologies can be considered as 3D techniques when three-dimensional objects are formed by multiple layering. The inkjet printing is used to precisely and accurately deposit small amounts of liquid on a substrate (like triple-coated inkjet paper, uncoated wood

free paper or double-coated sheet fed offset paper) based on digitally predesigned patterns. Thus, after the design of a printing pattern the deposition of a desired ratio of active pharmaceutical ingredient and excipient (so called ink formulation) onto a carrier substrate can be accomplished in a controlled manner (Sandler et al., 2011). And preparation of multiple layers can be done by depositing one or more layers on the top of the first with or without an intermediate base film layer. Furthermore, the printed layer can be shielded by a second base film layer. This will result in modified drug release profiles and protect the ink layer from detachment or mechanical stress during processing like cutting or packaging (Varan et al., 2017).

Flexographic printing is an offset, rotary printing process. It is a highly flexible and cost-effective alternative manufacturing method in which a drug-loaded substrate is deposited onto a polymeric thin film. Multilayer can be obtained by increasing the cycle of printing of drug-loaded substrate onto the polymeric support (Janßen et al., 2012).

Although a variety of different film-forming techniques can be used in multilayer films, it is desirable to select a method compatible with the polymers chosen for the formulation, with the aim to obtain a flexible film (Yang et al., 2014).

1.5.2 Design and choice of a multilayer film

In order to achieve suitable properties and specific release profile from a multilayer film, an ideal formulation design is necessary. It can be optimized by properly establishing the ratio of surface area to thickness of drug release-controlling layers. This design can be affected by changing the ratio of the water-soluble to water-insoluble polymers. Moreover, it may be desirable to have one or more layers free of active substance in order to obtain controlled release rate of the drug. Due to the high degree of variability of the manufacturing process, the layer build-up is preferably carried out sequentially, preferably starting with the adherent layer as the initial substrate for the successive active substance-containing layers and the cover layer on the support surface (Rupprecht and Zinzen, 2004).

1.5.3 Multilayer film applications in local drug delivery

Formulation aspects and technological platforms in multilayer films allowed use of this system in different strategies for local drug delivery, like administration of multiple drugs or of drug eluting implants, in wound healing and tissue regeneration.

Many examples of applications of multilayer films for local therapies have been disclosed, employing different film-forming techniques.

Sundararaj et al. (2013) designed a multilayered system that delivers multiple drugs directed at periodontitis treatment, produced by casting. This system includes four drugs, namely metronidazole, ketoprofen, doxycycline, and simvastatin, to eliminate infection, inhibit inflammation, prevent tissue destruction, and aid bone regeneration, respectively in four different layers with alternating single or double blank layers, which are said to be released in sequential manner for stepwise treatment of disease condition.

Varan et al. (2017) studied a multilayer film containing anticancer and antiviral drugs, manufactured by inkjet printing onto an adhesive film obtained by solvent casting for local treatment of cervical cancer as a result of HPV infection.

Lei et al. (2011) designed a PCL [poly(ε-caprolactone)]-based bi/trilayered film containing coating layer, drug reservoir layer and a backing layer for stent application in malignant stricture or stenosis, prepared by compression molding. This study revealed the potential of trilayered film in controlled drug delivery to intraluminal tumor due to its highly tunable zero order drug release.

Rong et al. (2012) developed a PCL-based bilayer/trilayered film containing surface layer (with or without drug), drug reservoir layer and a backing layer for stent application, using a hot melt extrusion method. This study proved that PCL-based films co-loaded with drugs have great potential for anti-tumor application, due to their unidirectional and rate-tunable drug release characteristics.

1.6 Multilayer films for local treatment of oral diseases

Local treatment of oral cavity related diseases have been achieved by use of local drug delivery systems for a long time. Though these diseases are often exceptionally responsive to local therapy, the mouth often presents a variety of difficulties in the application of topical dosage forms (owing to saliva and different functions of the mouth), resulting in a short retention time of applied dosage forms leading to a low therapeutic efficacy. To surmount these limitations, today research concentrates on the development of bioadhesive formulations (Paderni et al., 2012).

Recently, research on multilayer films for local drug administration in the oral cavity for certain indication areas, like oral cancer (Desai et al., 2011), oropharyngeal and periodontal infections (Tonglairoum et al., 2015) and pain (Abo Enin et al., 2016), (Juliano et al., 2008) has attracted considerable attention. The oral cavity is an attractive site for the delivery of drugs owing to the ease of administration and for its suitability for mucosal (local effect) and

transmucosal (systemic effect) drug administration. In the first case, the aim is to achieve a site-specific release of the drug on the mucosa.

Although there are diverse techniques for the extended drug release from formulations, like solid dosage forms, intended for buccal applications, they have the disadvantage that the form of preparation gives an extraneous feel to the patient when adhered to the gingiva and possibly causes pain. For this reason, multilayer films are assessed as an attractive and feasible dosage form to overcome some negative aspects of conventional oral dosage forms.

The properties of a film that satisfy the requirements for use in the buccal cavity are thickness, flexibility, mucoadhesion, control of the release of active substances and compatibility.

A non-exhaustive list of papers describing the formulation of multilayer films for oral application is reported in Table III.

Table III. Multilayer films for local drug delivery in oral diseases.

Drug substance	Multilayer type	Polymers	Technology	Reference
Metronidazole benzoate	2	Primary layer – chitosan Secondary layer - chitosan and poly(ε-caprolactone)	Solvent casting	El-Kamel et al. (2007)
Ipriflavone	3	Primary layer – chitosan Secondary layer - poly(ε-caprolactone) Tertiary layer – chitosan	Solvent casting	Perugini et al. (2003)
Prednisolone	2	Primary layer - sodium alginate Secondary layer - gellan gum Backing layer - ethylcellulose or white beeswax and white petrolatum	Solvent casting	Ragwa et al. (2017)
N/A	2	Mucoadhesive layer - polyethylene oxide and carmellose sodium	Solvent casting	Danek et al. (2017)
Imiquimod	2	Mucoadhesive layer - PVP K-90 and NaCMC Backing layer - poly(ethylene-co-vinyl acetate)	Solvent casting	Ramineni et al. (2013)
Phenytoin sodium	2	Mucoadhesive layer - carbopol 934, NaCMC, HPMC Backing layer - cellulose acetate phthalate	Solvent casting	Najafi et al. (2011)
Tetracycline hydrochloride and carvacrol	2	Mucoadhesive layer - carbopol 934 Backing layer - ethylcellulose	Solvent casting	Obaidat et al. (2011)
Chlorhexidine diacetate	2	Mucoadhesive layer - sodium alginate / HPMC / chitosan Backing layer - HPMC K100LV	Solvent casting	Juliano et al. (2008)
Lidocaine hydrochloride and diclofenac potassium	2	Mucoadhesive layer - sodium alginate, HPMC K4M, chitosan Backing layer - sodium alginate, HPMC K4M, chitosan	N/A	Abo Enin et al. (2016)

1.7 Choice of drug: chlorhexidine digluconate

Chlorhexidine digluconate is a potent bactericidal and broad-spectrum antimicrobial agent. Functioning as an antiseptic, it is an effective bactericidal agent against all categories of microbes, including bacteria, yeast, and viruses. It has been extensively studied by the researches and is considered to be the "gold standard" antimicrobial drug in oral hygiene. Moreover, it is useful in many clinical disciplines, including periodontics, endodontics, oral surgery and operative dentistry (Medlicott et al., 1999).

Chlorhexidine molecules being positively charged and whereas most bacteria and surface structures in the oral cavity, including the surfaces of teeth and mucous membranes, are negatively charged in nature. Chlorhexidine binds strongly to all these surface structures, based on the fact that the opposite charges attract. Hence, when chlorhexidine binds to microbial cell walls, it induces changes, damaging the surface structure, leading to an osmotic imbalance with consequent precipitation of cytoplasm and so causing cell death. These multiple effects of chlorhexidine enhance its bactericidal effect, which allows, due to the retention of chlorhexidine in the oral cavity, a prolonged residual antimicrobial activity for up to 12 hours or longer depending on the dosage and the form (Fardal et al., 1986; Schiøtt et al., 1972).

Chlorhexidine is safe and has an inherent advantage over antibiotics by not producing resistant microorganisms. As a result, chlorhexidine can be used repeatedly and over long periods of time. Furthermore, it destroys all categories of microbes, not just bacteria, and there is little risk for the development of opportunistic infections.

However, the patient compliance with the long term use of chlorhexidine is limited by its unpleasant taste and tendency to stain the teeth brown. These adverse effects may possibly as result of use of conventional delivery systems, including mouth rinses and irrigation solutions, which allow contact of high concentrations of chlorhexidine (typically 0.2%) with taste buds and visible tooth surfaces.

Currently, a great deal of evidence suggests that periodontitis occurs as intermittent bursts of disease progression combined with stable periods. As a result, only a few sites in an individual might show active disease at one time and require treatment (Goodson et al, 1982; Socransky et al., 1984).

Therefore, chlorhexidine delivery could be targeted to oral cavity and the area surrounding the periodontal pocket, thereby preventing recurrence of the subgingival infection.

1.8 Aims and objectives of the Ph.D. project

The prolonged life and the recurrent use of new dental implant technologies suggest in the immediate future a strong demand for buccal dosage forms for the treatment of different dental health problems, such as treating post-implant surgery complications or chronic diseases like periodontitis and gingival retraction.

Therefore, our research project has been focused on the development of a biopolymer-based multilayered film, which could be bioadhesive and biocompatible with the unhealthy tissue and simultaneously able to release the drug locally with a controlled rate.

To this aim chlorhexidine digluconate was selected as a model drug as its local delivery in the mouth may improve treatment of dental-associated oral diseases if its saliva concentrations can be maintained at effective levels for prolonged period.

Firstly, the idea was to develop a multilayered film consisting of a mucoadhesive layer, a supporting layer and a drug loaded layer which could exert a release rate control. With this aim, a preformulative study on film-forming polymers and a selection of the best candidates for the further development of a multilayer film is mandatory.

Secondly, the selected optimized multilayer film should be characterized for its physico-chemical properties like mucoadhesion, physical strength, and antimicrobial activity to prevent pathogen colonization.

Finally, other characteristics that should be taken into consideration to optimize a multilayer film for wound healing applications are: the ease of preparation and application on wound site, the controlled release of active molecules and the film ability of acting as a protective barrier.

CHAPTER 2

MATERIALS AND METHODS

2.1 Materials

Hydroxypropylcellulose (HPC G) (Klucel, Ashland), hydroxypropylmethylcellulose (HPMC K750) (Hypromellose, Ashland), hydroxyethylcellulose (HEC G) (Natrosol, Ashland), polyvinylalcohol (Parteck SRP 80, Merck Millipore), bovine collagen peptide (MW 1000-3000 Da) (Lapi Gelatine), edible gelatin (gel strength 166 g) (Rousselot 175 H30), bovine skin gelatin GLF 15 (gel strength 154 g) (Lapi Gelatine), chlorhexidine digluconate solution (20% in H_2O) (Sigma-Aldrich), mucin from porcine stomach, type II (Sigma-Aldrich), disodium hydrogen phosphate dihydrate ($Na_2HPO_4.2H_2O$) (Sigma-Aldrich), potassium dihydrogen phosphate anhydrous (KH_2PO_4) (Sigma-Aldrich), sodium chloride (NaCl) (Sigma-Aldrich).

2.2 Methods

2.2.1 Preformulation study

The rationale behind conducting this preformulative study was to select the best polymers with film-forming properties.

The film-forming polymers of interest for our application must feature properties like aqueous solubility, good flexibility without the use of plasticizers, mucoadhesive properties, good surface activity, availability in a wide range of viscosity types, and appropriate mechanical properties.

To this aim, initially pure polymers were screened for film-forming properties using water as a solvent. 4.85g of solutions of appropriate polymer concentration 3%w/w, obtained by careful dispersion of the powder in deionized water at room temperature, were casted on polystyrene plate lids (diameter 18 or 23 mm) and let dry at 45 °C for 1 h. The obtained films were then peeled off and only the ones that met our requirements in terms of mechanical resistance and flexibility were evaluated for *in vitro* adhesion, mechanical, *in vitro* residence time, swelling and erosion index properties.

2.2.2 Preparation of monolayer mucoadhesive films

To the best film-forming polymer with mucoadhesive properties a model biopolymer like bovine collagen peptide (MW 1000-3000 Da) was added in different ratios like (100/0, 80/20, 67/33, 50/50 %), and finally, the ratio that resulted in the most flexible films was selected for

further studies with other biopolymers like gelatin type A and B, collagen peptide (MW 5000 Da) and a undisclosed novel product (NP) of animal origin which is supposed to have wound healing and anti-inflammatory properties.

Solvent casting method was used to prepare the monolayer films. Briefly, the casting solutions containing 1.5% w/w biopolymers and 3.5% w/w film-forming polymer were prepared by dispersion of the powders in appropriate volumes of deionized water under continuous stirring at 37 °C. Then, the casting solutions (0.5 g of polymer solution per mould) were casted on polystyrene plate lids (diameter 23 mm) and dried at 45 °C for 1 h in a thermostated oven. Then the prepared films were evaluated for *in vitro* adhesion, mechanical, *ex vivo* residence time, swelling and erosion properties respectively.

2.2.3 Preparation of bilayer films

For bilayer films, a double casting method was used to prepare films: initially, polymer dispersions of supporting layer were cast and dried at 45 °C, then a mucoadhesive layer with or without drug was cast on the first layer and dried at the same temperature. The prepared films were evaluated for mechanical properties.

Composition of bilayer films:

(a1). Mucoadhesive layer without drug: a polymer mixture containing 3.5% w/w of HPC G and 1.5% w/w of novel product (NP)

(a2). Mucoadhesive layer with drug: a polymer mixture containing 3.5% w/w of HPC G, 1.5% w/w of NP and 0.5% w/w of chlorhexidine digluconate (CHX).

(b). Supporting layer: a polymer mixture containing 5% w/w HPC G alone or 3.5% w/w HPC G and 1.5% w/w of biopolymer (like gelatin type A and B) or film-forming polymers like pectin, sodium alginate and sodium carboxymethylcellulose.

2.2.4 Preparation of trilayer films

Trilayer films were prepared by a double casting method (Fig. 61). Briefly, casting solutions were prepared by dispersing selected polymer mixtures in appropriate volumes of deionized water in a closed container maintained at constant homogenization (magnetic stirring, 300 rpm) at 37 °C and at room temperature for 1 h. After complete homogenization, the casting solutions of the local drug delivery layer were cast (0.5 g of solution per mold) on polystyrene plate lids (diameter 23 mm) and dried at 45 °C in a thermostated oven for 1 h. Eventually, the casting solutions of supporting and mucoadhesive layers were cast and dried

at the same temperature for 2 and 3 h respectively. Finally, films were peeled from the mold and were used to evaluate their properties.

Composition of trilayer films:

(a) *Mucoadhesive layer:* a polymer mixture containing 3.5% w/w of HPC G, 1.5% w/w of novel product (NP) and 0.125% w/w of CHX.

(b) *Supporting layer:* a polymer solution containing 5% w/w of HPC G alone or a mixture containing 3.5% w/w of HPC G, 1.5% w/w of gelatin type A and 0.25% w/w of CHX.

(c) *Local drug delivery layer:* a polymer solution containing 5% w/w of HPC G alone and 0.5% w/w of CHX, or a mixture containing 2.5% w/w of HPC G, 2.5% w/w of HEC G and 0.5% w/w of CHX, or a mixture of 2.5% w/w of HPC G, 2.5% w/w of HPMC K750 and 0.5% w/w of CHX.

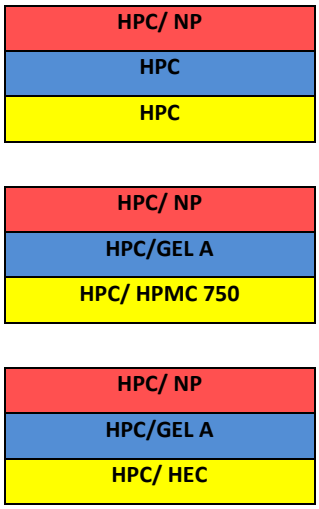

Figure 6. Formulation design of trilayer films.

2.2.5 Weight and thickness

The films (n = 5) were individually weighed on a digital analytical balance (Scaltec SBC 21). The film thickness was measured with the help of a digital calliper (Mitituyo, Aurora) in five random positions of the film. The average thickness value determined was also accounted for mechanical tests.

2.2.6 Surface morphology

The surface morphology of a mucoadhesive layer containing a film former in combination of a biopolymer (collagen peptide 3K) in different ratios was tested by optical microscopy

(Alphaphot-2YS2, Nikon) to confirm surface texture and homogeneity. The appearance of the films was observed at a magnification factor of 10. Illustrative digital images were taken at the same time.

2.2.7 *In vitro* mucoadhesion studies

In vitro mucoadhesion was evaluated by measurement of detachment force (referred to surface area, MPa) and calculation of the work (mJ) necessary for the detachment of the film from a substrate mimicking the mucosal surface (porcine mucin tablets, 13 mm diameter, 250 mg) (Fig. 7) using a material testing machine (LRX model, Lloyd Instruments) equipped with a 20 N load cell.

The film was pasted on the upper support connected to the material testing machine with cyanoacrylate glue. A porcine disc was glued on the lower support and was wetted with 100 µL of pH 6.8 phosphate buffer. Then the film was made to contact with the mucin tablet by lowering the upper support and a preload of 1 N was applied and the adhesive force was measured after 10 min by pulling the upper support at a speed of 0.1 mm/s.

Results are reported as the mean of 3 determinations ± SD. Maximum detachment force is the maximum applied force at which the patch detaches from mucin substrate (Fig. 8). Total Work, calculated from the area under the force-distance curve, is a measure of the work that must be done to remove a film from the mucin substrate. Peak work, is calculated from the area measured up to the maximum applied force, whereas work of adhesion is the area before initiation of viscoelastic behaviour (Fig. 9).

Preparation of mucin tablet

Porcine mucin powder of 250 mg was weighed and the tablet was prepared by using a 13 mm-die, under a compression force of 6 tons applied for 5 minutes by a hydraulic press (Fig. 7).

Figure 7. Mucin tablet preparation by a hydraulic press.

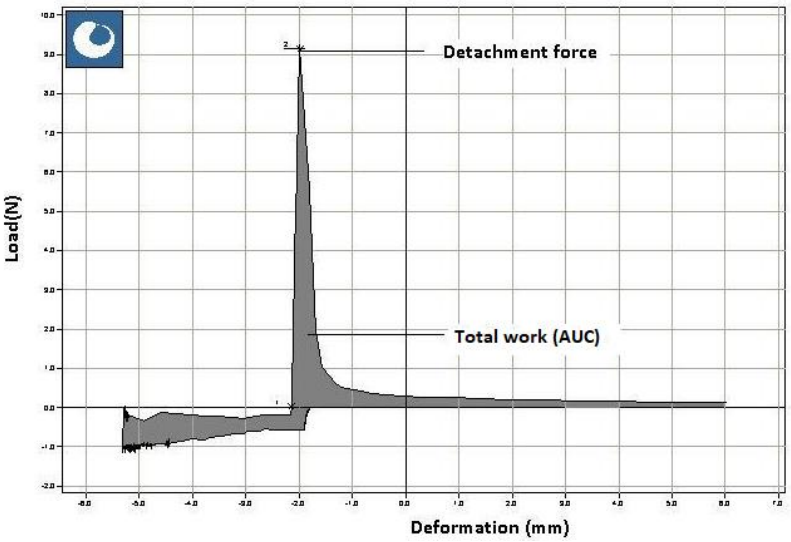

Figure 8. Representation of adhesion properties measurement from resulted graph.

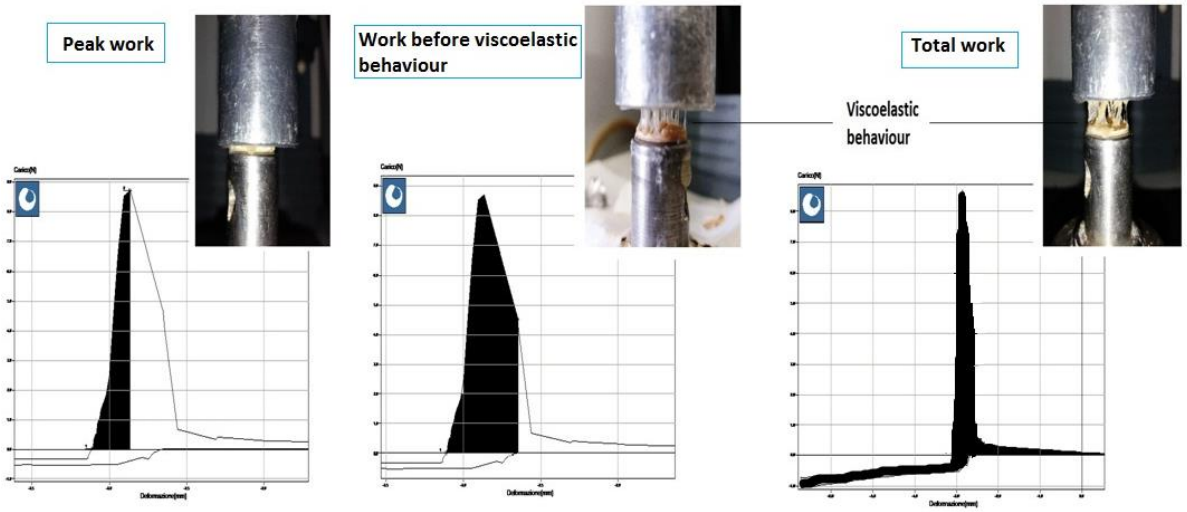

Figure 9. Schematic representation of work calculated at various points of detachment of film from the mucin substrate.

2.2.8 *Ex vivo* mucoadhesion studies

This test was performed on a material testing machine (LRX model, Lloyd Instruments) equipped with a 20 N load cell using three kinds of biological membranes. Firstly, the porcine buccal mucosa (Palem et al., 2011) was used due to its resemblance to human buccal mucosa. Secondly, the inverted chicken skin (Castan et al., 2015) was used to simulate the exposed submucosa in case of oral lesions and due to its surface homogeneity. Finally, a bovine liver tissue was used to simulate wounded tissue environment (Chen et al., 2014).

The film was pasted on the upper support connected to the material testing machine with cyanoacrylate glue. A piece of biological tissue was glued on the lower support and was wetted with 20 µL of aqueous porcine mucin solution (10% w/v), then the film was made to contact with the biological tissue by lowering the upper support and a preload of 1 N was applied and the adhesive force was measured after 10 min by pulling the upper support at a speed of 0.1 mm/s. Finally, maximum detachment force and total work parameters were calculated from the resulted graph. Results are reported as the mean of 3 determinations ± SD.

2.2.9 Mechanical properties

Yield strength (YS), Young's modulus (YM) and elongation at break (EB) were evaluated using the aforementioned testing machine equipped with mechanical grips. The film (10×10 mm) was placed between the two grips and tensile stress (Fig. 10) was applied at a velocity of 1 mm/min, until the film broke (Fig. 11).

Mechanical properties were calculated as follows:

Yield strength (YS) = Peak stress / Film cross-sectional area

Young's modulus (YM) = Stress / Strain

Elongation at break (EB) = Increase in length at break / Initial film length × 100

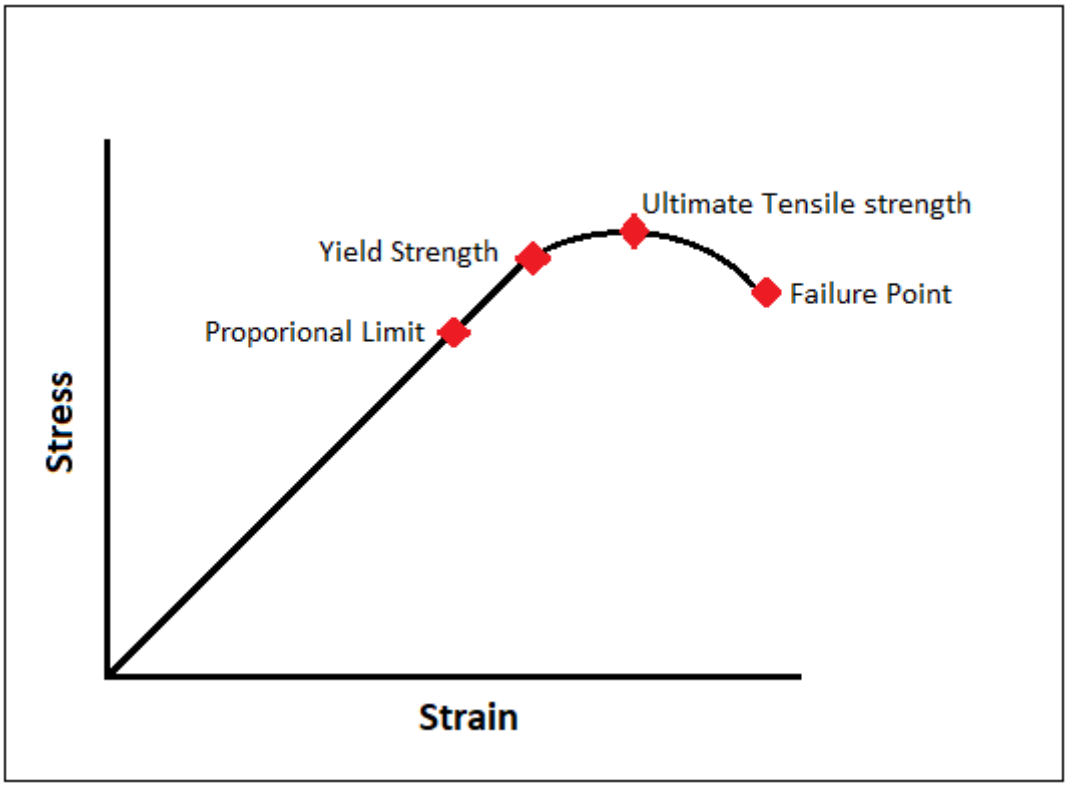

Figure 10. Stress-strain curve.

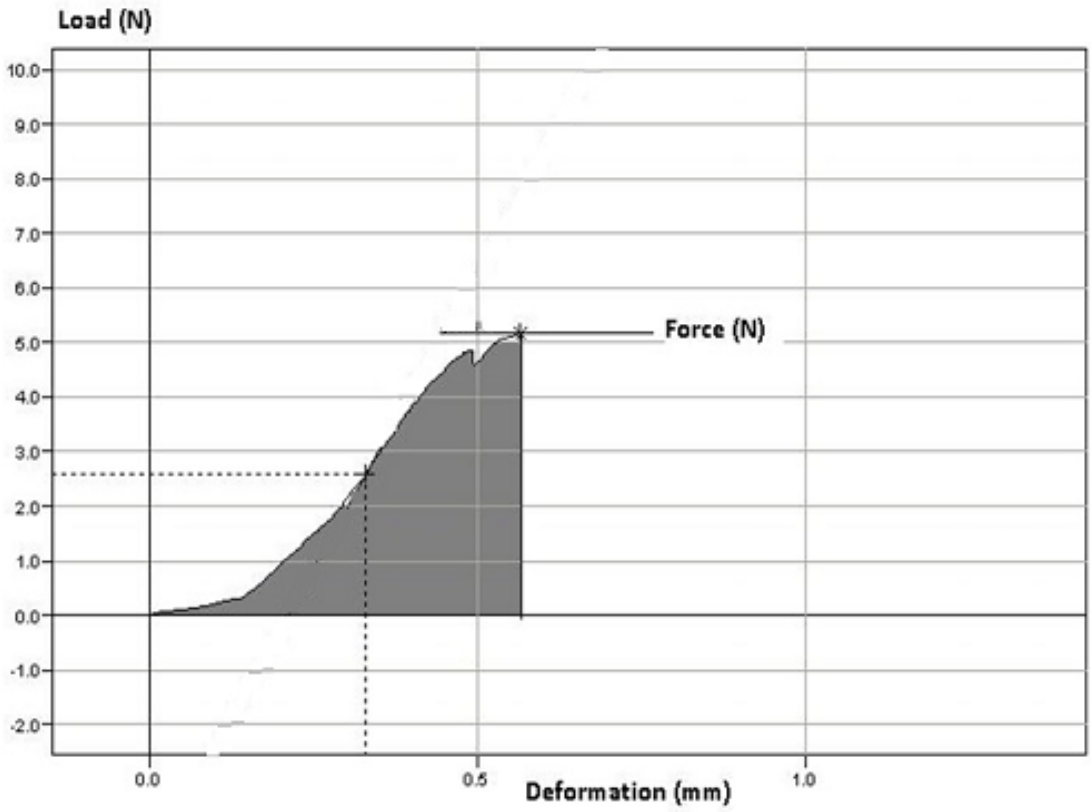

Figure 11. Representation of mechanical properties measurement from resulted graph.

Puncture strength was measured by letting a probe (5 mm diameter) pass with a velocity of 1 mm/min through a film fixed on a support and calculating the force required to rupture the film.

2.2.10 *Ex vivo*-residence time

This test was performed by sticking the films to a porcine tissue, which was fixed onto a glass plate hung on a movable support of a modified disintegrating compendial apparatus that moves vertically into and back out of a beaker containing 900 mL, pH 6.8, phosphate buffer solution maintained at 37 °C; the time (min) taken by the film to detach by complete erosion was recorded. Furthermore, a list of pure polymers like NaCMC L, PVA SRP 80, HEC G, carbopol 971, gelatin A in the mucoadhesive layer and HPC G alone in the backing layer were used to compare the adhesion capacity of biopolymers that have been used in this study. Additionally, a well-known very adhesive polymer like polycarbophil was also used to verify the residence of the aforementioned polymers.

2.2.11 *In vivo* residence time

This study was carried out on 5 healthy human subjects (2 males & 3 females) by applying a drug-free film on gingival mucosa. Each film was attached by pressing it against the gingival mucosa above the canine tooth for specific period of time (10 sec). The residence time was measured by the time of complete erosion or detachment of the film from the buccal mucus membrane.

2.2.12 Swelling and erosion index

These studies were measured in pH 6.8 phosphate buffer. For this purpose, each trilayer film was weighed (W1) and placed on a pre-weighed Petri dish (35 mm diameter), then 4 mL of phosphate buffer was poured and maintained at 37 °C for 30, 60, 120 and 180 minutes. Then, the excess liquid around the gelled films was carefully removed by means of a pipette and the Petri dishes were reweighed to determine the weight of swollen film (W2) and swelling index (SI) was calculated. Further, the films were dried for 1 h at 60 °C and reweighed to determine the weight (W3) for calculating the erosion index (EI).

$$SI = (W2-W1)/W1*100$$

$$EI= (W1-W3)/W1*100$$

2.2.13 *In vitro* drug release study

A modified version of previously used apparatus named home-made device (Baldassari et al., 2018) was used to perform the *in vitro* dissolution test: a plunger of a 50 mL syringe was inserted into the 50 mL polypropylene tube in inverted position to exploit the plunger flange as support to attach the films. An accurately weighed film(surface area 2.27cm^2) was then glued on the flange to limit the release of drug to only one side , and the plunger was moved to position the film in contact with the 5 or 10 ml of pH 6.8 PBS buffer solution [KH_2PO_4 0.19 g, $Na_2HPO_4.2H_2O$ 2.38 g, NaCl 8g], so that the film was just below the liquid surface. The dissolution medium was kept at a constant temperature of 37.0 ±0.2 °C and under soft orbital shaking (200 rpm) in a Peltier chilling-heating dry bath (Torrey Pines Scientific Inc.). For each sampling time (30 min, 1, 2, 2.30, 3, 4, 5,6 and 24 h) three devices were used, so that each time point in the release curves is the mean of 3 values. Chlorhexidine digluconate concentration in the dissolution medium was measured spectrophotometrically (Hewlett

Packard 8453) at 254 nm and the drug released was expressed as percentage w/w of the drug content.

Mass loss studies were performed in a similar way. The initial sample weight (W1) was recorded before the study, and final weight (W2) was measured after drying the eroded samples at 50 °C for 3 h. Percent mass loss was calculated and plotted against time.

2.2.14 *In vitro* sterility test

Films can be contaminated easily, which can lead to further infection when applied on wounded sites. Hence, a sterility test was performed on films employing two methods:

(i). *Incubation on rich medium agar plates*: each sample was placed aseptically on Columbia Agar plates (Oxoid) and incubated overnight at 37 °C. Plates were then carefully examined for visible growth and reincubated for 48 h for regrowth.

(ii). *Incubation in nutrient broth medium:* each sample was placed aseptically in 5 mL of Triptic Soy Broth (Biolife) and incubated overnight at 37 °C. Following that time, 20 µL from each culture broth were seeded on Columbia Agar plates and incubated overnight at 37 °C. Plates were then carefully evaluated for visible growth. Samples were subsequently kept at 37 °C for 14 more days and re-seeded on Columbia Agar plates.

Preparation procedure for films to be tested for sterility

Mainly four kinds of formulations like pure films made of HPC, films made of a solution of 5% w/w HPC pre-sterilized in autoclave, HPC+NP and HPC+NP+CHX were tested for sterility. Initially, all predefined polymers were weighed, placed in Petri dishes, positioned under a vertical laminar flow hood and finally UV sterilized overnight. The casting solutions were prepared in sterile vials. The polymer dispersions were prepared by adding sterile water and polymers into individual vials under continuous stirring by using a stirrer under the laminar flow hood for 1 h. Then, film formulations were casted (0.5 mL, equivalent to 0.5 g) on sterile polystyrene mould (18 mm) using a pipette and left to dry for 4 h. The dried films were exposed to UV light overnight, and finally carefully collected using sterile tweezers and placed in self-lock bags for sterility testing.

2.2.15 *In vitro* blood compatibility test: whole blood clotting

The films (2.54 cm^2) to be tested were placed into plastic dishes, and pre-warmed to 37 ˚C. Then 0.2 mL of whole blood [BD® vacutainer ACD type A (trisodium citrate 22 g/L, citric acid 8 g/L, dextrose 24.5 g/L)] was then dispensed onto the surface of the samples, and 50 µL of 0.2 M $CaCl_2$ solution were added to start coagulation. Subsequently, the plastic dishes

were placed at 37 ˚C in an incubator. After 10 min, red blood cells (RBCs) that were not trapped in the clot were hemolyzed with 10 mL of deionized water and centrifuged at 100 g for 30 s. Then 5 mL of supernatant were transferred carefully in to a tube and 20 mL of pure water were added. The absorbance of the resulting hemoglobin solution was measured at 542 nm (*Ds*), and the absorbance of 0.2 mL whole blood hemolyzed with 25 mL deionized water at 540 nm was denoted as *D0*. The blood clotting index (BCI) was calculated with the formula

$$\text{Blood clotting index (BCI)} = Ds / D0$$

2.2.16 Biological study

THP1 cells were maintained in RPMI medium at 37 °C with 5% CO_2, where culture medium was supplemented with 10% heat-inactivated fetal bovine serum (FBS), without antibiotics or antifungine supplements.

For viability/proliferation indexes and RT-PCR, about 3×10^4 and 5×10^5 THP1 cells were seeded in each well of 96-microwell plates and 75 cm^2 tissue flasks, respectively. After 24 h, THP1 were exposed to Lipopolysaccharide (LPS) alone, NP + LPS and NP alone, at a final dose of 3 mg/mL for NP and 5 µg/mL for LPS in complete growth medium for 6 and 24 h. LPS was added to the experimental medium as a positive control for monocyte activation. LPS, from Gram-negative bacteria, is commonly considered as one of the most potent innate immune-activating stimuli known. Gene expression of IL -1 and IL-8, chemokines produced by macrophages, was confirmed by RT-PCR. Whereas, NFkB, a transcription factor for damage response/adaptation genes, including inflammation and wound repair was confirmed by Western Blot.

MTS assay (CellTiter 96® Aqueous One Solution Cell Proliferation Assay, Promega), a colorimetric method, was used for testing any cytotoxic effects of the compounds and in parallel for measuring cell proliferation. It contains a tetrazolium compound [3-(4,5-dimethylthiazol-2-yl)-5-(3-carboxymethoxyphenyl)-2-(4-sulfophenyl)-2H-tetrazolium, inner salt] and an electron coupling reagent (phenazine ethosulfate, PES). The MTS was bioreduced by mithocondrial dehydrogenase enzymes into a colored formazan in metabolically active cells. MTS can be used to point out toxicity as well as proliferation, since the amount of formazan is time-dependent and proportional to the number of viable cells. The absorbance of formazan was measured in a microtiter plate-reader at 490 nm (Uniskan II, Labsystem). The potential toxicity of each treatment was extrapolated and

expressed as percentage vs. untreated LPS-stimulated cultures, respectively for toxicity and proliferation index, and presented as mean ± SD of three independent experiments with three replicates for each concentration.

2.2.17 Wound healing assay

To study cell migration *in vitro*, human keratinocytes HaCat cell line was used. $8.5x10^5$ cells/well were seeded and grown in DMEM medium supplemented with 10% fetal bovine serum at 37 °C with 5% CO_2, without antibiotics or antifungine supplements until a confluent monolayer was obtained. Then a scratch was created with a p200 pipet tip. To remove the debris and smooth the edge of the scratch, cells were washed once with PBS. Finally cells were added with medium with 10% FBS (positive control) or with medium alone (negative control) or treated with 3 mg/mL of NP in DMEM with 10% FBS. At time 0 and after 24 and 48 h cell images were acquired with a phase-contrast microscope and the distance of the scratched region was measured. For each image, distances between one side of scratch and the other were detected using Image J software. By comparing the images from time 0 to the last time point (24, 48 hours), the distance of each scratch closure was obtained on the basis of the distances that were measured by software to determine the migration of cells. Each experiment was performed with four replicates.

$$\text{Wound closure } \% = (W_0\text{-}Wt)/W_0 \times 100$$

W_0 represents the initial width of scratching, Wt represents scratching width t hours after test start.

2.2.18 Statistical analysis

Statistical analysis was performed by one-way analysis of variance (ANOVA). A post hoc comparison test of the means of individual groups was performed using the Tukey's HSD test. Statistical significance was set at $p<0.05$. Statistical evaluation of data was measured by means of Systat software, version 13.1.

CHAPTER 3

RESULTS AND DISCUSSION

3.1 Design of multilayer film

Technological purposes of multilayer films were studied to retain the dosage form in the site of application for prolonged time and to deliver one or more active substances**.** The adhesion properties of the polymer film depend on its composition, which in principle can be adjusted by carefully selecting polymer components. Moreover, an ideal film, apart from having good mucoadhesion, should be flexible, elastic, and strong enough to withstand breakage due to the stress endured during its residence in the mouth. In addition, controlled drug release from a film with the aforementioned properties still remains a challenge.

Therefore, in the present study, a mucus-membrane adhering multilayer film (Fig. 12) containing a mucoadhesive layer, a supporting layer and a local drug delivery layer has been rationally designed to act as a promising platform for wound healing applications in oral diseases.

The formulation was preceded by a preformulation step, allowing to choose the best polymer compositions for each layer and testing their properties.

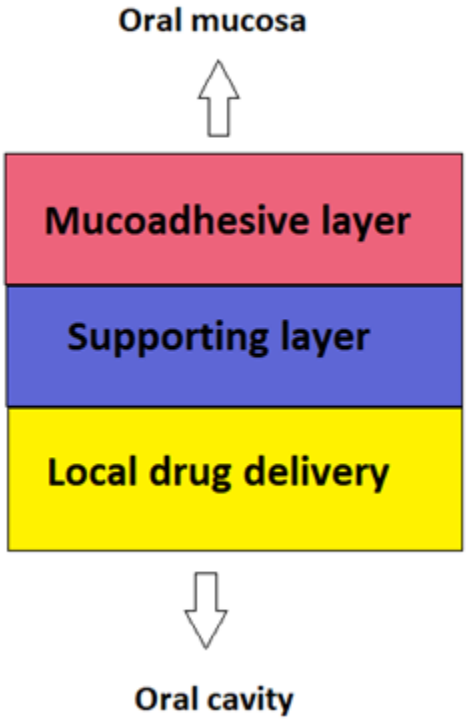

Figure 12. Scheme of a 3-layers planned dosage form.

Firstly, adhesive layer consists of a mucoadhesive polymer in combination with active substance having wound healing or anti-inflammatory properties. This layer has also a barrier-function to protect the wound or injury from the oral environment. This layer must not be irritating to the tissues or inhibit the coagulation process.

Secondly, the supporting layer consists of a polymeric mixture containing a film-forming agent with texture function, favoring the fabrication process, the mechanical properties of the final dosage form and counteracting the erosive action of the saliva.

Finally, the backing layer can contain polymer mixture to control the release of drug locally into the oral cavity, to prevent bacterial infection of the wounded site favoring the healing process.

Different substances having wound healing properties like collagen peptide, gelatin type A and B, have been tested in this thesis, while as model drug of antimicrobial substance the widely used chlorohexidine digluconate has been used.

3.2 Casting procedure of monolayer films

The solvent casting method was chosen to prepare monolayer films. It is a widely used manufacturing process for making films, well-known by its relative simplicity and the low cost that the system setup requires at a research laboratory scale (Morales et al., 2011).

In this method, monolayer films were successfully prepared by casting single aliquots of polymeric solutions on a polystyrene mold using a pipette (Fig. 13). Casting single aliquots would provide exact information about the amount of polymer and drug that has been cast and it does not require cutting the obtained film into pieces. Moreover, films produced by this method show good uniformity in the weight and thickness (Parodi et al., 2017).

Good homogenization of polymer dispersions was obtained by mixing the polymers at 37 °C and room temperature. To remove the air bubbles from the solution, it was further maintained at room temperature at rest for at least for 2-3 h before casting.

The casted films were dried in hot air oven at 45 °C. The prepared films were then peeled off and placed in self-lock bags for further evaluation.

Figure 13. Photo of a PS plate with twelve 18 mm pre-printed circular edge molds.

3.3 Preformulation study

The list of polymers studied is reported in Table IV.

Monolayer films casted with these polymers were evaluated for:

- *flowability of casting solution*
- *structure and appearance of films*
- *adhesion on mucin tablet*
- *tensile stress-strain behavior*
- *in vitro residence time*
- *swelling index*
- *erosion index*

3.3.1 Film properties

A number of potential film-forming polymers (Table V), suitable for casting from aqueous solution, were evaluated. The resulting films were studied for rheological properties of the casting colloidal solutions, shrinking tendency, ease of removal from the mold (detachability), rigidity/flexibility, thickness, transparency and texture smoothness.

Some water soluble, natural film-forming polymers, like sodium alginate and pectin resulted in rigid films (0.1 mm) not suitable for application on anatomic irregularities of gingival mucosa.

Furthermore, some cellulose-based polymers like NaCMC and low viscosity grades of PVP, like K30 and K64, produced rigid films. Though few polymers like PVP K90 and PEO-PVA

copolymers were flexible, the resulting films were too thin (0.02 mm). Therefore, these polymers were not considered for further studies.

Among the tested polymers, modified cellulosic polymers like hydroxypropylcellulose (HPC), hydroxypropylmethylcellulose (HPMC), hydroxyethylcellulose (HEC) and synthetic polymers like polyvinylalcohol (PVA) permitted to produce films with good flexibility without the use of the plasticizer agents (i.e. glycerin) and for this reason have been selected as possible candidates for the next steps of the preformulative evaluation.

Table IV. List of polymers used and their abbreviation and viscosity

Abbreviation	Polymer	Viscosity(mPa*s)	Solution conc (%)	Brand
PVA SRP 80	Polyvinyl alcohol	34-46	4	Parteck SRP 80
PVA Mowiol 4-88	Polyvinyl alcohol	3.5-4.5	4	Mowiol 4-88
HEC G	Hydroxyethyl cellulose	250-400	2	Natrosol G Pharm
HEC H	Hydroxyethyl cellulose	3,500-5,500	1	Natrosol H Pharm
HEC L	Hydroxyethyl cellulose	75-150	5	Natrosol L Pharm
HPC G	Hydroxypropyl cellulose	150-400	2	Klucel GF
HPC M	Hydroxypropyl cellulose	4,000-6,500	2	Klucel MF
NaCMC L	Sodium carboxy methyl cellulose	25-30	2	Blanose 7LP EP
NaCMC M	Sodium carboxy methyl cellulose	200-800	2	Blanose 7M8SF PH
PVP VA 64	Polyvinylpyrrolidone	8	10	Kollidon VA 64
PVP 30	Polyvinylpyrrolidone	5.5-8.5	10	Kollidon 30
PVP 90 F	Polyvinylpyrrolidone	300-700	10	Kollidon 90 F
HPMC E15	Hydroxypropyl methylcellulose	12-15	2	Methocel E15 LV
HPMC E3	Hydroxypropyl methylcellulose	2.4-3.6	2	Methocel E3
HPMC K15	Hydroxypropyl methylcellulose	13,275-24,780	2	Methocel K15
HPMC K100 LV	Hydroxypropyl methylcellulose	80-120	2	Benecel K100LV
HPMC K250	Hydroxypropyl methylcellulose	200-300	2	Benecel K250
HPMC K750	Hydroxypropyl methylcellulose	562-1050	2	Benecel K750
PEO WSR N-80	Polyethleneoxide	55-90	5	Polyox WSR N-80
PEO WSR N-12K	Polyethleneoxide	400-800	2	Polyox WSR N-12K
PEO WSR N-60K	Polyethleneoxide	2,000-4,000	2	Polyox WSR N-60K
MC A15	Methyl cellulose	12-18	2	Methocel A15
MC A4M	Methyl cellulose	2,663-4,970	2	Methocel A4M
HPSP	Hydroxypropyl peastarch polymer	900-1,300	25	LYCOAT RS720

Table V. List of polymers tested for film-forming properties.

Polymers	Flexibility/Rigidity	Detachability	Appearance
PVA SRP 80	Flexible	Detachable	Transparent
HEC G	Flexible	Detachable	Transparent
HPC G	Flexible	Detachable	Transparent
Pectin LM	Rigid	Detachable	Translucent
Pectin HM	Rigid	Detachable	Translucent
NaCMC L	Rigid	Detachable	Transparent
NaCMC M	Rigid	Detachable	Transparent
Sodium alginate	Rigid	Detachable	Translucent
PVP K64	Brittle	Undetachable	N/A
PVP K90	Flexible	Detachable	Transparent
PVP K30	Brittle	Undetachable	Transparent
HPMC E15	Flexible	Detachable	Transparent
HPMC E3	Flexible	Detachable	Transparent
HPMC K15	Too viscous to cast	N/A	N/A
PEO WSR N-80	Flexible	Detachable	Translucent
Methyl cellulose A15	Partially flexible to rigid	Detachable	Transparent
Methyl cellulose A4M	Partially flexible to rigid	Detachable	Transparent
Polaxomer 407	Brittle	Undetachable	N/A
PEO WSR N-12K	Flexible	Detachable	Translucent
PEO WSR N-60K	Flexible but Shrunken	Detachable	Translucent
Carbopol 971	Too viscous to cast	N/A	N/A
Polaxomer 407	Brittle	Detachable	Translucent
HPSP	Flexible	Detachable	Translucent
Kollicoat IR	Flexible	Detachable	Translucent
Kollicoat PROTECT	Flexible	Detachable	Translucent
PVA Mowiol 4-88	Flexible	Detachable	Translucent
HPC M	Too viscous to cast	N/A	N/A
HPMC K100 LV	Flexible	Detachable	Translucent
HEC H	Too viscous to cast	N/A	N/A
HPMC K250	Flexible	Detachable	Translucent
HPMC K750	Flexible	Detachable	Translucent
HEC L	Flexible	Detachable	Translucent

3.3.2 Adhesion on mucin tablet

This study has been performed using porcine mucin tablet as a substrate (Fig. 14). In Fig. 15 the maximum detachment force of films made of pure polymers are compared. HPC G and the two grades of PVA showed higher adhesion force compared to HEC G and HPMC K750. Whereas, work of adhesion (Fig. 16) was higher for HPC, HPMC and PVA based polymers compared to both grades of HEC.

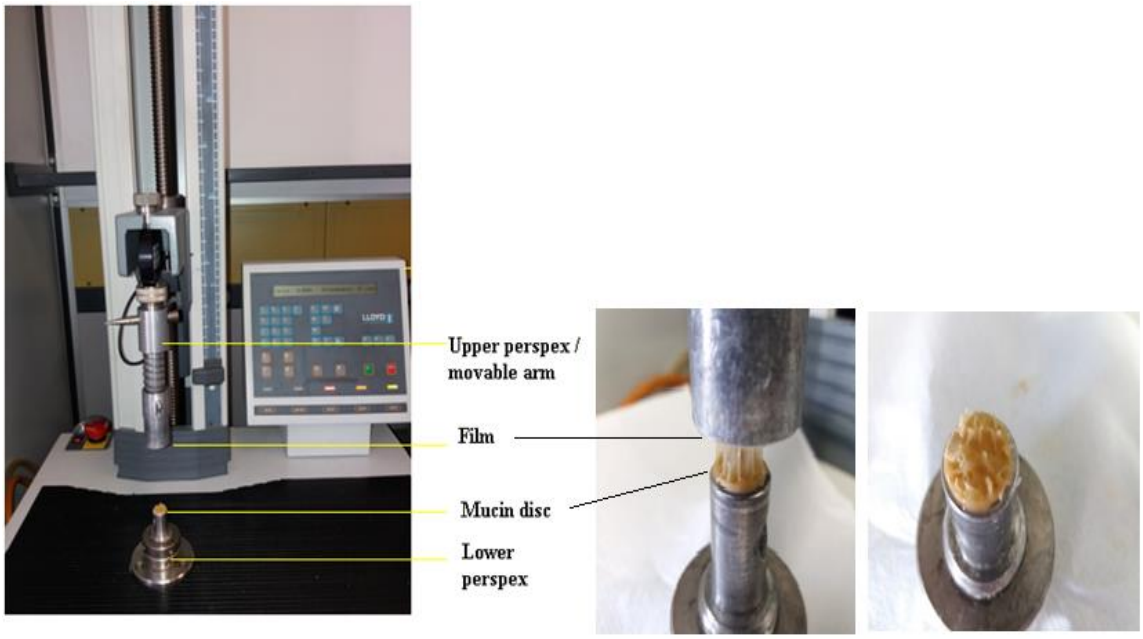

Figure 14. Setting used for measurement of *in vitro* mucoadhesion properties.

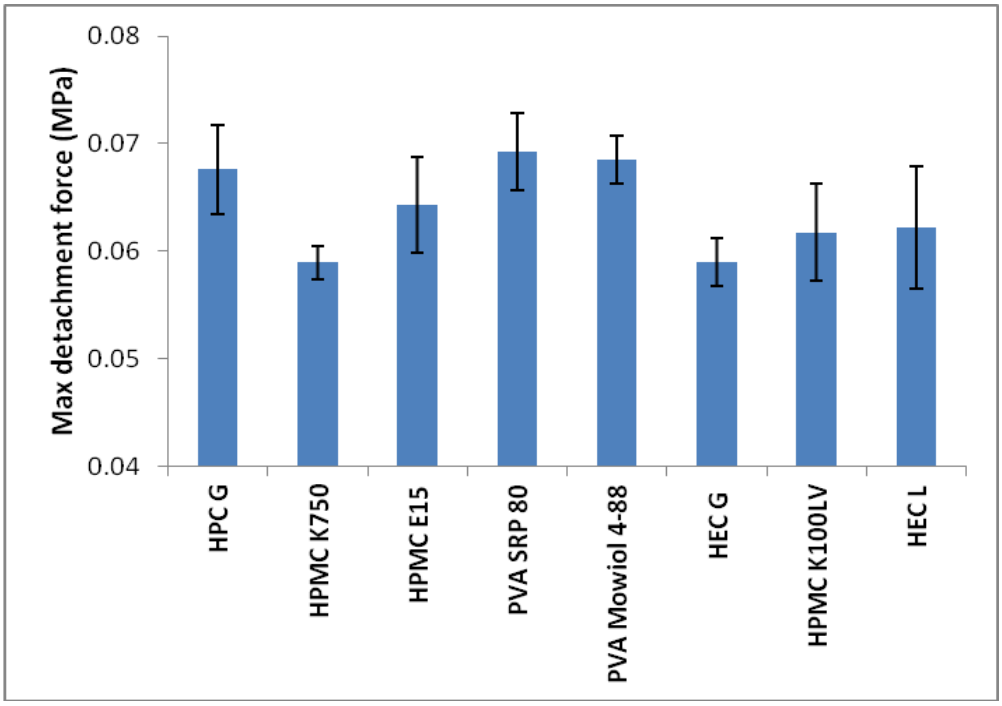

Figure 15. Comparision of maximum detachment force (MPa) of pure polymers tested on mucin tablet (values represented as mean (n = 3) and with error bar representing standard deviation).

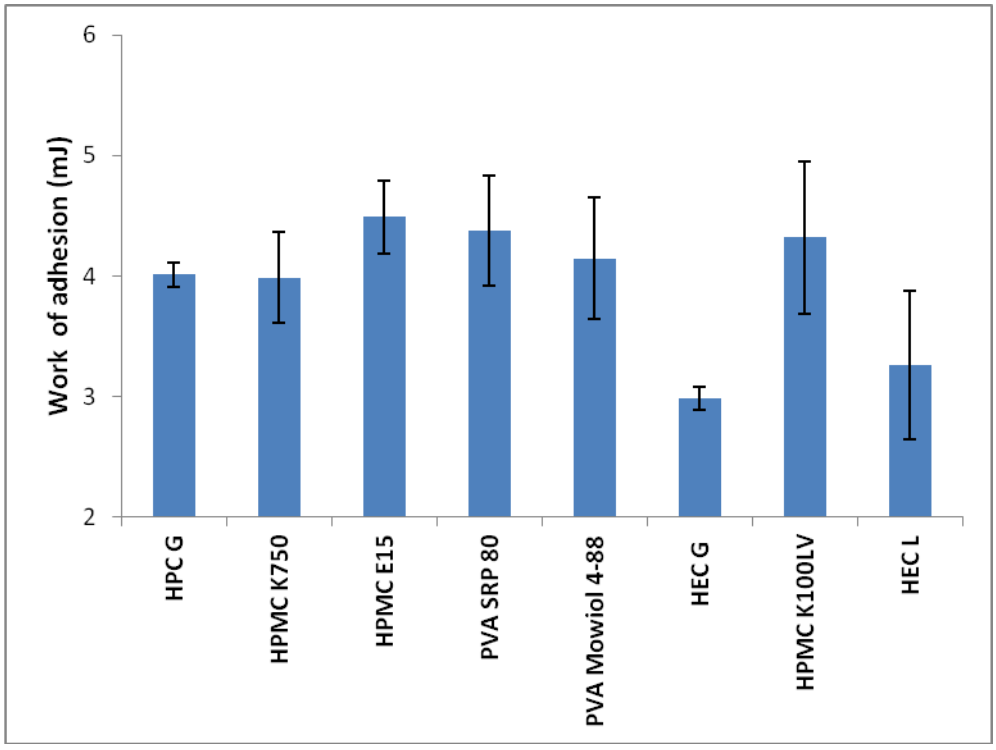

Figure 16. Adhesion properties of prepared films: work of adhesion (mJ) of pure polymers tested on mucin tablet (values represented as mean (n = 3) and with error bar representing standard deviation).

3.3.3 Tensile stress-strain behavior

The mechanical properties of the prepared films were tested using the same material testing machine, but with different equipment (Fig. 17). Figure 18 shows yield strength of the pure polymers tested. HPMC K750 and HPMC E15 showed good yield strength, whereas other polymers, like HPC G, the two grades of PVA and HEC, showed low yield strength: these polymer films, at a low stress, got deformed.

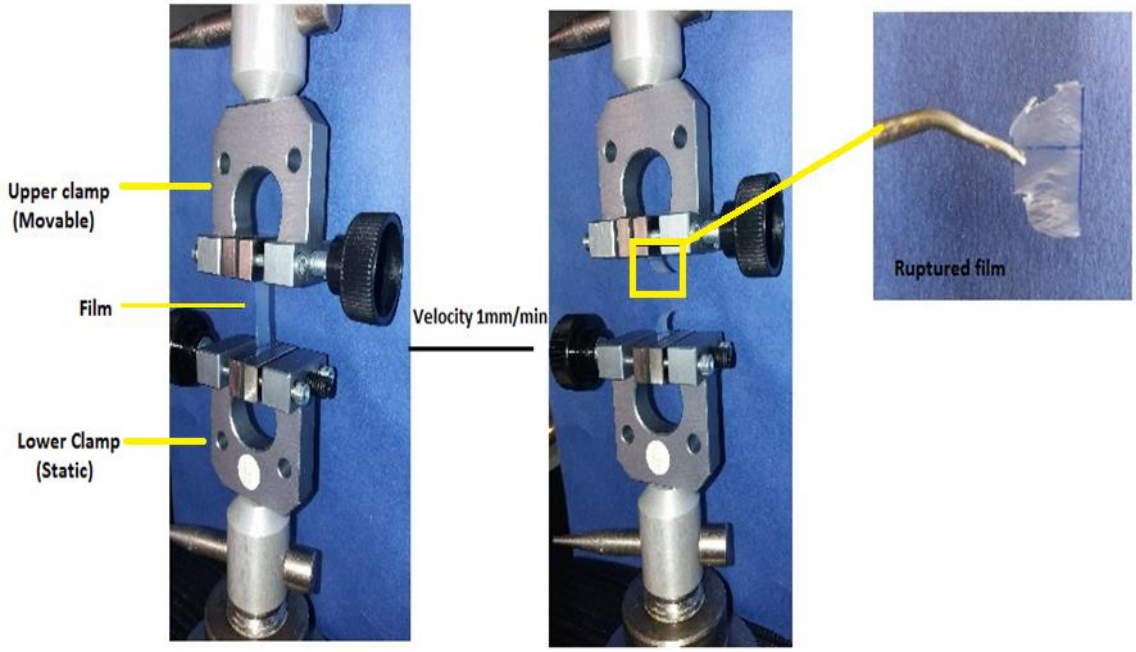

Figure 17. Illustration of material tester to measure tensile stress-strain curve of the films.

Figure 19 shows the Young's modulus comparison of the tested pure polymer film. The films made of pure HPC showed the most elastic behavior. This elastic nature of the polymer was well correlated with the results of the elongation at break (Fig. 20). Though films of PVA Mowiol 4-88 showed a low Young's modulus, its elasticity was poor as measured by the elongation at break value.

3.3.4 Swelling Index

Swelling index was measured on pure polymers by using the Petri dish method (Khan S et al., 2016) (Fig. 21) and using pH 6.8 phosphate buffer as the medium. The SI values comparison (Fig. 22) shows that HPMC K750 and HPMC E15 reached the highest value, while the two grades of PVA tested had the lowest swelling index.

3.3.5 Erosion Index

The erosion study results of the pure polymer films, performed in pH 6.8 phosphate buffer medium, are reported in Fig. 23. Among all the polymers tested, HPC G, HPMC K750 and HPMC E15 showed the lowest erosion index, while PVA type Mowiol 4-88, because of its lower viscosity and high solubility, showed the highest EI.

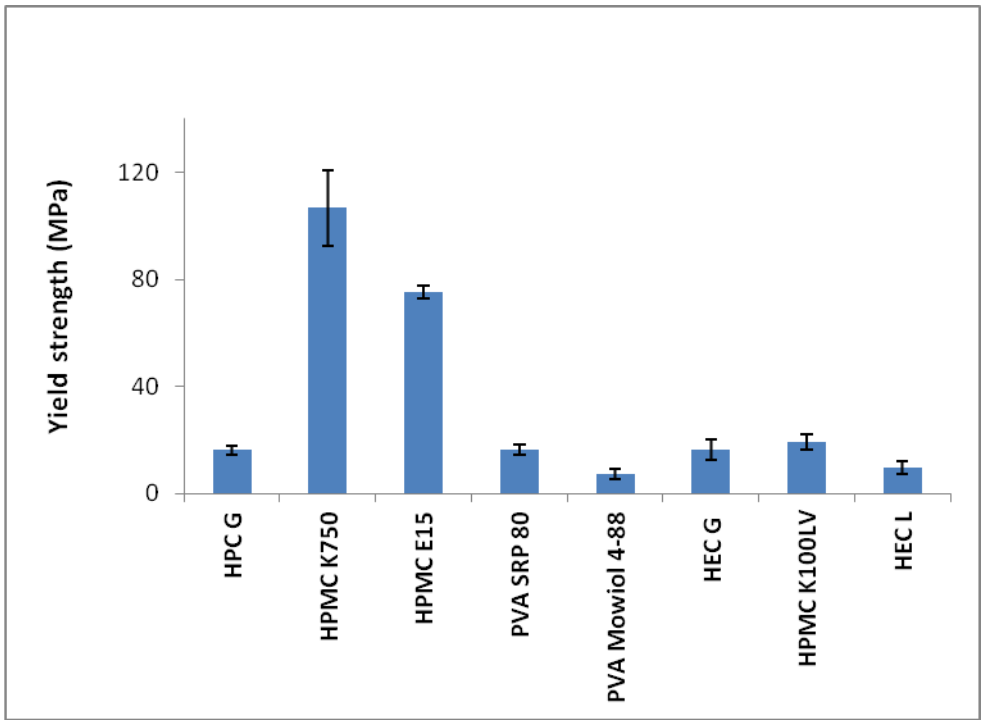

Figure 18. Mechanical properties of prepared films: yield strength (MPa) of pure polymers tested on material testing machine; (values represented as mean (n = 3) and with error bar representing standard deviation).

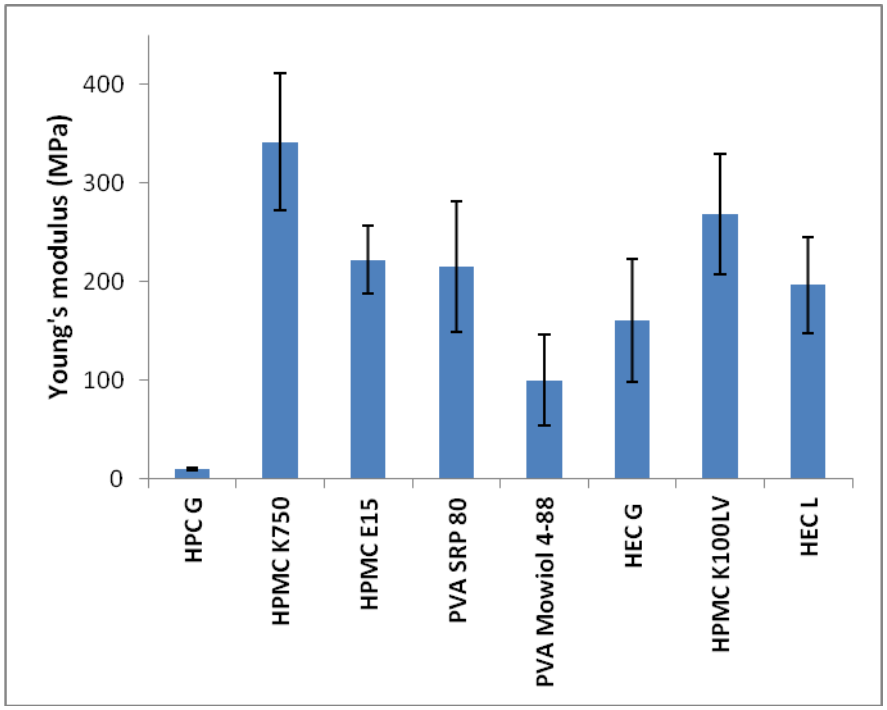

Figure 19. Mechanical properties of prepared films: Young's modulus (MPa) of pure polymers tested on material testing machine; (values represented as mean (n = 3) and with error bar representing standard deviation).

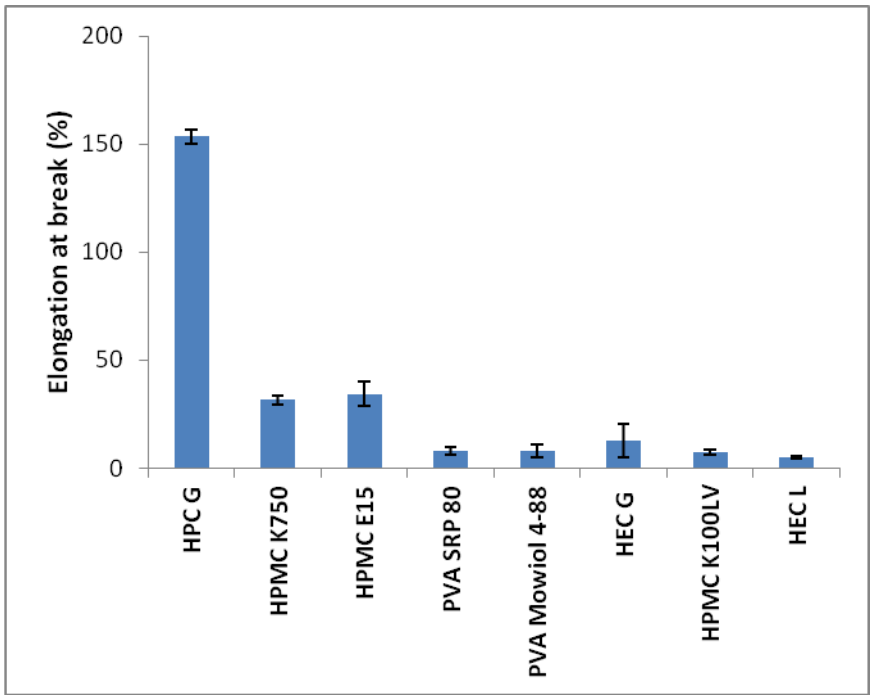

Figure 20. Mechanical properties of prepared films: Elongation at break (%) of pure polymers tested on material testing machine (values represented as mean (n = 3) and with error bar representing standard deviation).

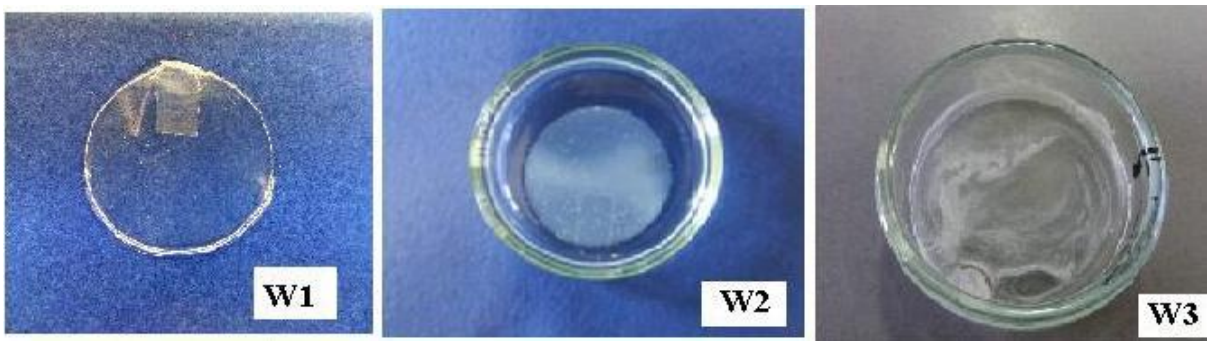

Figure 21. Method used to study the swelling behavior of films in pH 6.8 phosphate buffer.

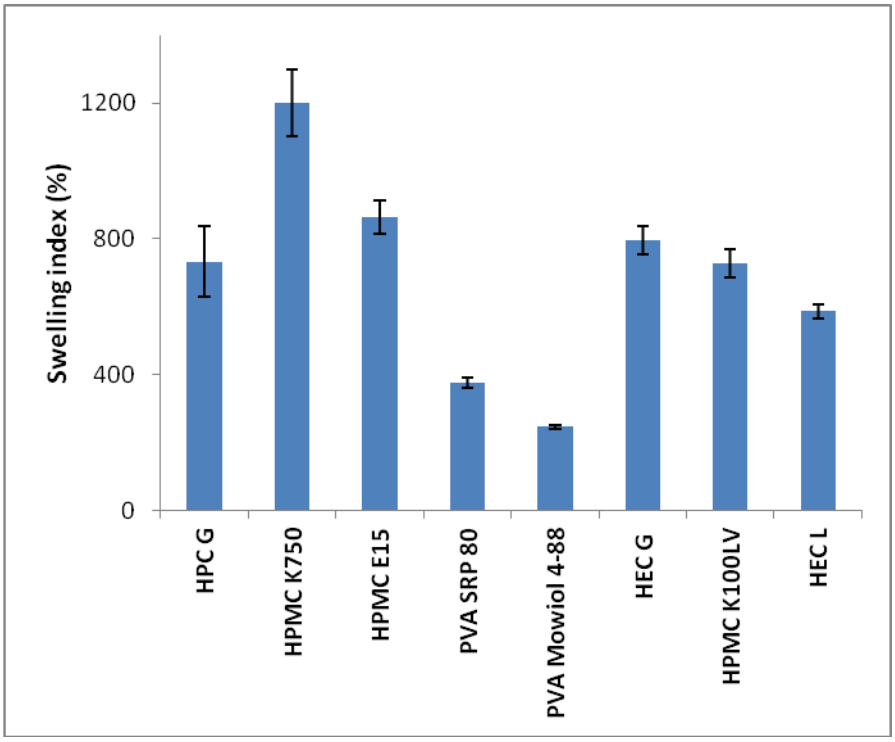

Figure 22. Swelling behavior of the prepared films tested in pH 6.8 phosphate buffer (values represented as mean (n = 3) and with error bar representing standard deviation).

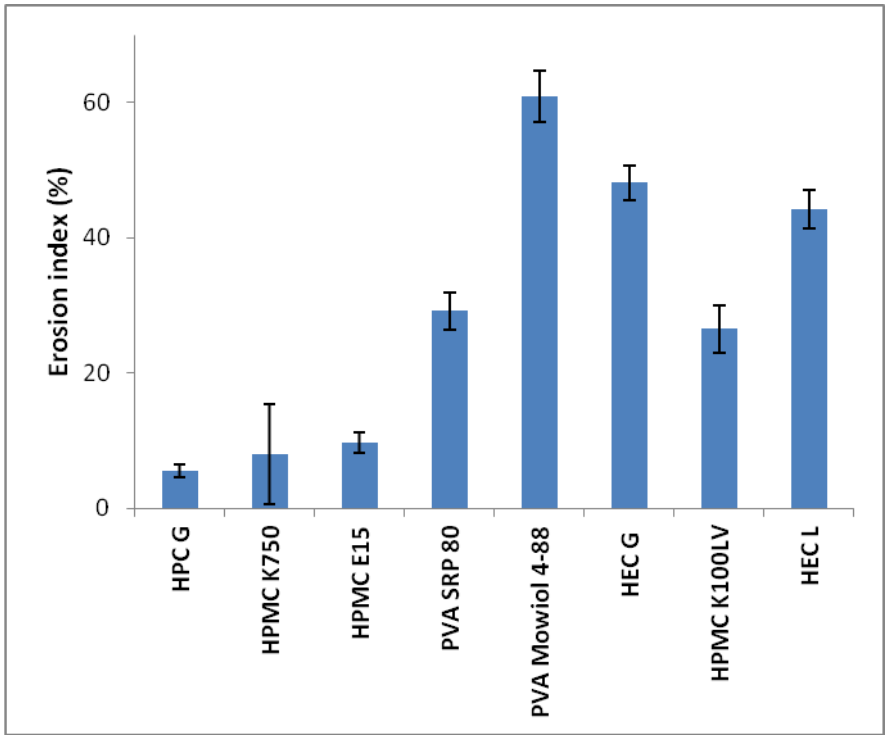

Figure 23. Erosion behavior of the prepared films tested in pH 6.8 phosphate buffer (values represented as mean (n = 3) and with error bar representing standard deviation).

3.3.6 Residence time

In vitro residence time study was performed by a modified disintegration apparatus using a glass slide as support (Fig. 24). Time comparison (Fig. 25) shows that HPC G polymer films remained attached for the longest time with respect to the other polymeric films, followed by HPMC K750. PVA and HEC based films showed the lowest residence time, probably due to their high erosion index.

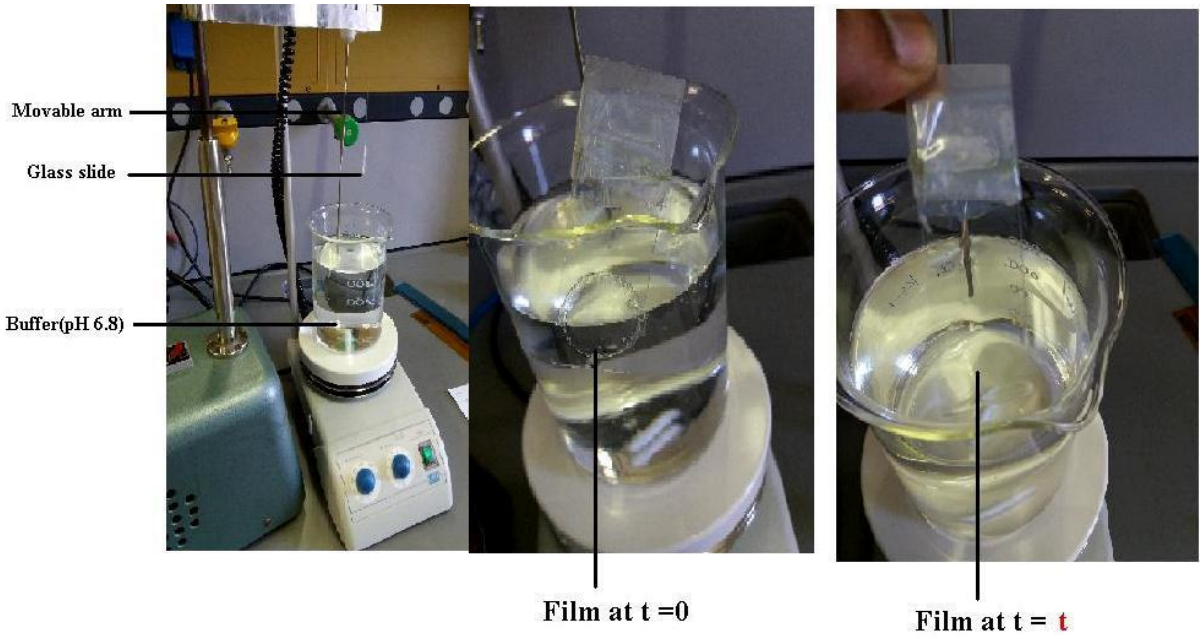

Figure 24. Modified compendial disintegration apparatus used to study residence time.

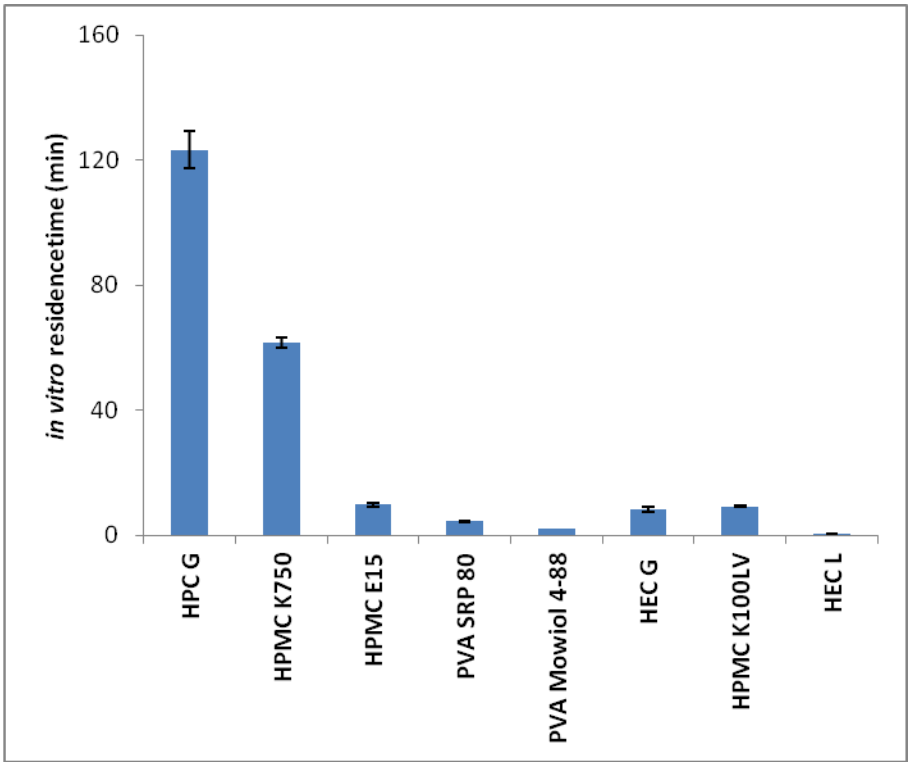

Figure 25. *In vitro* residence time of the pure polymer films tested by modified disintegration apparatus in pH 6.8 phosphate buffer (values represented as mean (n = 3) and with error bar representing standard deviation).

4. Selection of mucoadhesive layer

The first layer, which will be in contact with mucus membrane, must have the following characteristics: good mucoadhesive property, low SI and EI, good residence time and high mechanical resistance

HPC was selected as the best candidate for the mucoadhesive layer, because it showed all these properties.

Over the years, natural biopolymers like collagen, hyaluronic acid and derivatives have been used for wound healing applications (Table.VI).

Table VI. List of natural polymers used in wound healing.

Biopolymer	**Source**	**Uses**	**Reference**
Collagen	Bovine, pig skin	Many biomedical applications like wound dressing materials and hemostatic	Hafemann et al., 1999
Alginic acid and its salts	Natural polysaccharide derived from brown algae	Treatment for wounds due to their hemostatic properties	Thomas et al., 2000
Hyaluronic acid and its derivatives	Mammal's bond tissues and synovial fluids	Acceleration of tissue repair and wound healing	Saliba et al., 2001
Chitosan	Shells of shrimp and other crustaceans	Treatment of wounds due to its hemostatic effect	Senel et al, 2004
Fucoidan	Many species of brown seaweed	Used as anti-thrombotic, anti-inflammatory agent	Patankar et al., 1993

The properties of layer films obtained by combining the selected HPC polymer with biopolymers like collagen peptide (MW 1000-3000 Da and MW 5000 Da), gelatin type A, gelatin type B and a novel product of animal origin (NP), used for their anti-inflammatory and wound healing properties, were studied.

The NP used in the study is an animal extract containing, among other minor components, hyaluronic acid, collagen, elastin and chondroitin-4-sulphate, for which an anti-inflammatory and wound healing activity has been demonstrated in the biological study here reported.

4.1 Biological study on NP

4.1.1 Anti-inflammatory activity

In this study, the viability and proliferation of THP1 cells in the presence of NP were measured using the MTS assay, while proinflammatory cytokine gene expression was determined using RT-PCR mRNA. The obtained data of the viability index, extrapolated by

the MTS assay revealed that the exposure to NP at the tested doses did not exert toxicity on THP1 cells (Fig. 26) with respect to LPS treatment. Especially with athe dose of 3 mg/mL, the viability of the cells seems to be stimulated in a time-dependent way.

THP1 activation, after adding LPS, was assessed in terms of modulation of IL-1β and IL-8 gene expression, as representative of proinflammatory chemokines synthesis. LPS induced the expression of IL-1β and IL-8 in untreated cultures, both at 6 and 24 h (Figs.27 and 28), while NP exposure demonstrated a protective role of this extract.

In addition, NF-kB, which has a fundamental role in inflammatory condition to eliminate the initial cause of damage and to promote the process of repair of the involved tissue, has been studied. From the results, reported in Fig. 29, the increase in the ratio of phosphorylated NFkB to total NFkB indicated that the damage response was activated more when NP was used.

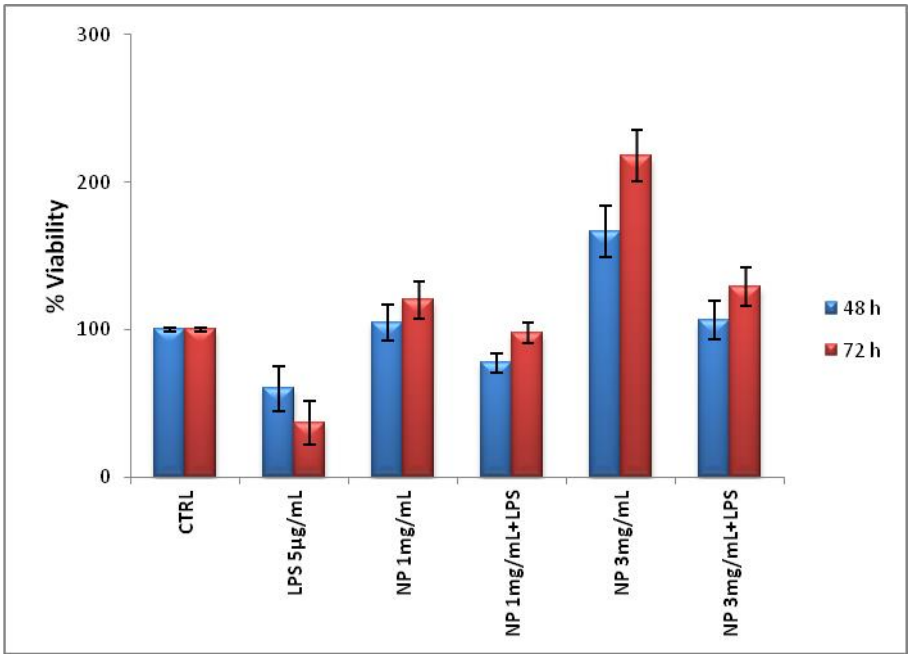

Figure 26. MTS assay performed on THP1 cell line treated with NP (values represented as mean (n = 3) and with error bar representing standard deviation).

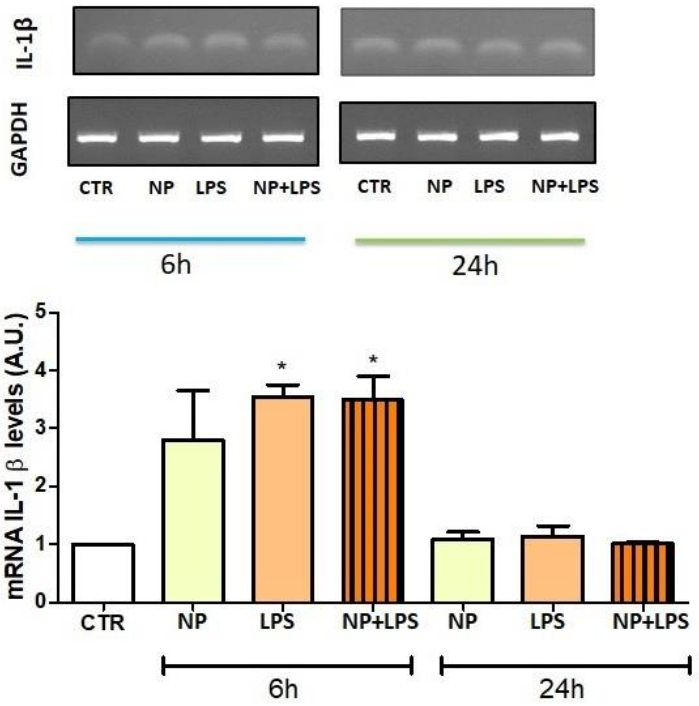

Figure 27. Study of IL-1 expression at 6 and 24 h(values represented as mean (n = 3) and with error bar representing standard deviation).

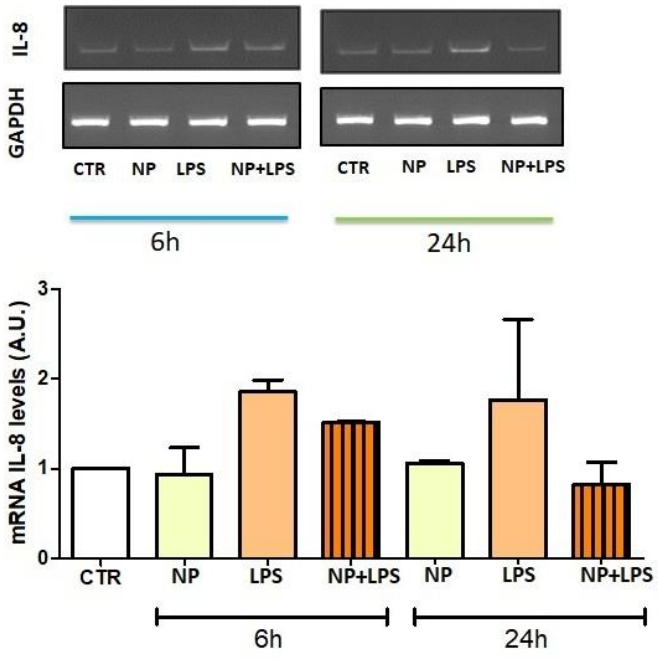

Figure 28. Study of IL-8 expression at 6 and 24 h (values represented as mean (n = 3) and with error bar representing standard deviation).

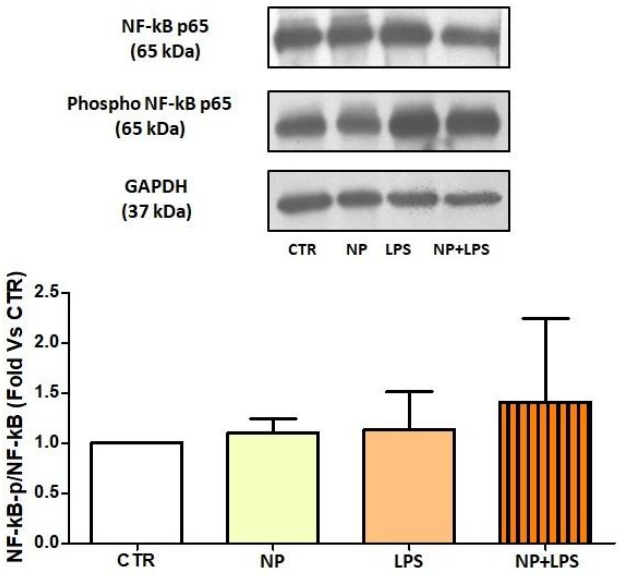

Figure 29. Study of NFkB expression at 24 h(values represented as mean (n = 3) and with error bar representing standard deviation).

4.1.2 Wound healing assay

The cell wound closure assay examines the ability of a particular cell line to migrate and subsequently close a wound made in a confluent plate of cells. As shown in Figs. 30, 31, 32, the migration of keratinocytes into the wounded area was distinctly increased in the presence of NP 3 mg/mL. In particular, the effect is clearly evident at 24 h after the treatment, where the treated cells showed a wound closure of 84±12 % vs positive control 30±9 %.

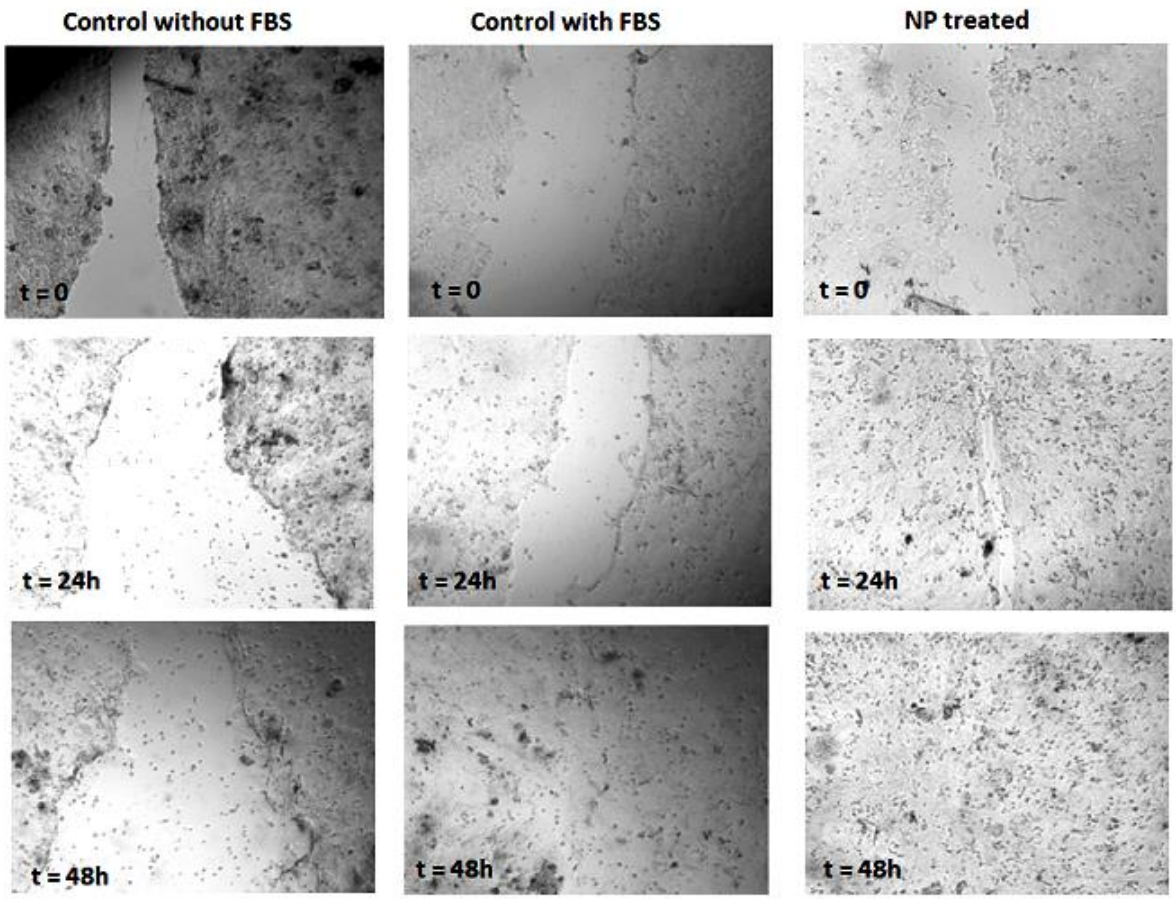

Figure 30. Effect of NP on migration of keratinocytes at different incubation times (0, 24 and 48 h) (values represented as mean (n = 3) and with error bar representing standard deviation).

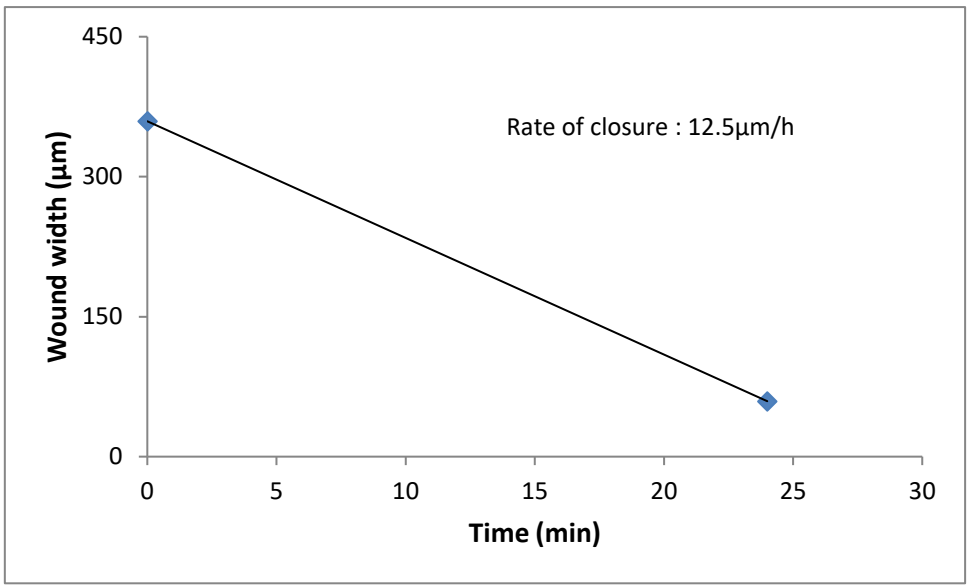

Figure 31. A scatter plot was used to display the width of the wound over time and the rate of wound closure in the presence of NP 3 mg/mL was calculated. To generate the r^2 value, a linear regression was run on the wound width data.

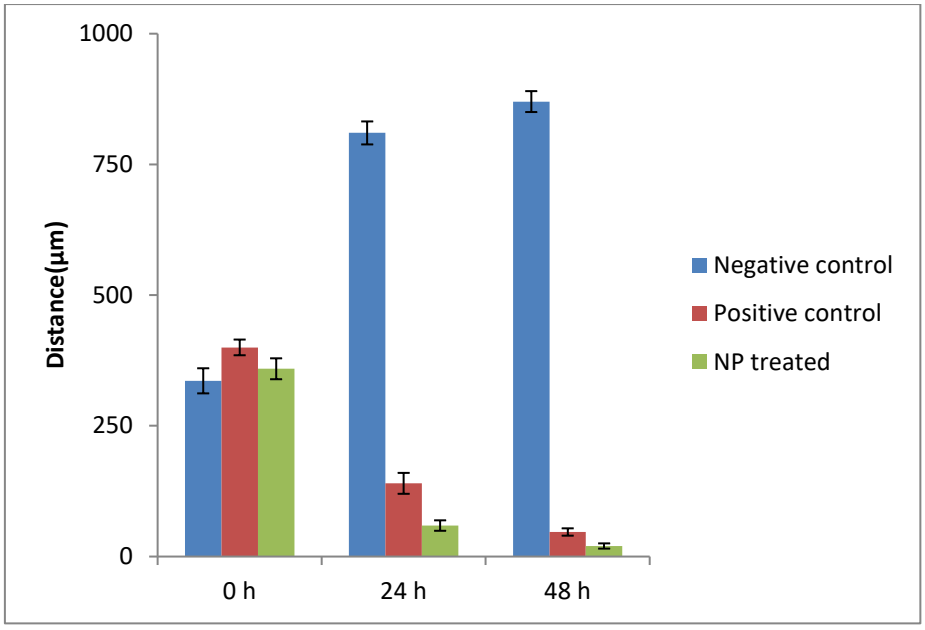

Figure 32. Quantitative analysis of wound healing for cell cultures incubated with positive control (FBS), negative control (without FBS), and NP treated (values represented as mean (n = 3) and with error bar representing standard deviation).

4.1.3 Blood clotting index

The first layer applied on wound must be protective and not inhibit blood coagulation. The blood clotting index of pure NP and of film composition containing HPC+NP and film of pure HPC were evaluated on whole human blood by a clotting experiment. PTFE and an insoluble NP were used as substrates and medical gauze as control. Human whole blood was allowed to contact with all the substrates used and then an amount of Ca^{2+} ion was added to promote coagulation. Then, the RBCs not trapped in clots were haemolysed by adding 25 mL of ultrapure water. The absorbance at 540 nm is related to the concentration of haemoglobin passed in solution from lysed free RBCs: a lower BCI value indicates a better blood clotting capability. BCI values of insoluble NP, NP coating the insoluble NP used as substrate and of the medical gauze were 0.03±0.014, 0.18±0.07 and 0.10±0.009, respectively. From Fig. 33, it is clear that NP has not a negative effect on blood clotting, while HPC inhibits blood clotting 3 times more than the medical gauze.

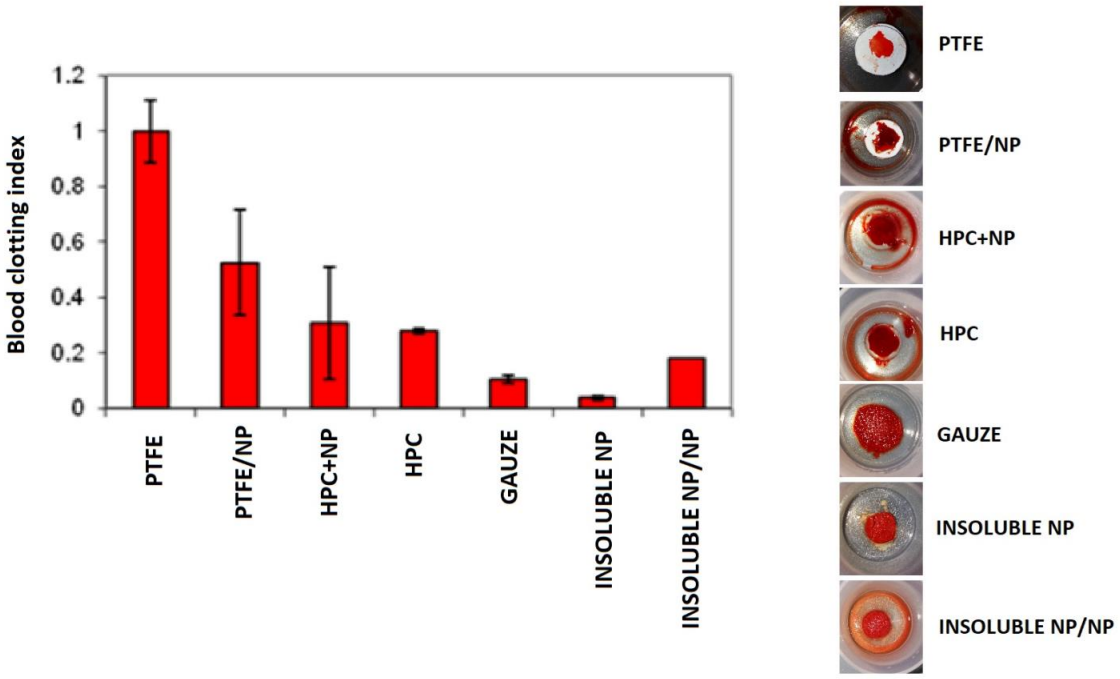

Figure 33. Blood clotting index. PTFE/NP denotes NP deposited on PTFE, Insoluble NP/NP denotes NP deposited on insoluble NP (values represented as mean (n = 3) and with error bar representing standard deviation).

These biological tests confirmed the anti-inflammatory and wound healing properties of NP. As said, after the biological tests, the selected best candidate from the preliminary study (HPC G) was combined with different biopolymers and was investigated for further properties.

4.2 Formulation study of first layer

The morphological characteristics of monolayer films produced are listed in Table VII.

Table VII. Physical characteristics of monolayer films.

Monolayer film	Thickness (mm)*	Weight (mg)*
HPC G	0.057 ± 0.012	25.6 ± 0.5
COLL PEP 3K + HPC G	0.052 ± 0.008	26.1 ±1.0
COLL PEP 5K + HPC G	0.058 ± 0.010	25.7 ± 1.2
NP + HPC G	0.053 ± 0.006	26.2 ± 1.1
GEL A + HPC G	0.055 ± 0.009	25.9 ± 0.7
GEL B + HPC G	0.060 ± 0.010	25.5 ± 0.4

*values represented as mean ± S.D. (n = 5)

4.2.1 Surface morphology

The feasibility and film forming nature of film formers with biopolymers in different ratios was tested by optical microscopy to confirm surface texture and homogeneity. It was evident that HPC G polymer maintained its film-forming property when ≥50% collagen peptide was added, but its mechanical properties were weak as cracks and surface roughness can be seen in the relevant microscopic images (Fig. 34). Hence, a mixture of HPC/collagen peptide 3K (70% / 30%) ratio was used for further studies.

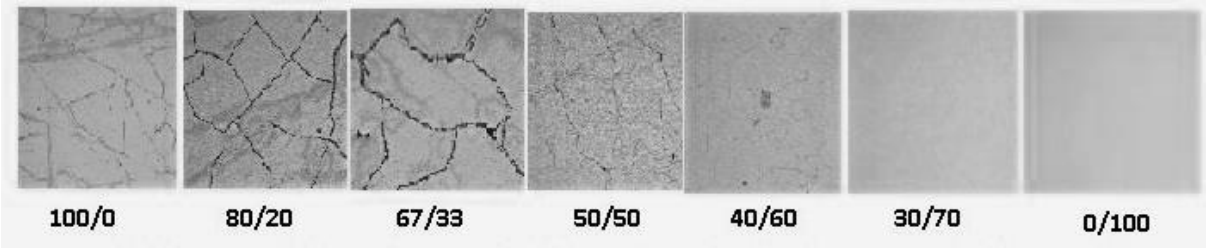

Figure 34. Surface morphology of films with different ratio of % collagen peptide / % HPC G.

4.2.2 Adhesive behavior

Figures 35-36 report the adhesive properties of the HPC polymer combined with different biopolymers. It was evident that the addition of NP had no negative effect on the detachment force of HPC (p>0.05) (Fig. 35) and, furthermore, increased the total work of adhesion. Whereas, other biopolymers seem to have a tendential negative effect on maximum detachment force of the HPC polymer and no considerable effect on total work (p>0.05) (Fig. 36), apart from gelatin A, which increased the adhesive energy of pure HPC.

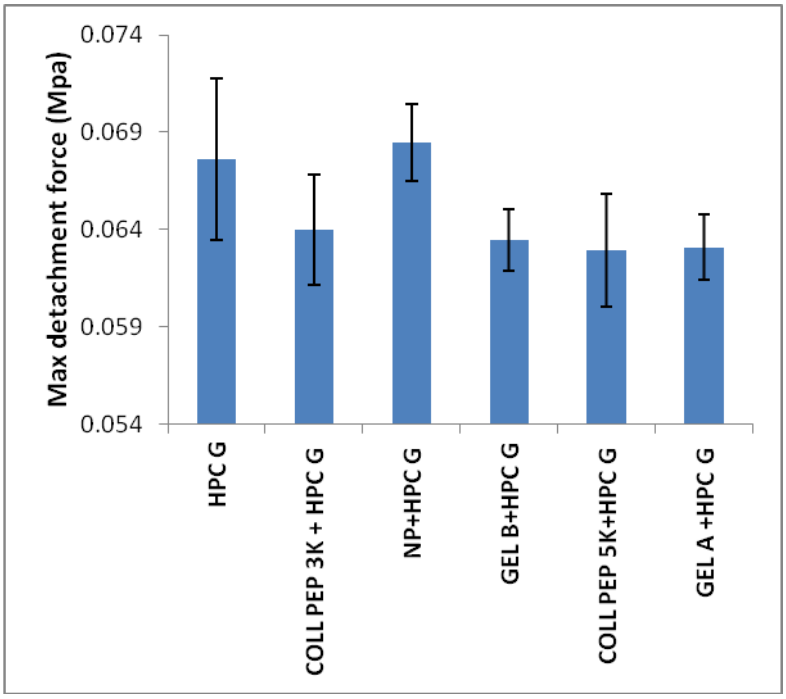

Figure 35. Adhesion properties of prepared films: maximum detachment force (MPa) of HPC and biopolymer mixtures tested on mucin tablet (values represented as mean (n = 3) and with error bar representing standard deviation).

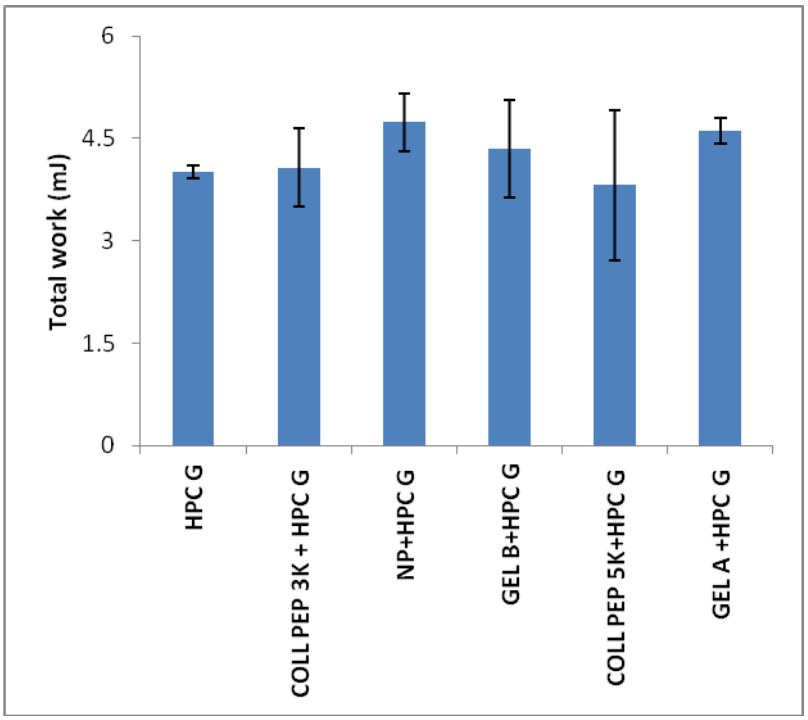

Figure 36. Adhesion properties of prepared films: work of adhesion (mJ) of HPC and biopolymer mixtures tested on mucin tablet (values represented as mean (n = 3) and with error bar representing standard deviation).

4.2.3 Mechanical properties

Mechanical properties of prepared films are shown in Figs. 37-39. From Fig. 37 it can be observed that the addition of collagen peptide 3k, collagen peptide 5k and NP to HPC had a negative effect on the yield strength, while gelatin type A and B did not show any significant effect.

The addition of biopolymers increased the rigidity of the HPC based film as shown in Figure 38 and confirmed by the clear reduction of the elongation at break of these films (Fig. 39).

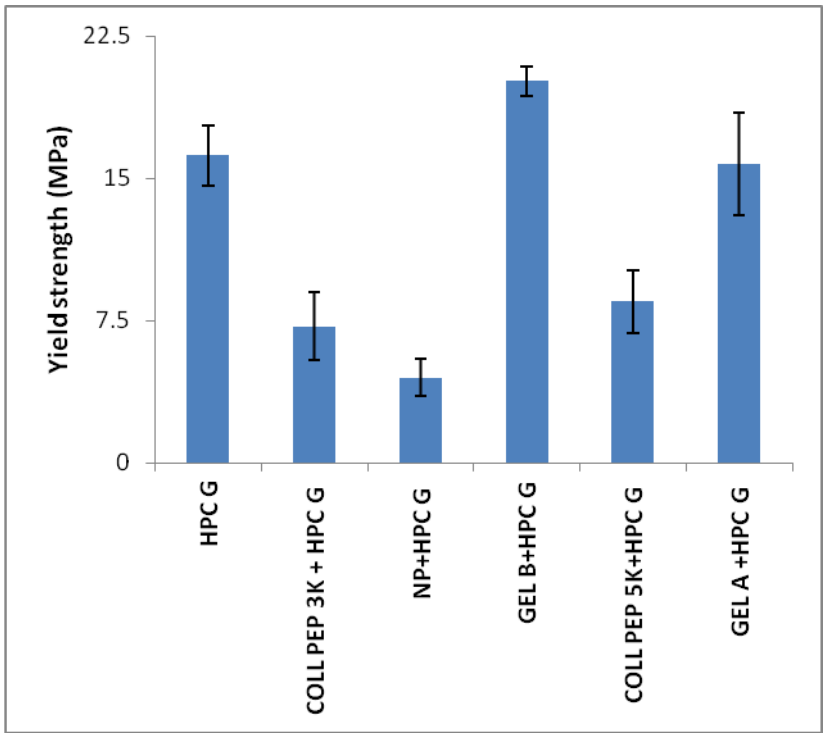

Figure 37. Mechanical properties of prepared films: yield strength (MPa) tested on material testing machine (values represented as mean (n = 3) and with error bar representing standard deviation).

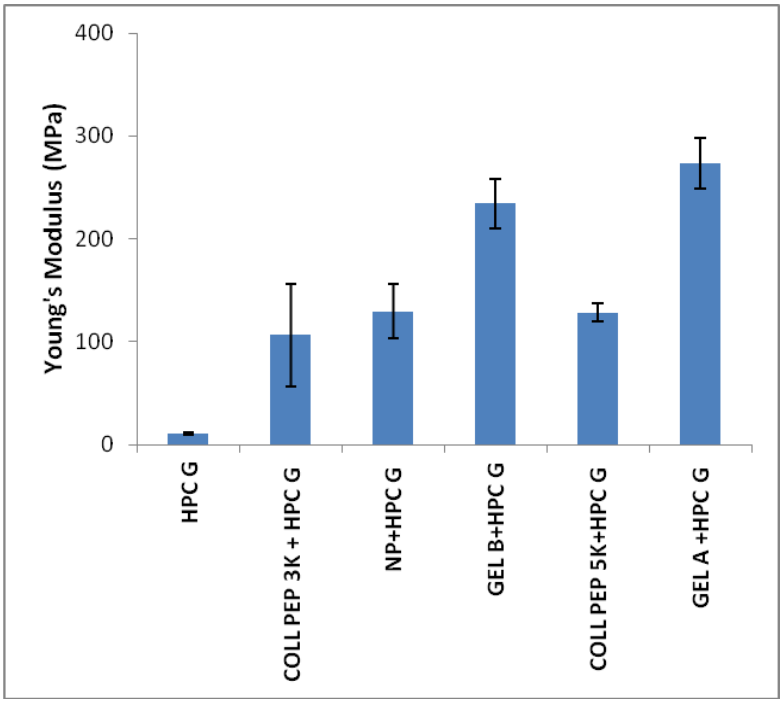

Figure 38. Mechanical properties of prepared films: Young's modulus (MPa) tested on material testing machine (values represented as mean (n = 3) and with error bar representing standard deviation).

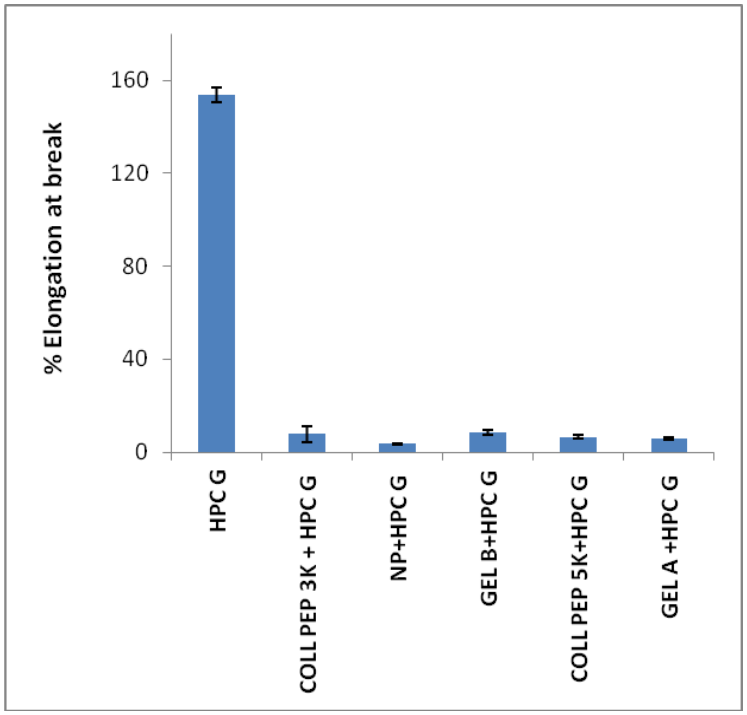

Figure 39. Mechanical properties of prepared films: elongation at break (%) tested on material testing machine (values represented as mean (n = 3) and with error bar representing standard deviation).

4.2.3 Swelling and erosion properties

The addition of the considered biopolymers had not a significant effect on the swelling behaviour of the HPC-based films (Fig. 40). On the other hand, the erosion index (Fig. 41) increased in the presence of both grades of collagen peptides and NP (p<0.05). Conversely, gelatin type A and B slightly decreased the erosion compared to pure HPC film. The reduction in erosion might be due to the low solubility of gelatine at 37 °C.

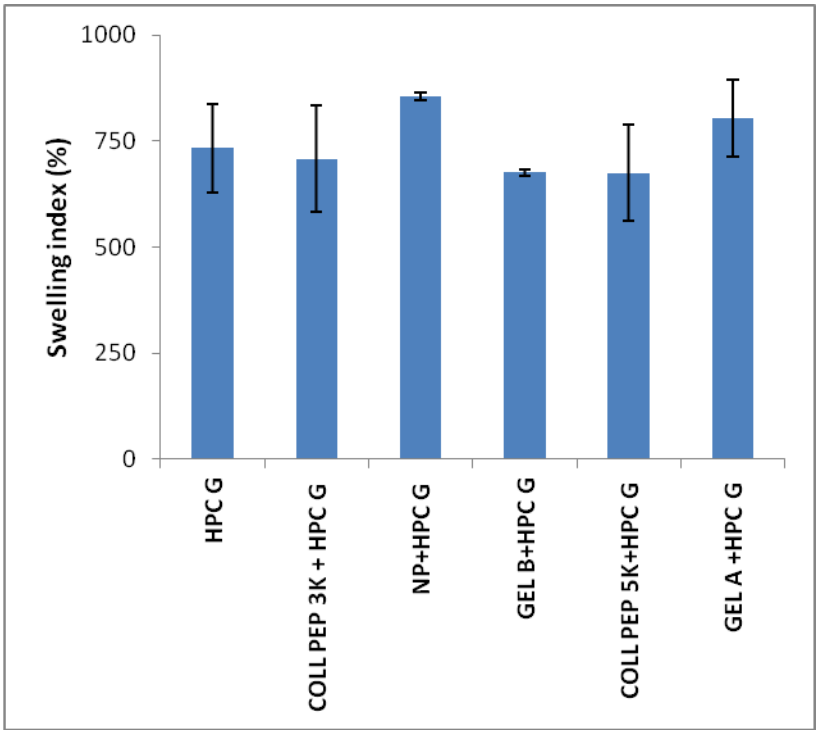

Figure 40. Swelling behavior of the prepared films tested in pH 6.8 phosphate buffer (values represented as mean (n = 3) and with error bar representing standard deviation).

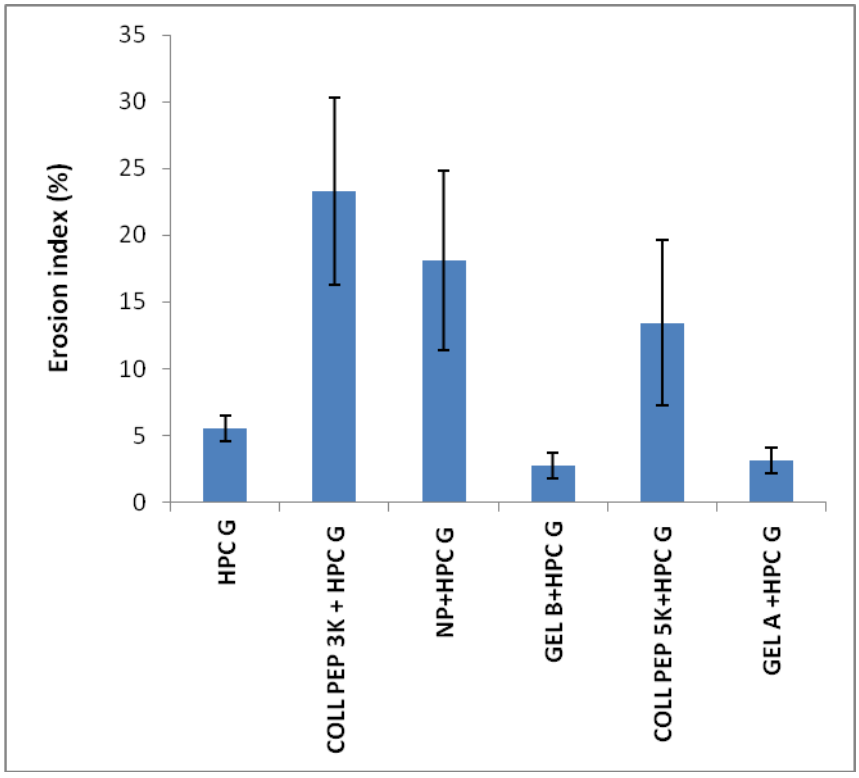

Figure 41. Erosion behavior of prepared films tested in pH 6.8 phosphate buffer (values represented as mean (n = 3) and with error bar representing standard deviation).

4.2.4 *Ex vivo* residence time

These films were tested for *ex vivo* residence time (Fig. 42) using porcine mucosa substrate in the apparatus described in Fig. 24. The pure HPC film showed the highest residence time equal to about 2 hours. The addition of biopolymers to HPC films led to a strong reduction in the residence time, with HPC+collagen peptide 5k having the lowest time measured, equal to only 2.2 minutes.

The films tested can be divided into 3 classes of behavior for residence time:

1) Over 60 min (HPC alone)
2) Between 30-60 min (HPC+collagen peptide 3k, HPC+NP, HPC+geatin A, HPC+gelatin B)
3) Below 30 min (HPC+collagen peptide 5k)

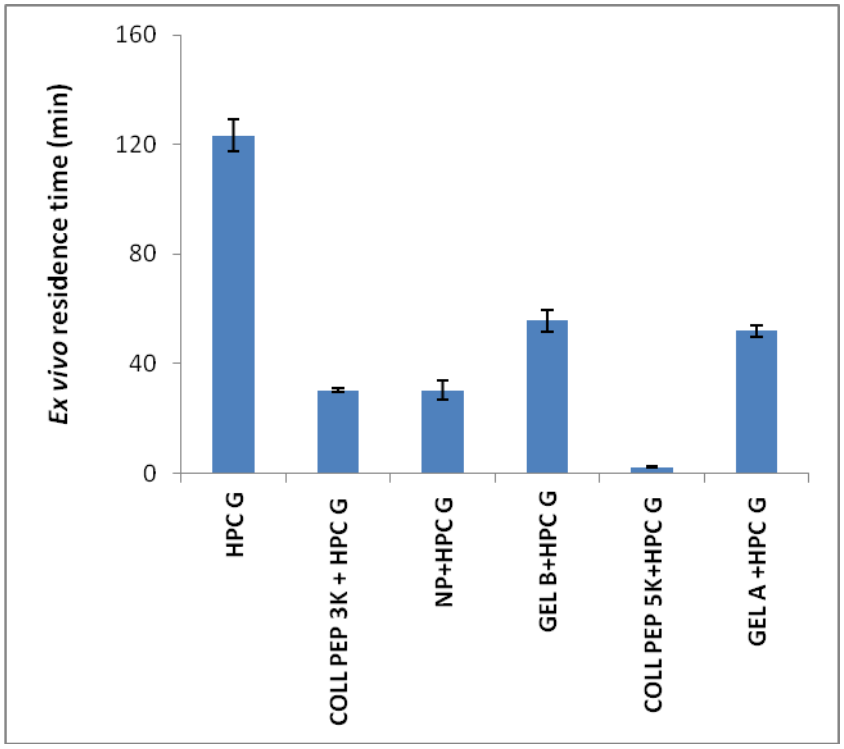

Figure 42. *Ex vivo* residence time of the prepared films tested using porcine mucosa as a substrate (values represented as mean (n = 3) and with error bar representing standard deviation).

The experiment was replied using a HPC layer as a support of the previous mixtures, observing a net increase of the residence time (Fig. 43). Notably, for the HPC+NP/HPC film residence time increased to 180 min. Furthermore, the addition of the model drug chlorhexidine digluconate (CHX) increased the residence time further to 410 min. This effect could be explained considering the possible electrical interaction between mucin (anionic) and the drug (cationic).

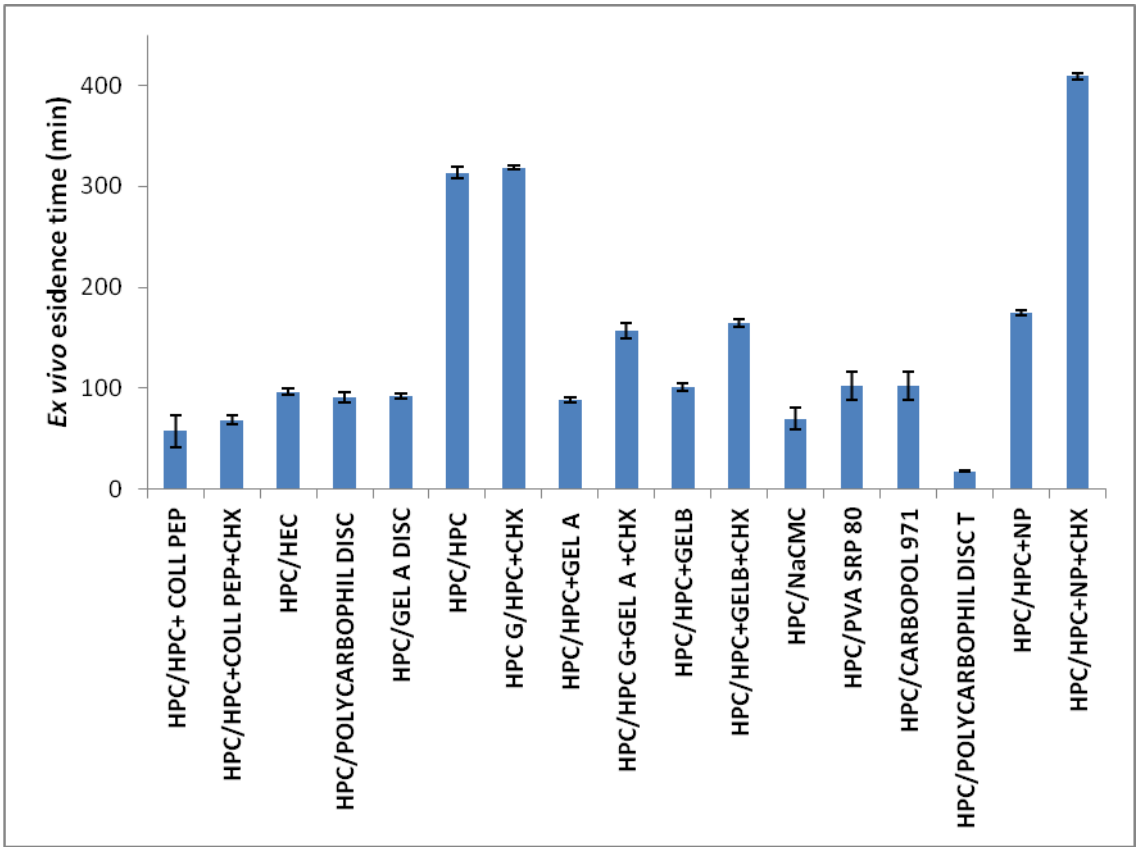

Figure 43. *Ex vivo* residence time of the prepared films containing HPC as back support tested using porcine mucosa (values represented as mean (n = 3) and with error bar representing standard deviation).

5. Selection of supporting layer

From the studies performed on the first layer it was evident that NP did notshow any negative effect on adhesion, but it weakened the mechanical properties of the HPC polymer.

Therefore, a support layer was required for giving texture to the entire multilayer structure.

To this aim, polymer combinations of HPC and those polymers that gave rigid films when used alone were studied: HPC+gelatin A, HPC+gelatin B, HPC+pectin, HPC+sodium alginate, HPC+NaCMC were tested as a second or support layer, with the aim to enhance the mechanical properties.

5.1 Formulation study of second layer

The physical characteristics of bilayers are listed in Table VIII.

Table VIII. Physical characteristics of bilayer films.

Bilayer film composition		Thickness (mm)*	Weight (mg)*
First layer	**Second layer**		
HPC+ NP	HPC+GELA	0.118 ± 0.018	51.8 ± 1.1
HPC+ NP	HPC+GELB	0.116 ± 0.018	52.2 ± 0.4
HPC+ NP	HPC+Pectin	0.124 ± 0.021	51.4 ± 1.3
HPC+NP	HPC+Sodium alginate	0.112 ± 0.026	51.4 ± 1.3
HPC+ NP	HPC+NaCMC	0.116 ± 0.011	51.9 ± 1.1
HPC+ NP	HPC	0.110 ± 0.007	51.9 ± 1.1

*values represented as mean ± S.D. (n = 3)

5.1.1 Mechanical properties

In Figures 44-48 the mechanical properties of the bilayer films tested are reported.

The yield strength (Fig. 44) of the films containing HPC+pectin, HPC+sodium alginate and HPC+NaCMC was slightly increased, in comparison with the other films tested, but these films were too rigid: in fact, films with HPC+GELA, HPC+GELB showed higher elasticity (Fig. 45) with respect to the aforementioned combinations. HPC+GELA was slightly more elastic and had higher yield strength if compared to HPC+GELB.

Due to their elastic nature, elongation at break (Fig. 46) was higher for films containing HPC+GELA, HPC+GELB, while HPC+pectin, HPC+sodium alginate and HPC+NaCMC support based films had low elongation.

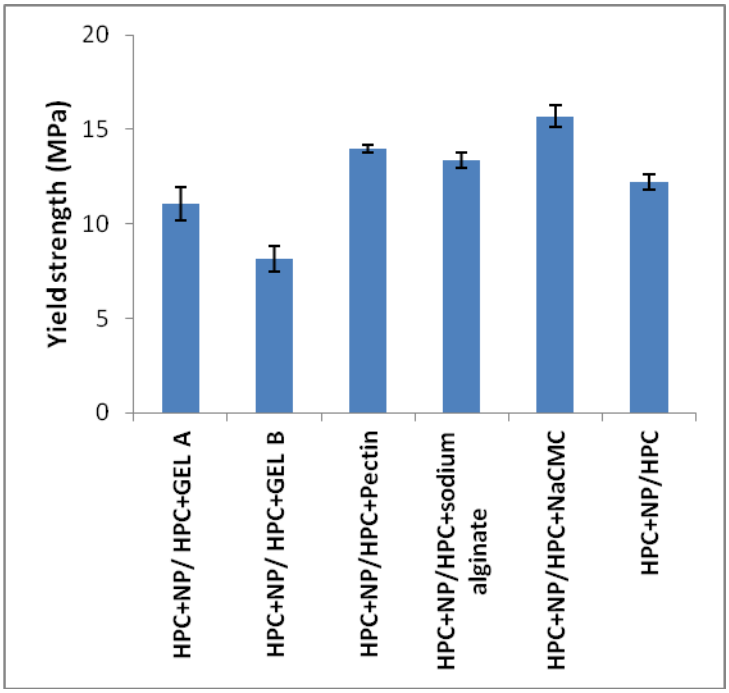

Figure 44. Mechanical properties of prepared films: yield strength (MPa) tested on material testing machine (values represented as mean (n = 3) and with error bar representing standard deviation).

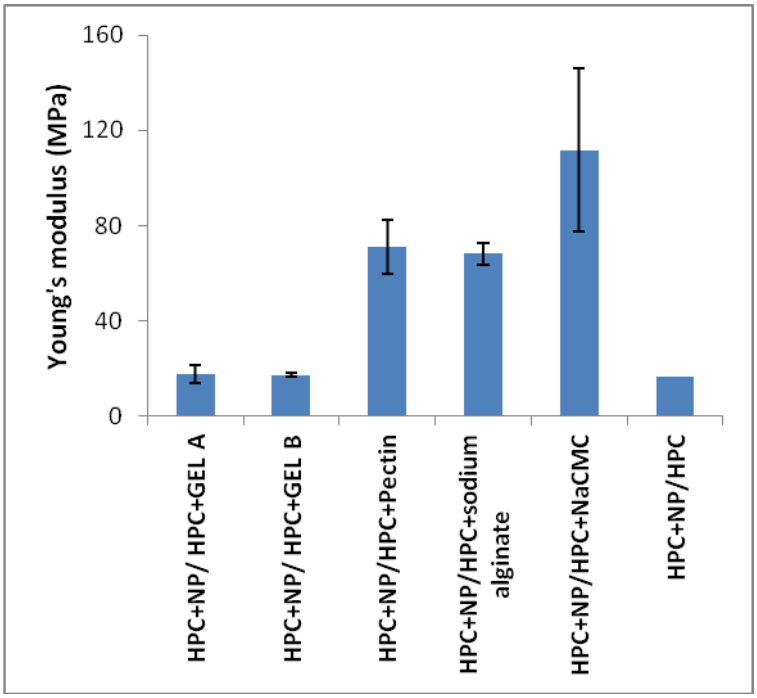

Figure 45. Mechanical properties of prepared films: Young's modulus (MPa) tested on material testing machine (values represented as mean (n = 3) and with error bar representing standard deviation).

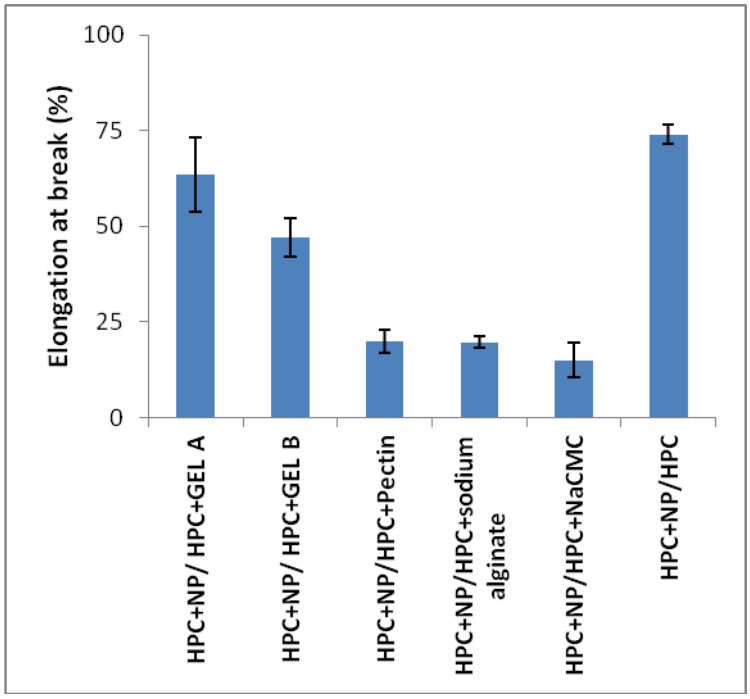

Figure 46. Mechanical properties of prepared films: elongation at break (%) tested on material testing machine (values represented as mean (n = 3) and with error bar representing standard deviation).

In addition, the results of puncture strength (Fig. 47) showed that the films with HPC+GELA, HPC+GEL B got ruptured at higher load compared to HPC+pectin, HPC+sodium alginate and HPC+NaCMC as support layer, and this behavior can be related to the elastic nature of these films (Fig. 48).

In the end, based on the results obtained from the previous study of mechanical properties, HPC+GEL A and HPC alone were selected as components for a potential supporting layer.

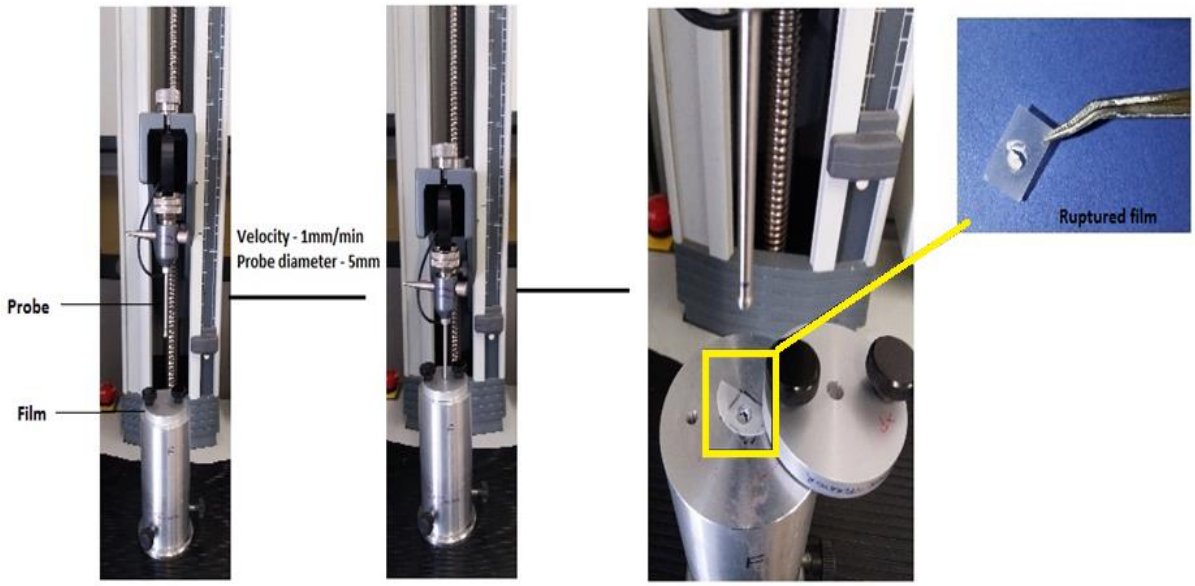

Figure 47. Puncture strength equipment using material testing machine.

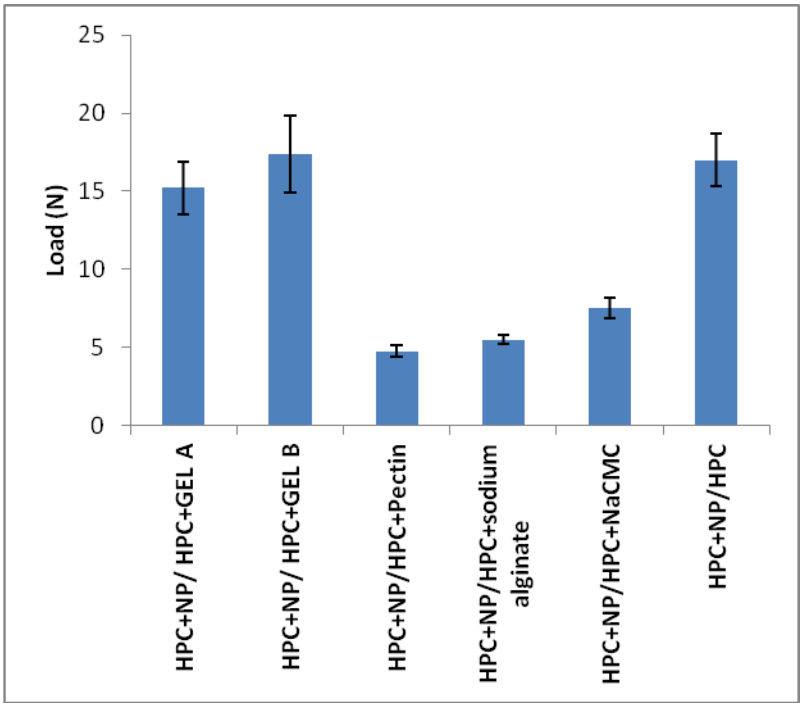

Figure 48. Mechanical properties of prepared films: puncture strength (N) tested on material testing machine using 5 mm probe (values represented as mean (n = 3) and with error bar representing standard deviation).

6. Selection of third layer

The third layer or backing layer was planned to control the release of antimicrobial drug .To this aim, for continuing the study we selected HPMC K750, HEC G and HPC alone, which are film-forming agents but also known for their ability to control the drug release.

The tested trilayer films were prepared by double casting method. The prepared films were evaluated for adhesion, mechanical, residence, swelling, erosion and *in vitro* drug release properties.

6.1 Formulation study of third layer

The morphological characteristics of trilayer films studied are listed in Table IX.

Table IX. Physical characteristics of trilayer films.

Trilayer composition			Thickness (mm)*	Weight (mg)*
Mucoadhesive layer	**Supporting layer**	**Backing Layer**		
HPC (70%)+NP(30%)	HPC(100%)	HPC(100%)	0.164 ± 0.013	75.6 ± 1.34
HPC (70%)+NP(30%)	HPC(70%)+GELA(30%)	HPC(50%)+HEC(50%)	0.166 ±0.011	75.4 ± 0.90
HPC (70%)+NP(30%)	HPC(70%)+GELA(30%)	HPC(50%)+HPMC(50%)	0.162 ±0.008	75.2 ± 0.59

*values represented as mean ± S.D. (n = 5)

6.1.1 *In vitro* adhesion properties

Figures 49-53 show *in vitro* adhesion properties of the prepared trilayer films on mucin substrate.

The results of max detachment force (Fig. 49) show that there is a slight increase in adhesion in films containing HPMC and HEC as third layer compared to films with HPC alone as third layer. However, the difference is not significant ($p>0.05$).

Even in the case of total work (Fig. 50), peak work (Fig. 51) and work of adhesion (Fig. 52) there is no significant difference ($p>0.05$) among the prepared trilayer films, when three different kinds of polymers were used in the third layers.

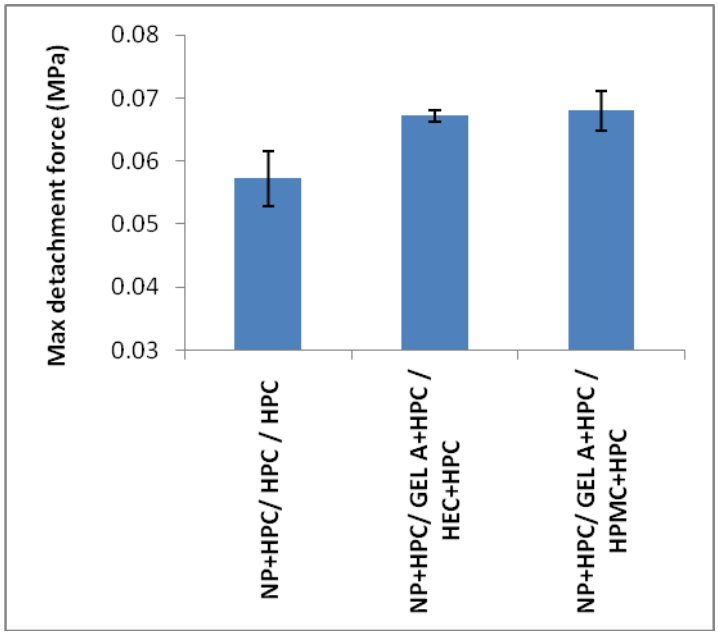

Figure 49. Adhesion properties of prepared films: maximum detachment force (MPa) of a trilayer film tested on mucin tablet (values represented as mean (n = 3) and with error bar representing standard deviation).

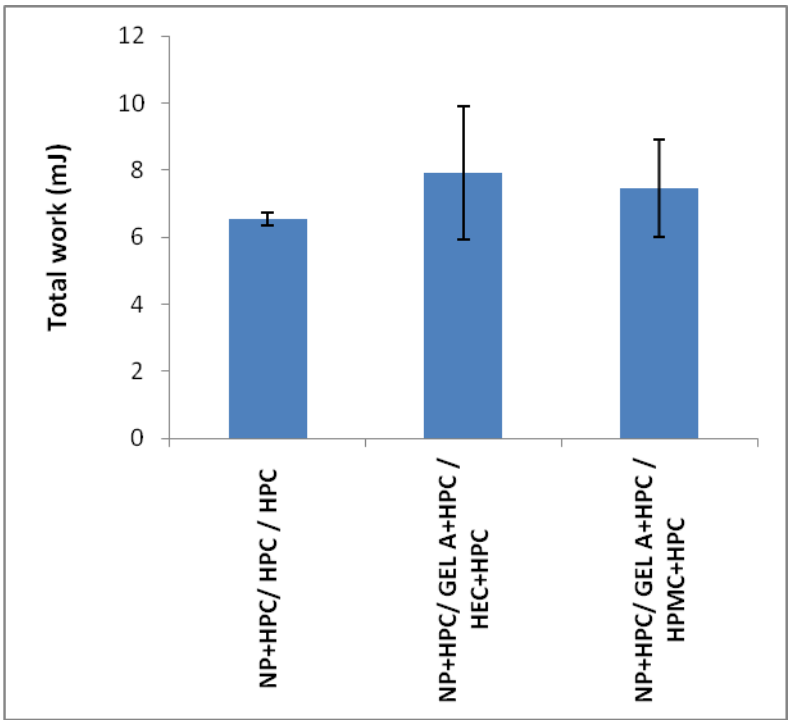

Figure 50. Adhesion properties of prepared films: total work (mJ) of trilayer films tested on mucin tablet (values represented as mean (n = 3) and with error bar representing standard deviation).

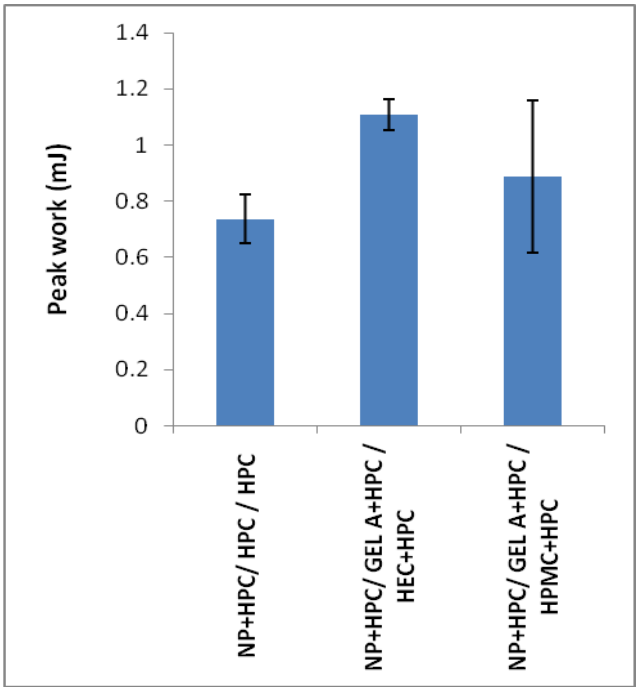

Figure 51. Adhesion properties of prepared films: peak work (mJ) of trilayer films tested on mucin tablet (values represented as mean (n = 3) and with error bar representing standard deviation).

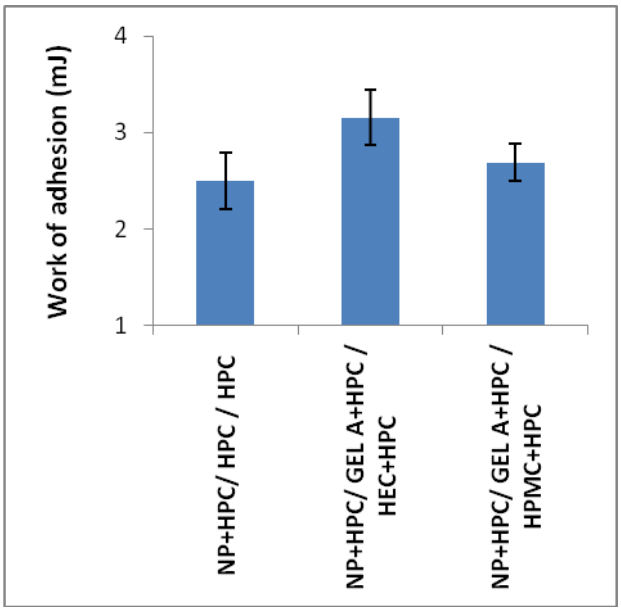

Figure 52. Adhesion properties of prepared films: work of adhesion (mJ) of trilayer films tested on mucin tablet (values represented as mean (n = 3) and with error bar representing standard deviation).

6.1.2 *Ex vivo* mucoadhesion studies

Three different kinds of biological substrates were used for *ex vivo* mucoadhesion study (Fig. 53): porcine buccal mucosa, which mimics the human buccal tissue, the inverted chicken skin, which mimics the undermucosa tissue, and bovine liver to simulate the bleeding wound condition.

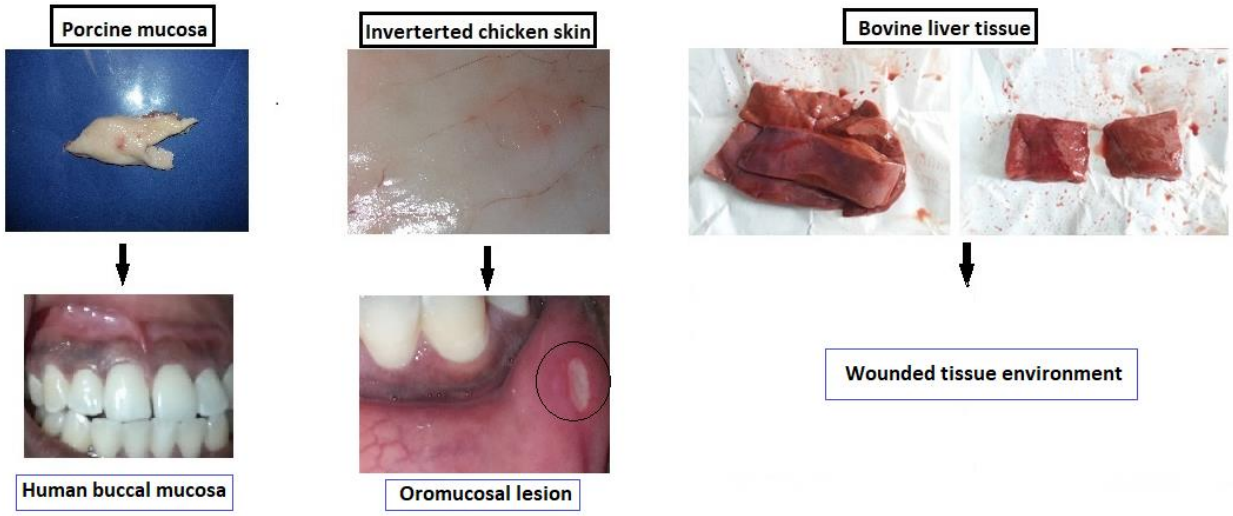

Figure 53. Schematic representation of biological substrates used for *ex vivo* mucoadhesion study.

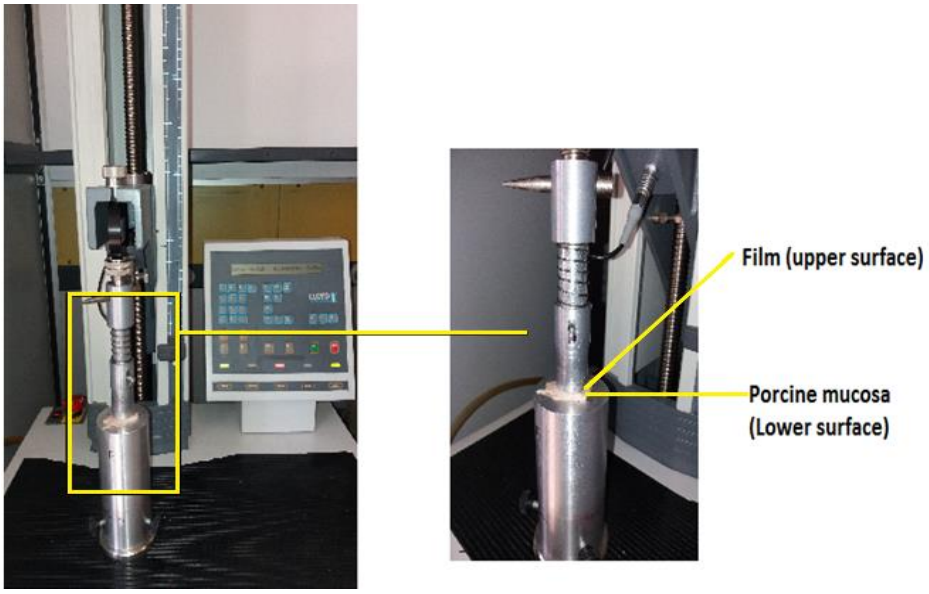

Figure 54. Equipment for *ex vivo* mucoadhesion test performed using porcine mucosa as biological substrate.

The results of *ex vivo* mucoadhesion study on porcine mucosa (Fig. 54) show that the maximum detachment force (Fig. 55) increased for films containing HPC+HEC as third layer compared to other trilayer films; on the contrary, for total work (Fig. 56) there were no considerable differences.

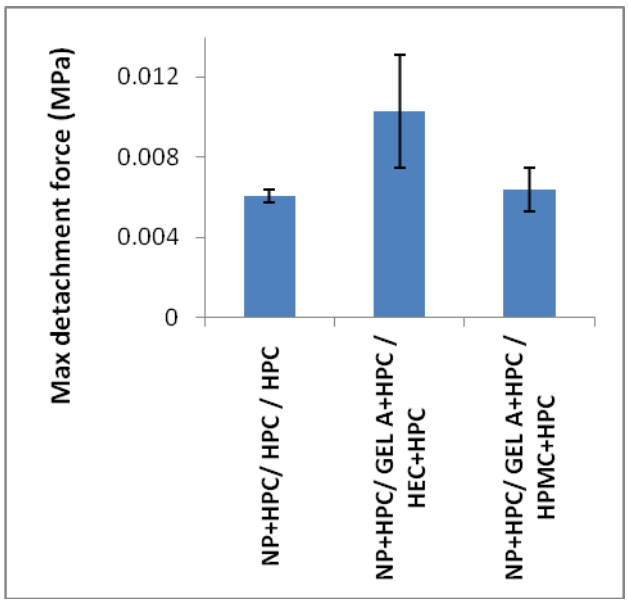

Figure 55. Adhesion properties of prepared films: maximum detachment force (MPa) of trilayer films tested on porcine mucosa (values represented as mean (n = 3) and with error bar representing standard deviation).

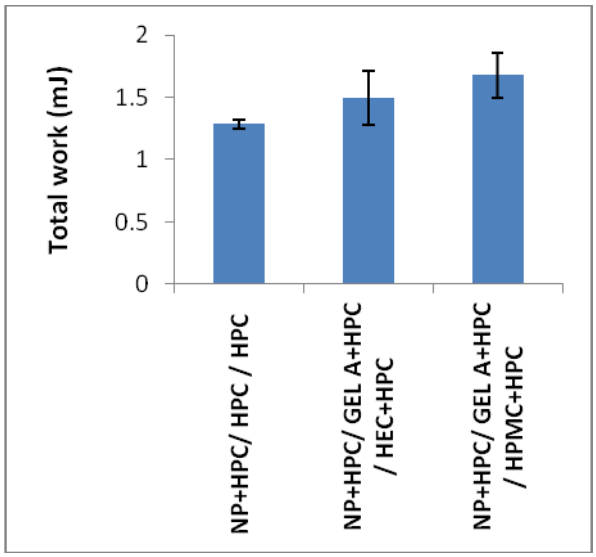

Figure 56. Adhesion properties of prepared films: total work (mJ) of trilayer films tested on porcine mucosa (values represented as mean (n = 3) and with error bar representing standard deviation).

Secondly, *ex vivo* mucoadhesion was tested on inverted chicken skin as biological substrate (Fig. 57).

Figure 57. Equipment for *ex vivo* mucoadhesion tested on inverted chicken skin as biological substrate.

On inverted chicken skin the results showed that the maximum detachment force (Fig. 58) was slightly increased in films containing HPC+HEC as the third layer. Whereas, for total work (Fig. 59), no considerable differences were observed among the films tested.

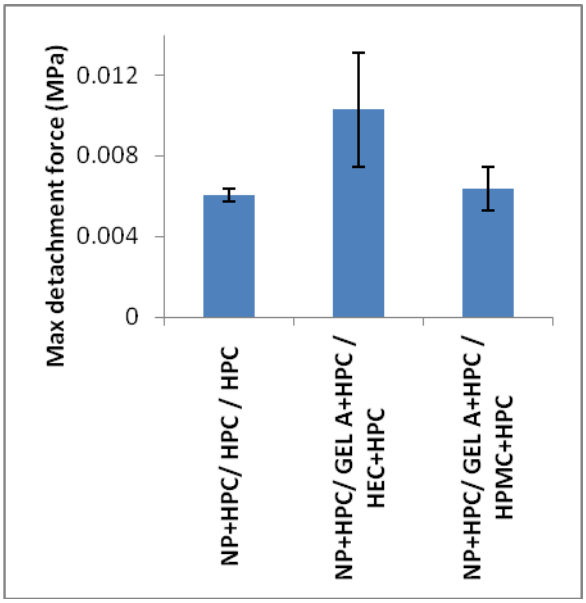

Figure 58. Adhesion properties of prepared films: max detachment force (MPa) of trilayer films tested on inverted chicken skin (values represented as mean (n = 3) and with error bar representing standard deviation).

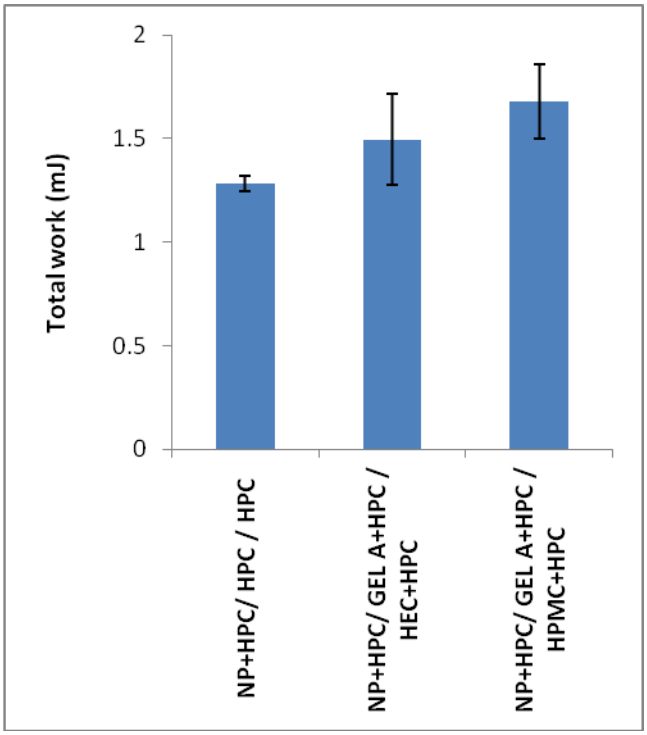

Figure 59. Adhesion properties of prepared films: total work (mJ) of trilayer films tested on inverted chicken skin (values represented as mean (n = 3) and with error bar representing standard deviation).

Finally, *ex vivo* adhesion was tested on liver tissue to simulate the wounded environment (Fig. 60).

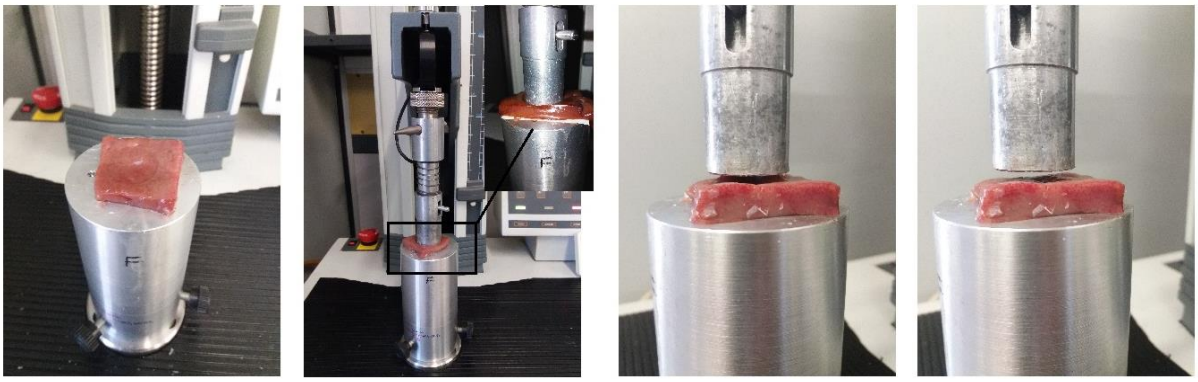

Figure 60. Equipment for *ex vivo* mucoadhesion tested on bovine liver tissue as biological substrate.

The results demonstrate that among the prepared trilayer films tested, maximum detachment force (Fig. 61) and total work (Fig. 62) were not significantly different. But comparing, the results on the three biological substrate the maximum detachment force were relatively low when tested on liver tissue.

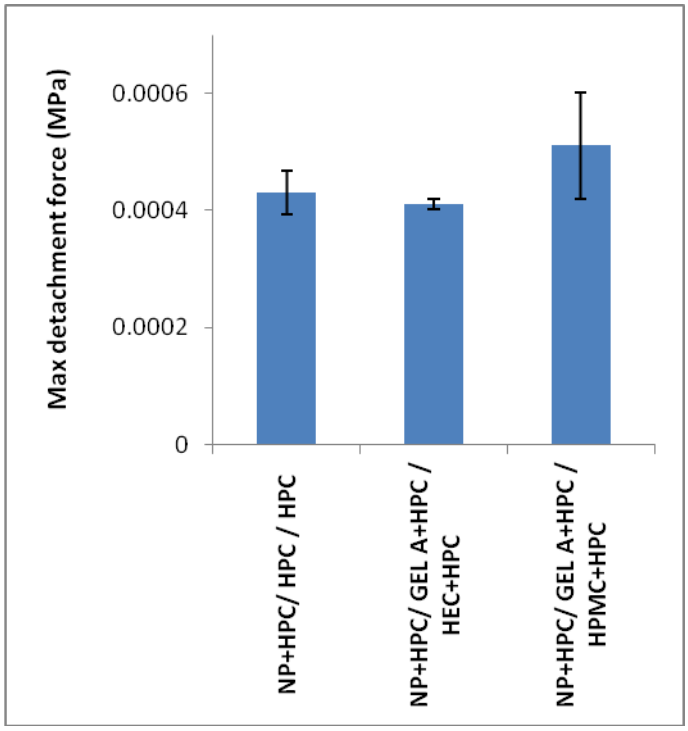

Figure 61. Adhesion properties of prepared films: maximum detachment force (MPa) of trilayer films tested on bovine liver tissue (values represented as mean (n = 3) and with error bar representing standard deviation).

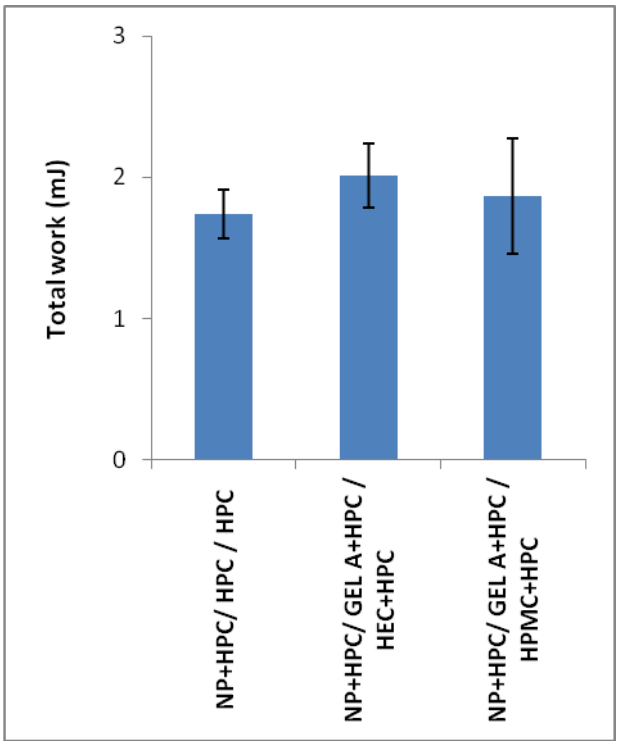

Figure 62. Adhesion properties of prepared films: total work (mJ) of trilayer films tested on bovine liver tissue (values represented as mean (n = 3) and with error bar representing standard deviation).

6.1.3 Mechanical properties

The tensile mechanical resistance of the trilayer films studied showed that there was no significant difference (p>0.05) in yield strength (Fig. 63).

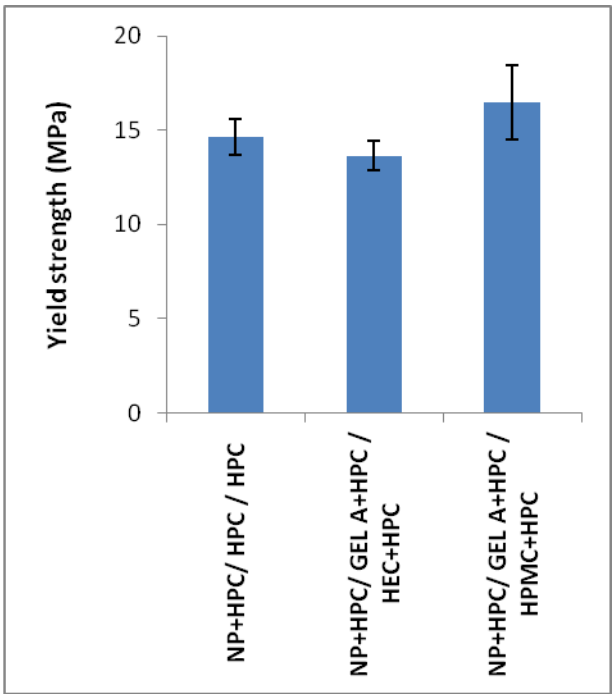

Figure 63. Mechanical properties of prepared trilayer films: yield strength (MPa) tested on material testing machine (values represented as mean (n = 3) and with error bar representing standard deviation).

Whereas, films containing HPC alone and HPC+HEC in the third layer were more elastic (Fig. 64) than films containing HPC+HPMC in the third layer (p<0.05).

As for the elongation at break (Fig. 65), it was relatively low and significantly different (p<0.05) for films containing HPC+HEC or HPC+HPMC in the third layer. The addition of HEC and HPMC to third layer, and the addition of GELA to the second layer, significantly reduced the elongation of these films.

In addition, puncture strength (Fig. 66) was relatively low significantly different (p<0.05) for films containing HPC+HEC or HPC+HPMC in the third layer.

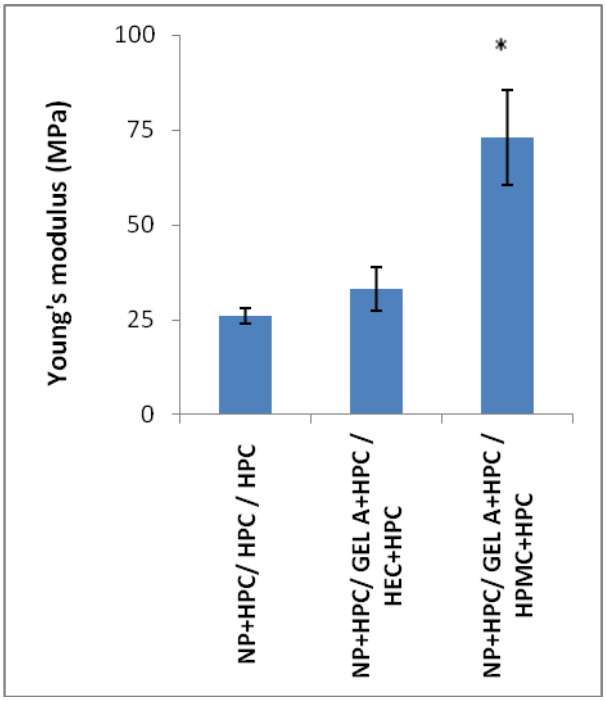

Figure 64. Mechanical properties of prepared trilayer films: Young's modulus (MPa) tested on material testing machine (values represented as mean (n = 3) and with error bar representing standard deviation). Films with HPC alone in the third layer were set as control. The symbol (*) denotes statistical significance from the control group (p<0.05).

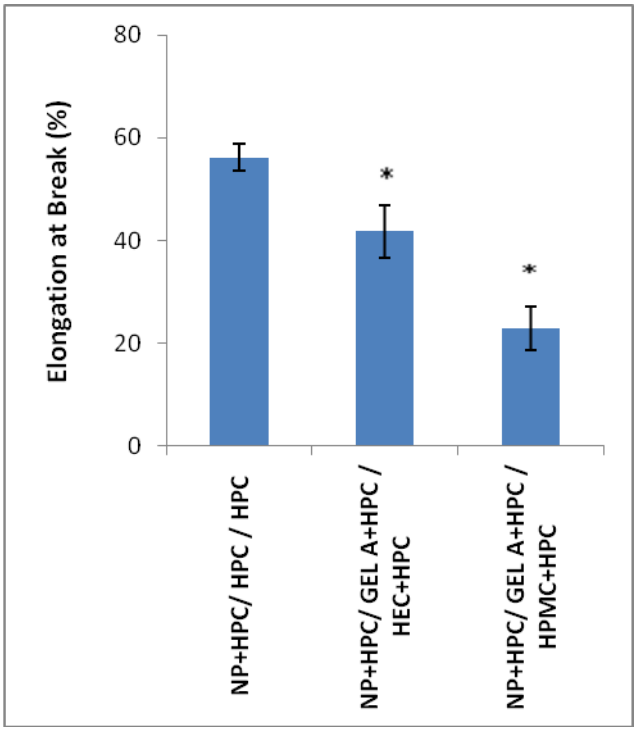

Figure 65. Mechanical properties of prepared films: elongation at break (%) tested on material testing machine (values represented as mean (n = 3) and with error bar representing

standard deviation). Films with HPC alone in the third layer were set as control. The symbol (*) denotes statistical significance from the control group (p<0.05).

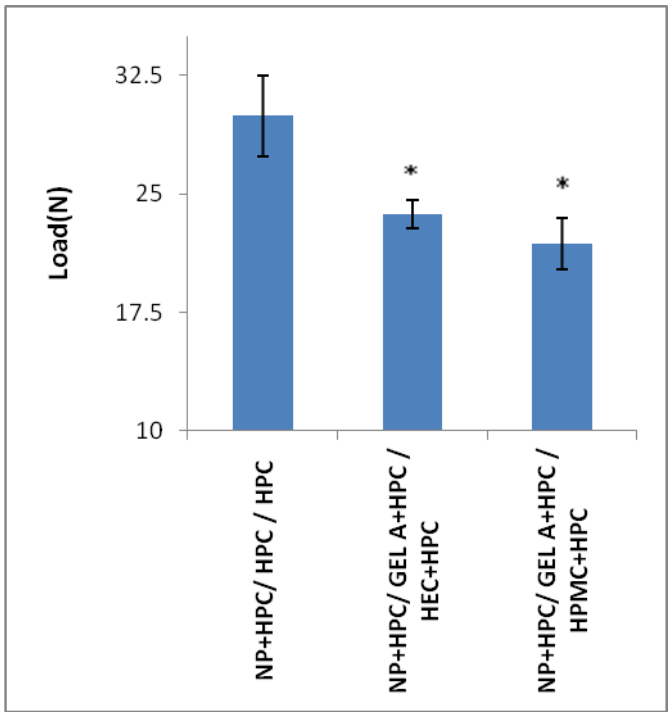

Figure 66. Mechanical properties of prepared trilayer films: puncture strength (N) tested on material testing machine (values represented as mean (n = 3) and with error bar representing standard deviation). Films with HPC alone in the third layer were set as control. The symbol (*) denotes statistical significance from the control group (p<0.05).

6.1.4 Measurement of *in ex vivo* residence time

The *ex vivo* residence time was measured using porcine mucosa and a modified compendial disintegration apparatus. The results obtained are presented in Table X.

Table X *Ex vivo* residence time of the trilayer films tested on porcine mucosa.

Formulation	*Ex vivo* residence time (min)*
NP+HPC/ HPC / HPC	289 ± 9.64
NP+HPC/ GEL A+HPC / HEC+HPC	163 ± 2.65
NP+HPC/ GEL A+HPC / HPMC+HPC	221 ± 3.61

*values represented as mean ± S.D. (n = 3)

6.1.5 Measurement of *in vivo* residence time

In vivo residence time for all the formulations was determined in healthy human volunteers and the results are presented in Figure 67. No volunteer felt heaviness of the buccal patch at the place of attachment because of the moderate thickness (0.15 mm) and light weight (75 mg) of the patch.

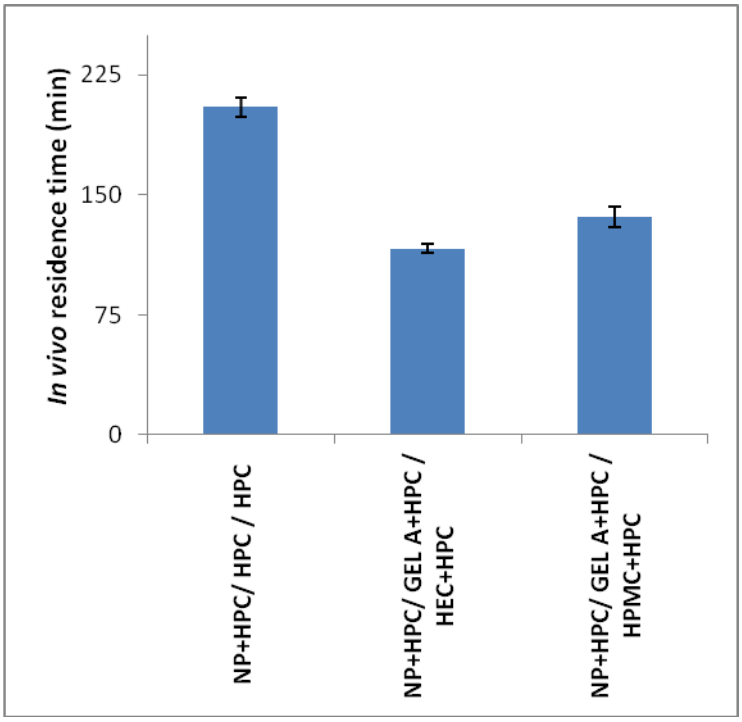

Figure 67. *In vivo* residence time of the trilayer films tested in healthy volunteers (values represented as mean (n = 3) and with error bar representing standard deviation).

6.1.6 Swelling and erosion index

The swelling properties of the prepared films were measured in pH 6.8 phosphate buffer solution. The determination of the swelling properties of the prepared films was extremely difficult, because the gelled films were very fragile, making their recovery from the Petri dish and weighing impossible. A method consisting in removing the excess of liquid around the swollen film directly in the weighing container was then adopted.

The films exhibited a high degree of swelling (Fig. 68), while still maintaining their structural integrity for a reasonable time period. The degree of swelling increased with time. The higher swelling values (1612±115 %) were obtained from films containing HPMC+HPC as the third layer.

Erosion index (Fig. 69) was calculated by drying the swollen film in an oven. The films showing higher swelling index had higher erosion index, although their erosion index was

low in the beginning. On the whole, the erosion index was low in the case of films containing HPC alone as the third layer.

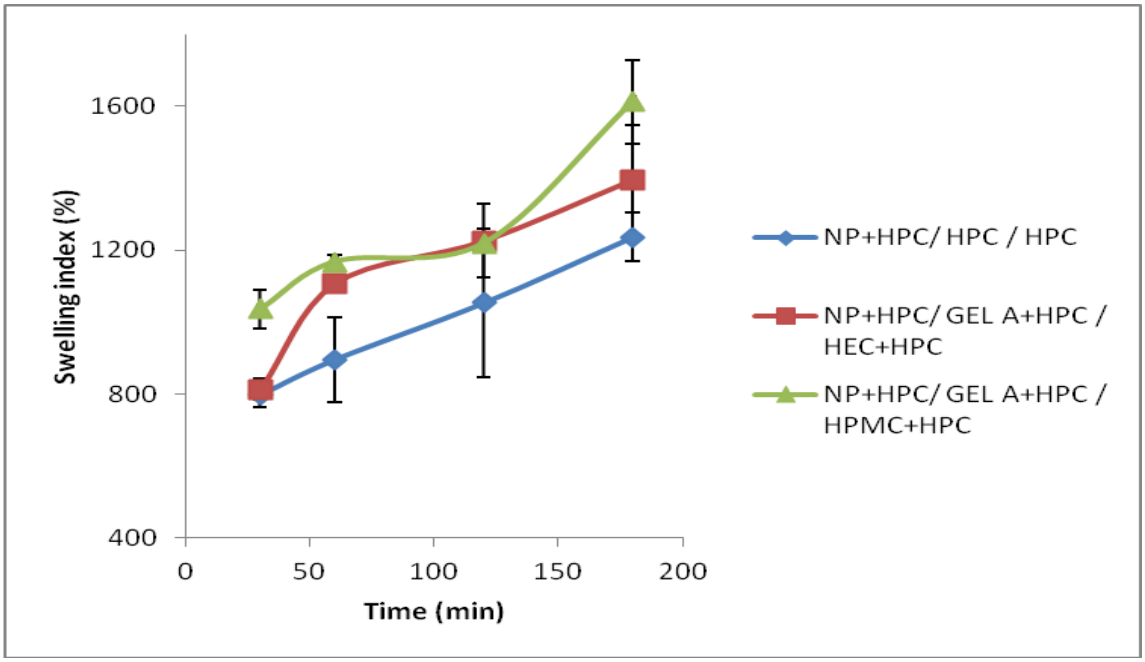

Figure 68. Swelling behavior of the prepared trilayer films tested in pH 6.8 phosphate buffer (values represented as mean (n = 3) and with error bar representing standard deviation).

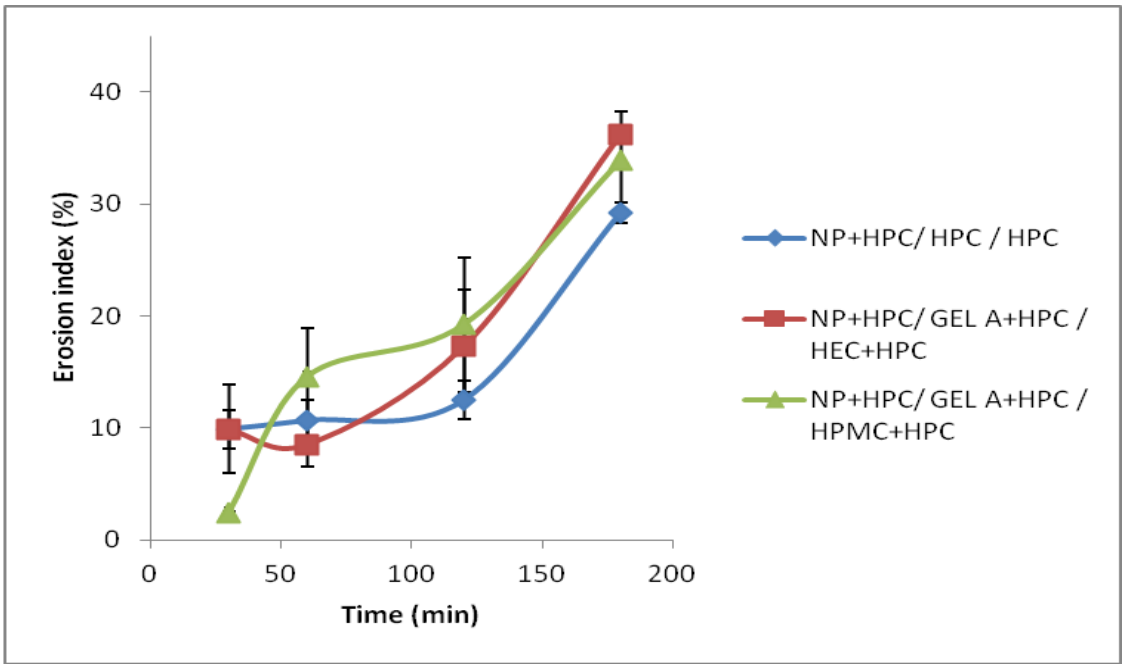

Figure 69. Erosion behavior of the prepared trilayer films tested in pH 6.8 phosphate buffer (values represented as mean (n = 3) and with error bar representing standard deviation).

6.1.7 *In vitro* drug release study

A homemade device was used to study the *in vitro* drug release profile from HPMC and HEC based trilayer films (Fig. 70) and the theoretical weights and percentage weights of each individual layer in trilayer films are reported in Fig. 71. This study was performed using 5 mL and 10 mL of simulated saliva as the dissolution medium.

The release of CHX from HPC+NP/HPC+GELA/HPC+HPMC films in 5 mL dissolution medium is shown in Fig. 72. The mean percentage of drug released was 39.3±0.9 % at the end of the test (after 6 h, Fig. 73), corresponding to 1.780±0.040 mg of the drug (Fig. 74). The drug released at 6 h was slightly less than the amount released at 5 h (46.16±0.65 %). This behaviour could be due to the second layer swelling, generating a temporary reduction of drug concentration in the medium, justifiable by a specific hydrodynamic condition. In fact, when the volume of the dissolution medium was increased to 10 mL, the curve showed only a brief stop in the drug release. The 10 mL release profile (Fig. 73) showed a higher percentage of drug released at 6 h (48.5±3.9 %, corresponding to 2.170±0.150 mg of the drug) than the release profile measured in 5 mL dissolution medium, and after 24 h the drug released was 90.7±3.5 % (Fig. 73). The reason for higher drug release at 6 h using 10 mL of release medium was due to higher percent of mass loss of films (23.63±3.21 %) compared to 5 mL release medium (18.9 ±0.79 %).

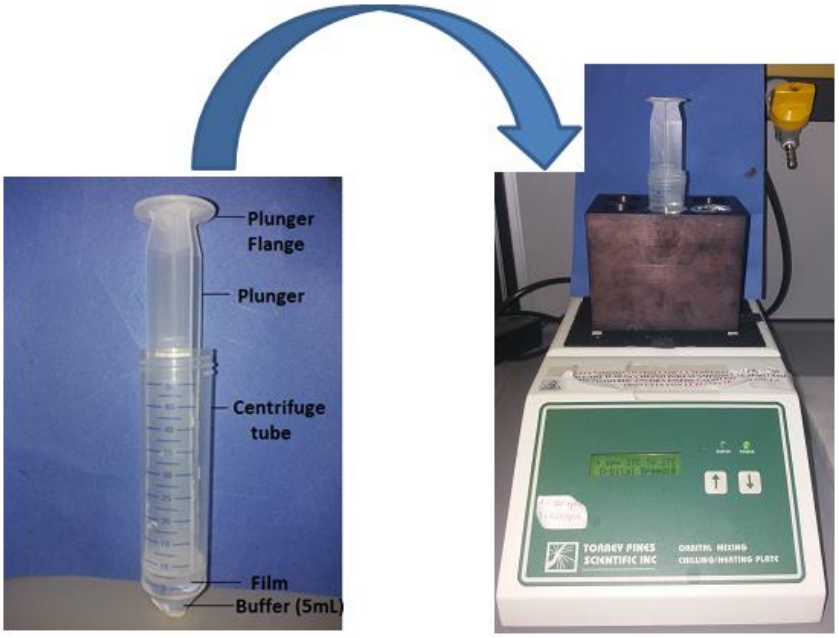

Figure 70. Homemade device based on a plunger for drug release study from a film.

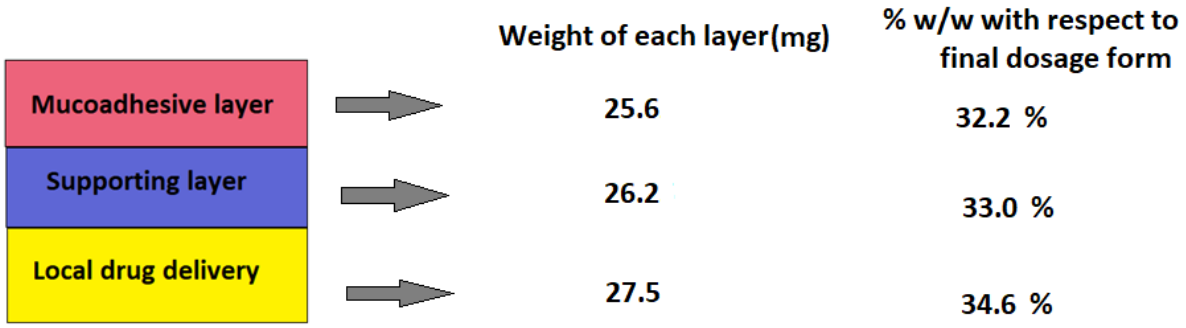

Figure 71. Representation of theoretical weights of each individual layer in a tri-layer film.

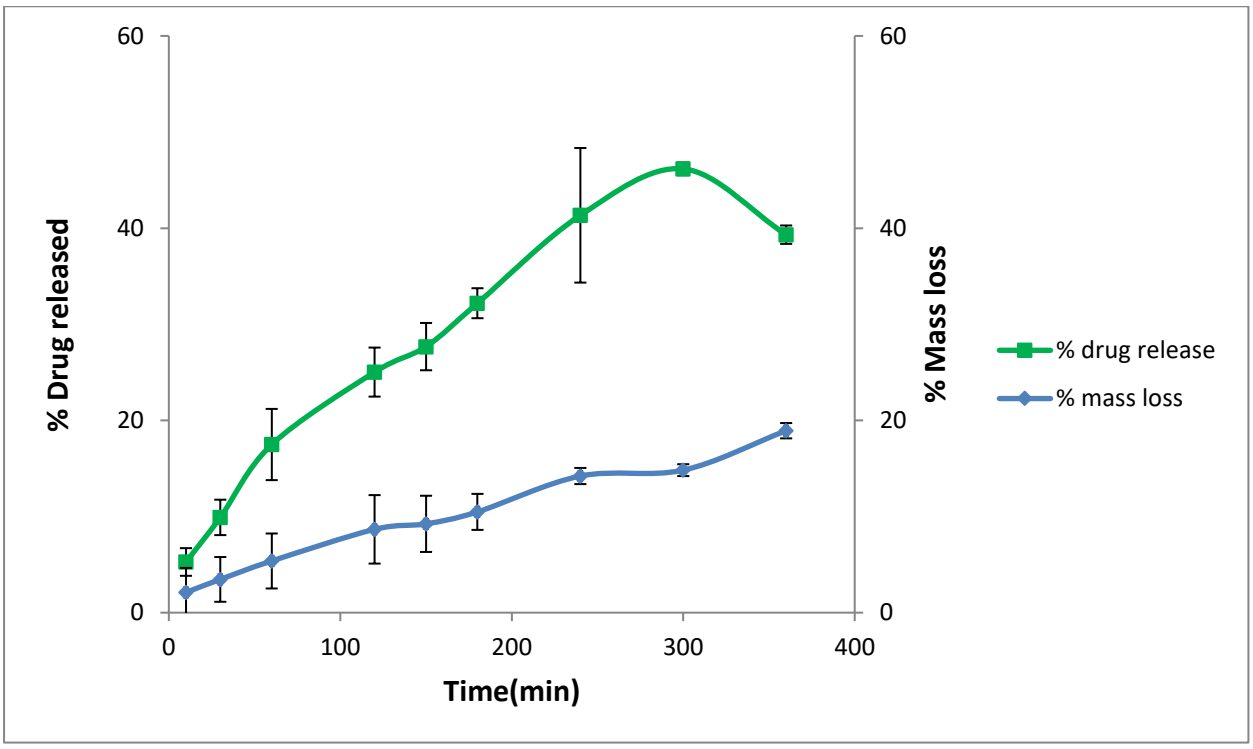

Figure 72. *In vitro* drug release and mass loss profile of the HPMC-based trilayer films tested in 5 mL of simulated saliva (values represented as mean (n = 3) and with error bar representing standard deviation).

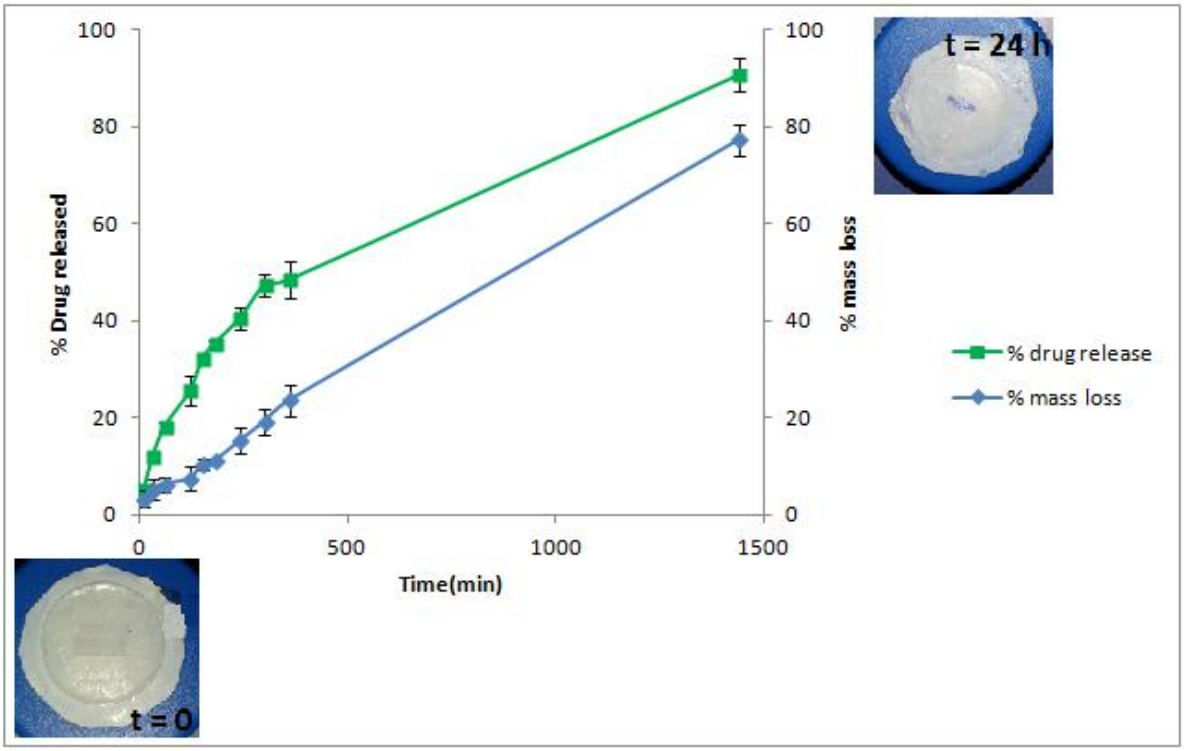

Figure 73. *In vitro* drug release and mass loss profile of the HPMC-based trilayer films tested in 10 mL of simulated saliva (values represented as mean (n = 3) and with error bar representing standard deviation).

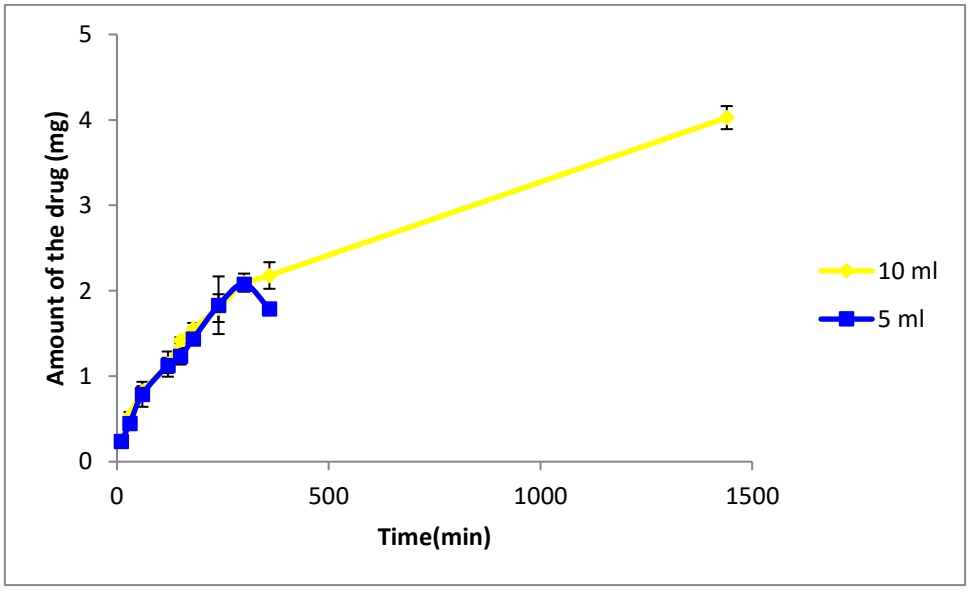

Figure 74. Profile of the amount of drug released from the HPMC-based trilayer films tested in 5 and 10 mL of simulated saliva (values represented as mean (n = 3) and with error bar representing standard deviation).

The CHX release from HPC+NP/HPC+GELA/HPC+HEC films is shown in Figs. 75 and 76. The profile of drug released using 5 mL of the release medium (Fig. 75) shows 37.6±3.8 % of drug released after 4 h, which is equivalent to 1.67±0.16 mg of the drug (Fig. 77). Then, a small decrease to 28.8±7.73 %, equivalent to 1.28±0.35 mg of CHX, was observed at 5 h. This, like in the previous case, may be attributed due to absorption of the drug from the dissolution medium in the empty swelled layer, hence the movement of diffusing drug was temporary reversed from dissolution medium towards the film. Unlike the previous release profile (Fig. 73), a similar behaviour was observed also when 10 mL of release medium were used (Fig. 76), but the decrease in the drug release was anticipated at 4 h (19.43±7.75 %, equivalent to 0.88±0.36 mg of CHX) in comparison to the 3 h time point (33.63±0.84 %). However, after 4 h the drug release progression was restored, and after 24 h the final drug release resulted to be 80.0±0.6 %. It has to be considered that after 6 h the amount of the drug released in 10 mL dissolution medium was higher (2.32±0.09 mg) with respect to 5 mL dissolution medium (1.94±0.34 mg, Fig. 77). It was also observed that the release behaviour was related to the mass loss of the film. Actually, in the release study performed using 10 mL release medium, the percent mass loss was 13.0±2 % at 4 h and 21.6±2.32 % at 5 h: this increase in mass loss from 4 h to 5 h can be related to the restoring of the drug release profile (45.19±2 % drug released after 5 h).

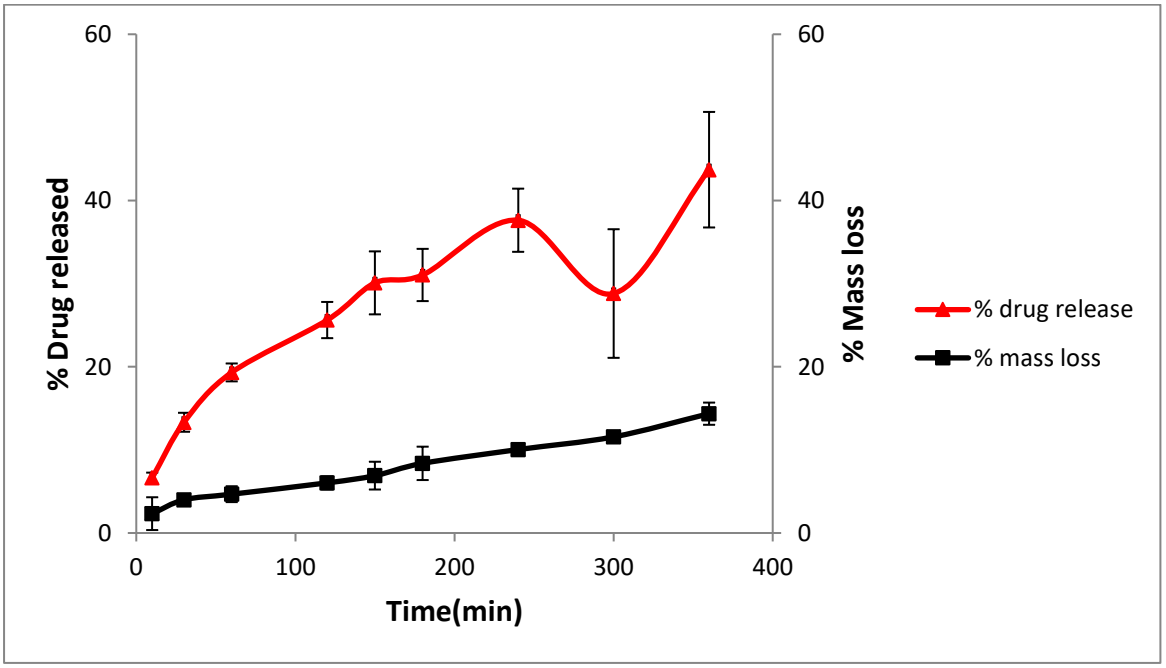

Figure 75. *In vitro* drug release and mass loss profile of the HEC-based trilayer films tested in 5 mL simulated saliva (values represented as mean (n = 3) and with error bar representing standard deviation).

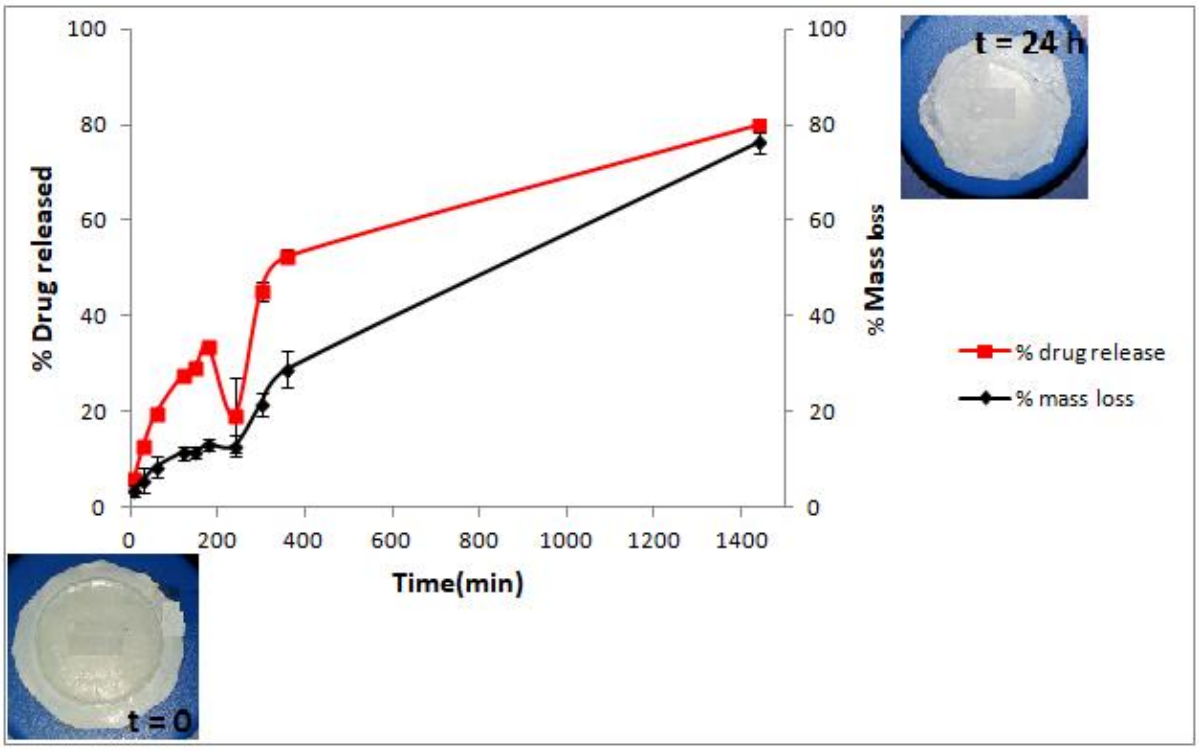

Figure 76. *In vitro* drug release profile of the HEC-based trilayer films tested in 10 mL simulated saliva (values represented as mean (n = 3) and with error bar representing standard deviation).

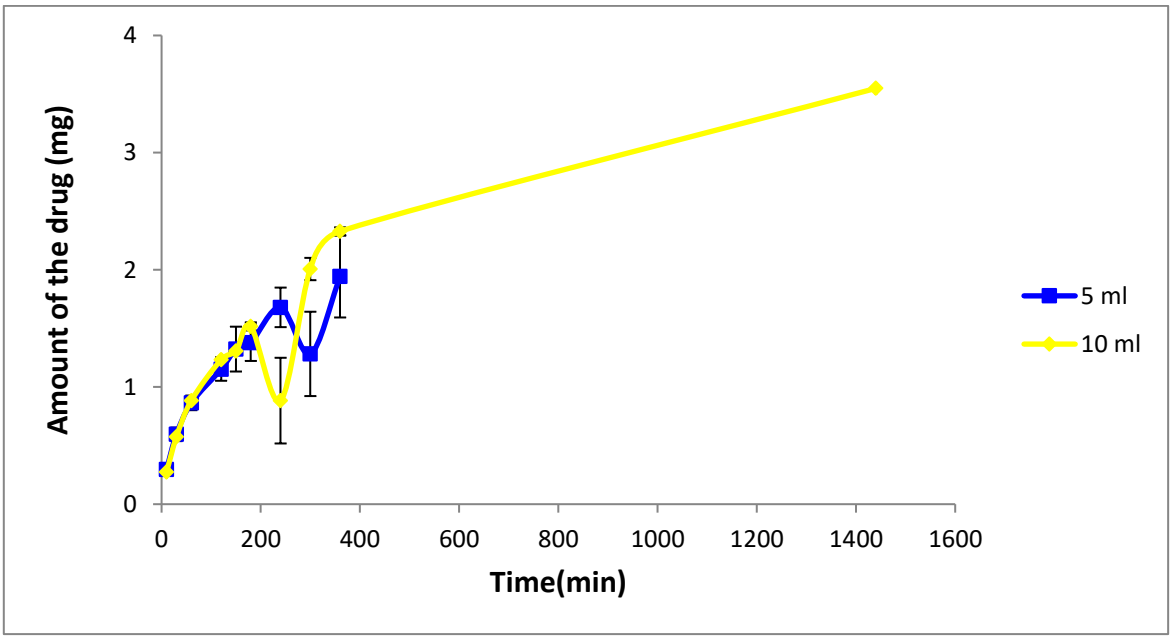

Figure 77. Profile of the amount of drug released from HEC-based trilayer films tested in 5 and 10 mL simulated saliva (values represented as mean (n = 3) and with error bar representing standard deviation).

Figures 78 and 79 show the comparative release profiles of HPMC- and HEC-based trilayer films in different volumes of the dissolution medium. Relatively, the percent drug release from the HEC-based films was higher in 5 mL (43.7±6.9 %) at 6 h and lower in 10 mL (80.0±0.6 %) dissolution medium at 24 h. Whereas, HPMC-based films showed percent drug release of 39.3±0.9 % in 5 mL at 6 h and 90.7±3.5 % in 10 mL dissolution medium at 24 h. The percent mass loss of HPMC- and HEC-based films at 6 h when 5 mL of dissolution medium was used were 18.9±0.79 % and 14.35±1.33 %, respectively. These values suggest that 15.01 mg of HPMC-based films and 11.38 mg of HEC-based-films have been eroded respectively. Whereas, when 10 mL release medium was used, the percent mass loss of HPMC- and HEC-based films at 24 h were 77.29±3.33 % and 76.22±2.21 %, these values corresponding to the erosion of 61.3±3.23 mg and 60.75±2.21 mg respectively. At the end of the dissolution, i.e. after 24 h, a portion of the film, that was supposed to be the first layer, was still attached to the flange (as shown in Figs. 74 and 76).

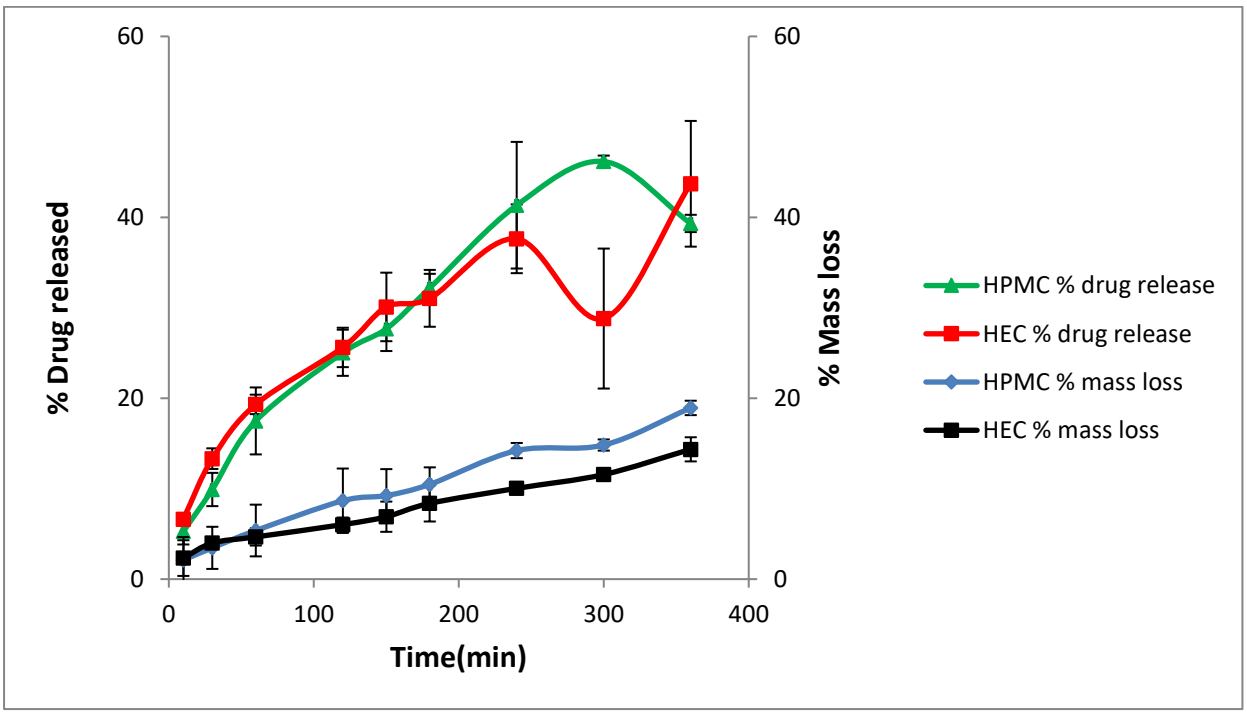

Figure 78. Comparison of *in vitro* drug release and mass loss profiles of the HPMC- and HEC-based trilayer films tested in 5 mL simulated saliva (values represented as mean (n = 3) and with error bar representing standard deviation).

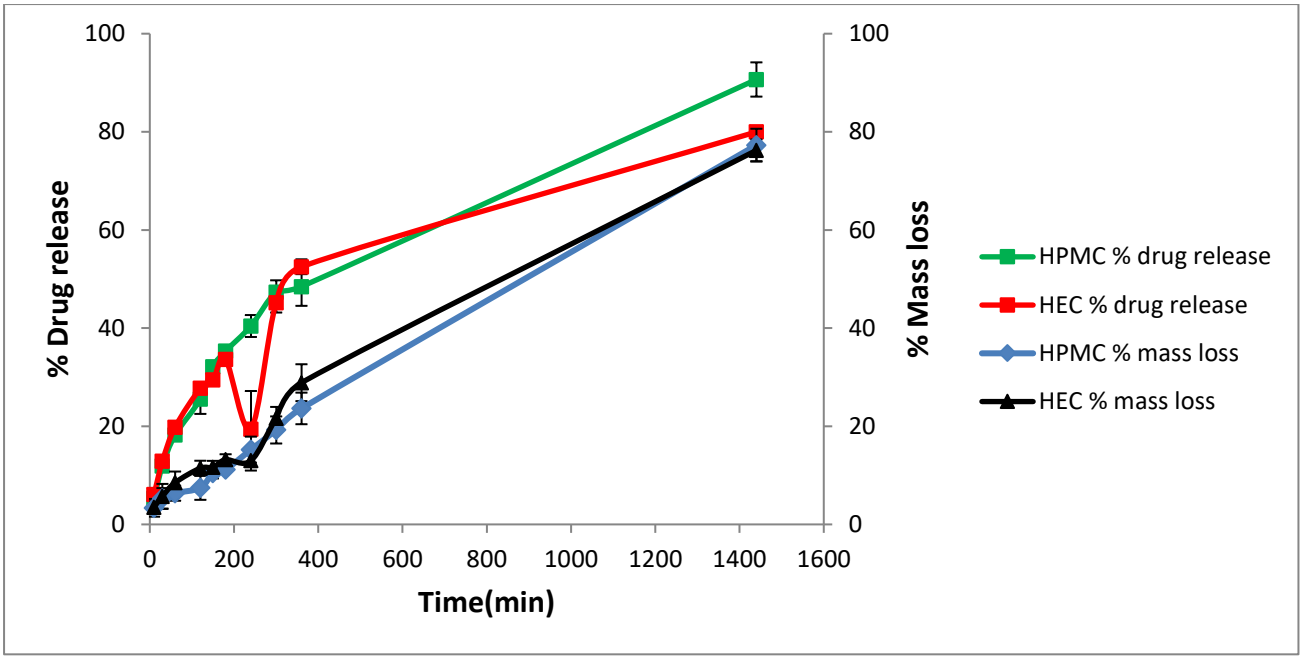

Figure 79. Comparison of *in vitro* drug release and mass loss profiles of the HPMC- and HEC-based trilayer films tested in 10 mL simulated saliva (values represented as mean (n = 3) and with error bar representing standard deviation).

The comparison of the amount of drug released from HPMC- and HEC-based trilayer films are shown in Figs. 80 and 81.The percentage amount of drug loaded in the third layer for both formulations was 57.14% (equivalent to 2.5 mg) with respect to the total amount of the drug in all the three layers (equivalent to 4.4 mg). When the *in vitro* release was performed using 5mL of the dissolution medium, 1.78±0.04 mg of CHX for HPMC- and 1.94±0.34 mg of CHX for HEC-based films were released in 6 h (Fig. 80). Whereas, in the case of 10 mL release medium, 4.0±0.1 mg of CHX for HPMC- and 3.5±0.0 mg of CHX for HEC-based films were released in 24 h (Fig. 81). In comparison, HEC-based films showed slightly higher drug release with respect to HPMC-based films when 5 mL of dissolution volume were used. Whereas, HPMC-based films showed higher percent drug release (p>0.05) compared to HEC-based films when 10 mL of dissolution volume were used. Hence, the results suggest that the HPMC polymer in the third layer confers the film a superior drug release profile compared to the HEC polymer.

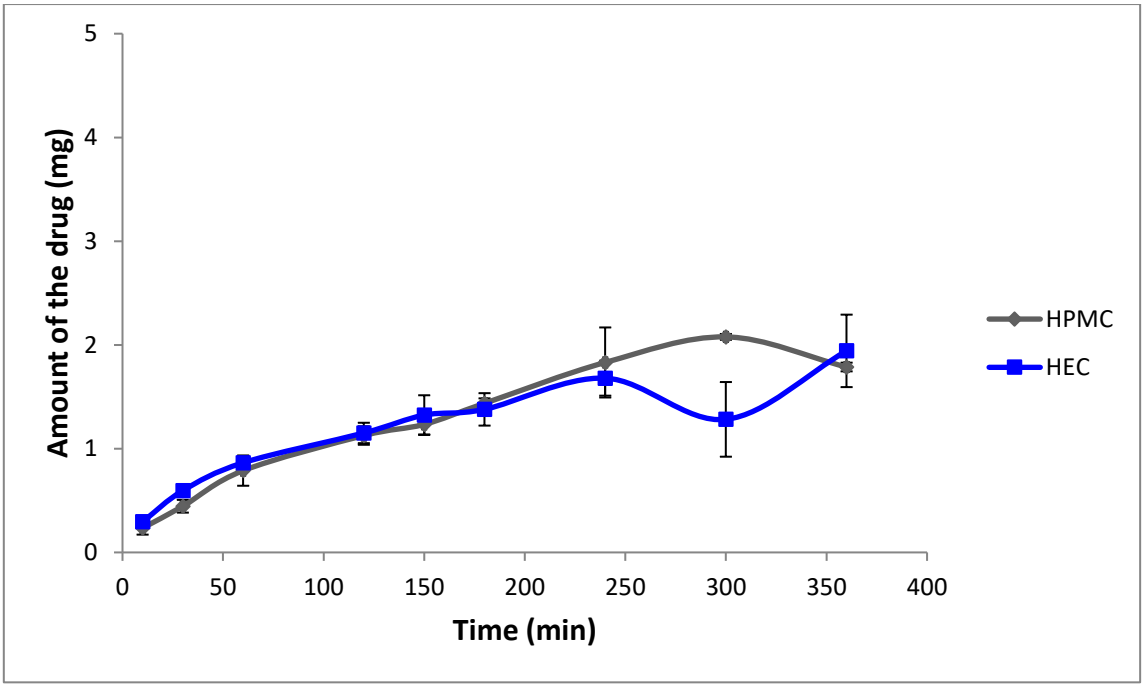

Figure 80. Comparison of the amount of drug released from HPMC- and HEC-based trilayer films tested in 5mL of simulated saliva (values represented as mean (n = 3) and with error bar representing standard deviation).

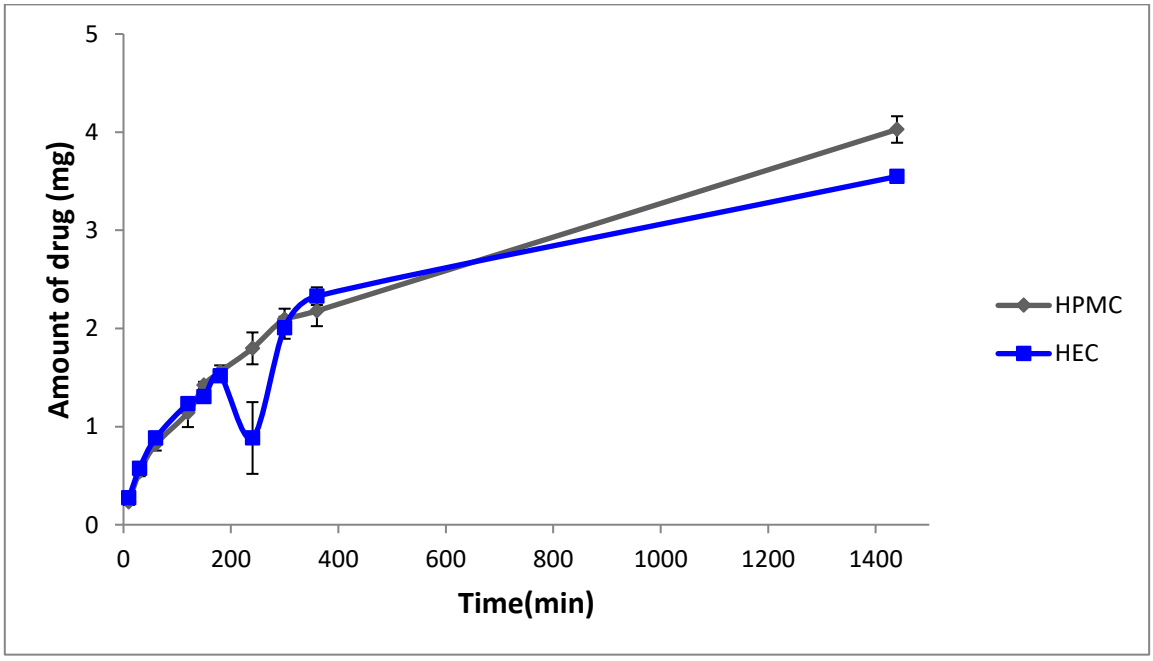

Figure 81. Comparison of the amount of drug released from HPMC- and HEC-based trilayer films tested in 10 mL of simulated saliva (values represented as mean (n = 3) and with error bar representing standard deviation).

In addition, the comparison of *in vitro* release profiles for HPMC- and HEC-based films coupled with their respective mass loss profiles showed that both release profiles were better when 10 mL of dissolution medium were used. In both trilayer films the polymer content in the third layer produced a water-swollen gel-like state controlling the drug release. Furthermore, it was clear from the plots that the drug release was governed by the volume of the dissolution medium used and by swelling and erosion of the polymer present in the third layer.

Finally, these findings suggest that the polymers used in the third layer adequately controlled the release of the drug from the films. Therefore, a rate-controlling layer in the film could be used to control the drug release to have a local action in the oral cavity.

6.1.8 *In vitro* sterility test

The sterility test was intended for detecting the presence of viable forms of bacteria in the preparations using agar medium. The tests were carried out under aseptic conditions to avoid contamination of the films during the test.

The films tested did not show any growth of microorganisms for 14 days, which indicates that the adopted manufacturing conditions assured the production of sterile dosage forms and might be used for wound healing applications in oral diseases.

CONCLUSIONS

The rational design of the multilayer film allowed us to develop a mucoadhesive, flexible, film for local delivery of chlorhexidine digluconate in the oral cavity for the treatment of oral diseases and wound healing applications.

Initial preformulaton studies led to selection of the best film forming polymers.

The biopolymer-based multilayer films were successfully prepared by double casting method.

The mucoadhesive layer containing HPC and the novel product showed good mucoadhesion that led to good residence time of the dosage form. Furthermore, a biological study of novel product successfully demonstrated its anti-inflammatory and wound healing properties.

The supportive layer containing HPC alone or HPC+GEL A enhanced the mechanical properties of the multilayer films for their convenient detachment from the substrate and handling purposes.

The local drug delivery layer containing HPC+HPMC and HPC+HEC enabled the controlled release of chlorhexidine digluconate, which could reduce the possibility of bacterial infection in the wound site and accelerate the wound healing process.

The good swelling index and convenient *in vitro* residence of the trilayer films provided prolonged drug release, therefore can be selected for the development of multilayer films for effective therapeutic uses.

Whereas, *ex vivo* studies on different biological substrates provided information on possible adhesion of our final formulation in oral diseases or dental complications.

The sterility test of the films successfully confirmed that the films were sterile and might be used for wound healing applications.

Finally, our studies suggest that the ease of preparation of multilayer films, their adhesion on the wounded site, the mechanical flexibility of films makes their application simpler, furthermore the release control of active molecules and their protective function pave the path for wound healing application in the oral cavity.

References

1. The Challenge of Oral Disease - A call for global action. The Oral Health Atlas. 2nd ed. Geneva: FDI World Dental Federation; 2015.

2. Perschbacher K. (2018). Mucocutaneous diseases of the oral cavity, Mini-symposium: head and neck pathology, Diagn Histopathol 24(5):161-190.

3. Jain N, Jain GK, Javed S, Iqbal Z, Talegaonkar S, Ahmad FJ, Khar RK. (2008). Recent approaches for the treatment of periodontitis. Drug Discov Today 13:932–43.

4. Zilberman M, Elsner JJ. (2008). Antibiotic-eluting medical devices for various applications. J Control Release 130:202–15.

5. Pihlstrom BL, Michalowicz BS, Johnson NW. (2005). Periodontal diseases. Lancet 366:1809–20.

6. Singh K, Arora N, Garg T. (2012b). Superbug: antimicrobial resistance due to NDM-1. Int J Institutional Pharmacy Life Sci 2:58–66.

7. Jacob S. (2012). Global prevalence of periodontitis: a literarure review. Int Arab J Dentistry 3:26–30.

8. Singh K, Arora N, Garg T. (2012a). RFID: a trustable security tool in pharmaceutical industry. Am J Pharm Tech Res 2:113–27.

9. Ismail G, Dumitriu HT, Dumitriu AS, Ismail SB. (2013). Periodontal disease: a covert source of inflammation in chronic kidney disease patients. Int J Nephrol 2013:1–6.

10. Singh H, Sharma R, Joshi M, Garg T, Goyal AK, Rath G.(2015).Transmucosal delivery of docetaxel by mucoadhesive polymeric nanofibers. Artif Cells Nanomed Biotechnol 43(4):263-269.

11. Parnami N, Garg T, Rath G, Goyal AK.(2013). Development and characterization of nanocarriers for topical treatment of psoriasis by using combination therapy. Artif Cells Nanomed Biotechnol.

12. Lalla E, Papapanou PN. (2011). Diabetes mellitus and periodontitis: a tale of two common interrelated diseases. Nat Rev Endocrinol 7:738–48.

13. Santos VR, Lima JA, Miranda TS, Feres M, Zimmermann GS, Nogueira-Filho Gda R, Duarte PM (2012). Relationship between glycemic subsets and generalized chronic periodontitis in type2 diabetic Brazilian subjects. Arch Oral Biol 57:293–9.

14. Kaur M, Malik B, Garg T, Rath G, Goyal AK. (2015). Development and characterization of guar gum nanoparticles for oral immunization against tuberculosis. Drug Deliv. 22(3):328-334.

15. Kaur R, Garg T, Malik B, Gupta UD, Gupta P, Rath G, Goyal AK.(2016). Development and characterization of spray-dried porous nanoaggregates for pulmonary delivery of anti-tubercular drugs. Drug Deliv 23(3):882-7.

16. Esfahanian V, Shamami MS, Shamami MS. (2012). Relationship between osteoporosis and periodontal disease: review of the literature. J Dent 9:256–64.

17. Guiglia R, Di Fede O, Lo Russo L, Sprini D, Rini GB, Campisi G.(2013). Osteoporosis, jawbones and periodontal disease. Med Oral Patol Oral Cir Bucal 18(1):E93–99.

18. Van Dyke TE, Dave S. (2005). Risk factors for periodontitis. J Int Acad Periodontol 7:3–7.

19. Saini R, Saini S, Sharma S. (2010). Periodontitis: a risk factor to respiratory diseases. Lung India 27:189.

20. Dhadse P, Gattani D, Mishra R. (2010). The link between periodontal disease and cardiovascular disease: how far we have come in last two decades? J Indian Soc Periodontol 14:148–54.

21. Nair SC, Anoop KR. (2012). Intraperiodontal pocket: An ideal route for local antimicrobial drug delivery. J Adv Pharm Technol Res 3(1):915.

22. Listgarten MA.(1980). Periodontal probing: what does it mean?. J Clin Periodontol 7(3):165–76.

23. Tariq M, Iqbal Z, Ali J, Baboota S, Talegaonkar S, Ahmad Z, Sahni JK (2012).Treatment modalities and evaluation models for periodontitis. Int J Pharm Investig 2(3):106–122.

24. Sanz I, Alonso B, Carasol M, Herrera D, Sanz M. (2012). Nonsurgical treatment of periodontitis. J Evid Based Dent Pract 12(3 Suppl):76-86.

25. Herrera D, Matesanz P, Bascones-Martínez A. (2012). Local and systemic antimicrobial therapy in periodontics. J Evid Based Dent Pract. 12(3 Suppl):50-60.

26. Ahuja A, Baiju CS, Ahuja V. (2012). Role of antibiotics in generalized aggressive periodontitis: A review of clinical trials in humans. J Indian Soc Periodontol 16(3):317-23.

27. Arweiler NB, Pietruska M, Pietruski J, Skurska A, Dolińska E, Heumann C, Auschill TM, Sculean A. (2014). Six-month results following treatment of aggressive periodontitis with antimicrobial photodynamic therapy or amoxicillin and metronidazole. Clin Oral Investig 18(9):2129-2135.

28. Schwach-Abdellaoui K, Vivien-Castioni N, Gurny R. (2000). Local delivery of antimicrobial agents for the treatment of periodontal diseases. Eur J Pharm Biopharm 50(1):83-99.

29. Kaur M, Garg T, Rath G, Goyal AK. (2014a). Current nanotechnological strategies for effective delivery of bioactive drug molecules in the treatment of tuberculosis. Crit Rev Ther Drug Carrier Syst 31:49–88.

30. Kataria P, Kaur J, Parvez E, Maurya RP. (2014). Statins: The paradigm shift in periodontal regeneration. SRM J res Dental Sci 5(1):26-30.

31. Garg T, Singh O, Arora S, Murthy R. (2011d). Dendrimer – a novel scaffold for drug delivery. Int J Pharma Sci Rev Res 7:211–20.

32. Goyal G, Garg T, Malik B, Chauhan G, Rath G, Goyal AK.(2015). Development and characterization of niosomal gel for topical delivery of benzoyl peroxide. Drug Deliv 22(8):1027-1042.

33. Garg T, Singh O, Arora S. (2011c). Opportunities and growth of conduct clinical trials in India. Int J Pharm Sci Rev Res 8:152–60.

34. Labib GS, Aldawsari HM, Badr-Eldin SM. (2014). Metronidazole and pentoxifylline films for the local treatment of chronic periodontal pockets: preparation, in vitro evaluation and clinical assessment. Expert Opin Drug Deliv 11:855–65.

35. Cetin EO, Buduneli N, Atlıhan E, Kirilmaz L. (2005). In vitro studies of a degradable device for controlled-release of meloxicam. J Clin Periodontol 32:773–7.

36. Perugini P, Genta I, Conti B, Modena T, Pavanetto F.(2003). Periodontal delivery of ipriflavone: new chitosan/PLGA film delivery system for a lipophilic drug. Int J Pharm 252:1–9.

37. Ikinci G, Senel S, Akincibay H, Kaş S, Erciş S, Wilson CG, Hincal AA. (2002). Effect of chitosan on a periodontal pathogen Porphyromonas gingivalis. Int J Pharma 235: 121–7.

38. Minabe M, Takeuchi K, Nishimura T, Hori T, Umemoto T.(1991). Therapeutic effects of combined treatment using tetracycline-immobilized collagen film and root planing in periodontal furcation pockets. J Clin Periodontol 18:287–90.

39. Friesen LR, Williams KB, Krause LS, Killoy WJ. (2002). Controlled local delivery of tetracycline with polymer strips in the treatment of periodontitis. J Periodontol 73:13–19.

40. Somayaji B, Jariwala U, Jayachandran P, Vidyalakshmi K, Dudhani RV. (1998). Evaluation of antimicrobial efficacy and release pattern of tetracycline and metronidazole using a local delivery system. J Periodontol 69:409–13.

41. Ozcan G, Taner IL, Doğanay T, Iscanoğlu M, Taplamacioğlu B, Gültekin SE, Baloş K. (1994). Use of membranes containing 20% chlorhexidine and 40% doxycycline for treatment of chronic periodontal pockets. J Nihon Univ School Dent 36:191–8.

42. Taner IL, Ozcan G, Doğanay T, Iscanolu M, Taplamacioğlu B, Gültekin SE, Baloş K. (1994). Comparison of the antibacterial effects on subgingival microflora of two different resorbable base materials containing doxycycline. J Nihon Univ School Dent 36:183–90.

43. Deasy P, Collins AE, Maccarthy DJ, Russell RJ. (1989). Use of strips containing tetracycline hydrochloride or metronidazole for the treatment of advanced periodontal disease. J Pharm Pharmacol 41: 694–9.

44. Rao N, Pradeep A, Bajaj P, Kumari M, Naik SB. (2013). Simvastatin local drug delivery in smokers with chronic periodontitis: a randomized controlled clinical trial. Aust Dent J 58:156–62.

45. Pradeep AR, Bajaj P, Agarwal E, Rao NS, Naik SB, Kalra N, Priyanka N (2013a). Local drug delivery of 0.5% azithromycin in the treatment of chronic periodontitis among smokers. Aust Dent J 58:34–40.

46. Pradeep AR, Kumari M, Rao NS, Naik SB. (2013b). 1% Alendronate gel as local drug delivery in the treatment of class II furcation defects: a randomized controlled clinical trial. J Periodontol 84:307–15.

47. Pradeep AR, Priyanka N, Kalra N, Naik SB, Singh SP, Martande S. (2012a). Clinical efficacy of subgingivally delivered 1.2-mg simvastatin in the treatment of individuals with class II furcation defects: a randomized controlled clinical trial. J Periodontol 83:1472–9.

48. Pradeep AR, Sharma A, Rao NS, Bajaj P, Naik SB, Kumari M. (2012b). Local drug delivery of alendronate gel for the treatment of patients with chronic periodontitis with diabetes mellitus: a double-masked controlled clinical trial. J Periodontol 83:1322–8.

49. Reise M, Wyrwa R, Müller U, Zylinski M, Völpel A, Schnabelrauch M, Berg A, Jandt KD, Watts DC, Sigusch BW (2012). Release of metronidazole from electrospun poly (L-lactide-co-D/L-lactide) fibers for local periodontitis treatment. Dental Mater 28:179–88.

50. Chaturvedi T, Srivastava R, Srivastava A, Gupta V, Verma PK. (2013). Doxycycline poly e-caprolactone nanofibers in patients with chronic periodontitis - a clinical evaluation. J Clin Diagn Res 7:2339–42.

51. Kearns VR, Williams RL, Mirvakily F, Doherty PJ, Martin N. (2013). Guided gingival fibroblast attachment to titanium surfaces: an in vitro study. J Clin Periodontol 40:99–108.

52. Zhang S, Huang Y, Yang X, Mei F, Ma Q, Chen G, Ryu S, Deng X.(2009). Gelatin nanofibrous membrane fabricated by electrospinning of aqueous gelatin solution for guided tissue regeneration. J Biomed Mater Res A 90:671–9.

53. Laurell L, Bose M, Graziani F, Tonetti M, Berglund T. (2006). The structure of periodontal tissues formed following guided tissue regeneration therapy of intra-bony defects in the monkey. J Clin Periodontol.33 (8):596–603.

54. Stavropoulos A, Sculean A. (2017). Current Status of RegenerativePeriodontal Treatment. Curr Oral Health Rep 4:34-43.

55. Wheeler S, Bollinger C. (2009). Complication or Substandard Care? Risks of Inadequate Implant Training. CDA J 37(9):647-51.

56. Bornstein MM, Halbritter S, Harnisch H, Weber HP, Buser D.(2008). A retrospective analysis of patients referred for implant placement to a specialty clinic: indications, surgical procedures, and early failures. Int J Oral Maxillofac Implants 23(6), 1109-16.

57. Misch K, Wang HL. (2008). Implant surgery complications: etiology and treatment. Implant Dent 17(2):159-68.

58. Lamas Pelayo J, Penarrocha Diago M, Marti Bowen E. Intraoperative complications during oral implantology. (2008). Med Oral Patol Oral Cir Bucal 13(4) : E239-43.

59. Greenstein G, Cavallaro J, Romanos G, Tarnow D. (2008). Clinical recommendations for avoiding and managing surgical complications associated with implant dentistry: a review. J Periodontol 79(8):1317-29.

60. Annibali S, Ripari M, LA Monaca G, Tonoli F, Cristalli MP.(2008). Local complications in dental implant surgery: prevention and treatment. Oral Implantol (Rome) 1(1):21-33.

61. Curtis JW, McLain JB, Hutchinson RA. (1985). The Incidence and Severity of Complications and Pain following Periodontal Surgery. J Periodontol 56(10):597-601.

62. Laurell L, Bose M, Graziani F, Tonetti M, Berglund T. (2006). The structure of periodontal tissues formed following guided tissue regeneration therapy of intra-bony defects in the monkey. J Clin Periodontol 33(8):596–603.

63. Stavropoulos A, Sculean A. (2017). Current Status of Regenerative Periodontal Treatment. Curr Oral Health Rep 4:34–43.

64. Balasubramani M, Kumar TR, Babu M. (2001). Skin substitutes: a review. Burns 27:534-544.

65. Jones I, Currie L, Martin R. (2002). A guide to biological skin substitutes, Brit J Plast Surg 55:185-193.

66. Still J, Glat P, Silverstein P, Griswold J, Mozingo D. (2003). The use of a collagen sponge/living cell composite material to treat donor sites in burn patients, Burns 29(8):837-841.

67. Stashak TS, Farstvedt E, Othic A. (2004). Update on wound dressings: indications and best use, Clinical Techniques in Equine Practice 3:.148-163.

68. Preis M, Woertz C, Schneider K, Kukawka J, Broscheit J, Roewer N, Breitkreutz J. (2014). Eur J Pharm Biopharm 86(3):552-61.

69. Repka MA, Repka SL, Mcginity JW.(2000). Bioadhesive hot-melt extruded film for topical and mucosal adhesion applications and drug delivery and process for preparation thereof.US patent US6375963B1.

70. Preis M, Breitkreutz J, Sandler N.(2015). Perspective: Concepts of printing technologies for oral film formulations. Int J Pharm 494(2):578-584.

71. Rupprecht H, Zinzen S. (2004). Active substance-containing multi-layer film of hydrophilic polymers crosslinked in situ. US patent US6780504.

72. Yang RK, Fuisz RC, Myers GL, Fuiz M. (2014). Process for manufacturing a resulting multi-layer pharmaceutical film. US patent US8900498.

73. Paderni C, Compilato D, Giannola LI, Campisi G. (2012). Oral local drug delivery and new perspectives in oral drug formulation. Oral Surg Oral Med Oral Pathol Oral Radiol 114(3):e25-34.

74. Desai KGH, Mallery SR, Holpuch AS, Schwendeman SP. (2011). Development and *in vitro-in vivo* evaluation of fenretinide-loaded oral mucoadhesive patches for site-specific chemoprevention of oral cancer. Pharm Res 28(10):2599-2609.

75. Tonglairoum P, Ngawhirunpat T, Rojanarata T, Panomsuk S, Kaomongkolgit R, Opanasopit P .(2015). Fabrication of mucoadhesive chitosan coated polyvinylpyrrolidone/cyclodextrin/clotrimazole sandwich patches for oral candidiasis. Carbohyd Polym.132:173-179.

76. Sundararaj SC, Thomas MV, Peyyala R. (2013). Design of a multiple drug delivery system directed at periodontitis. Biomaterials 34(34):8835-42.

77. Varan C, Wickström H, Sandler N, Aktaş Y, Bilensoy E .(2017). Inkjet printing of antiviral PCL nanoparticles and anticancer cyclodextrin inclusion complexes on bioadhesive film for cervical administration. Int J Pharm 531(2):701-713.

78. Lei L, Liu X, Shen YY, Liu JY, Tang MF, Wang ZM, Guo SR, Cheng L. (2011). Zero-order release of 5-fluorouracil from PCL-based films featuring trilayered structures for stent application. Eur J Pharm Biopharm 78(1):49-57.

79. Rong HJ, Chen WL, Guo SR, Lei L, Shen YY. (2012). PCL films incorporated with paclitaxel/5-fluorouracil: Effects of formulation and spacial architecture on drug release. Int J Pharm 427(2):242-51.

80. El-Kamel AH, Ashri LY, Alsaraa IA.(2007). Micromatricial metronidazole benzoate film as a local mucoadhesive delivery system for treatment of periodontal diseases. AAPS Pharmscitech.8(3):E184-E194.

81. Perugini P, Genta I, Conti B, Modena T, Pavanetto F.(2003). Periodontal delivery of ipriflavone: new chitosan/PLGA film delivery system for a lipophilic drug. Int J Pharm 252(1-2):1-9.

82. Ragwa M. Farid, Ming Ming Wen . (2017).Promote Recurrent Aphthous Ulcer Healing with Low Dose Prednisolone Bilayer Mucoadhesive Buccal Film. Curr Dr Del. 14(1):123-125.

83. Daněk Z, Gajdziok J, Doležel P, Landová H, Vetchý D, Štembírek J.(2017). Buccal films as a dressing for the treatment of aphthous lesions. J Oral Pathol Med 46 (4):301-306.

84. Ramineni SK, Cunningham LL, Dziubla TD, Puleo DA.(2013). Development ofimiquimod-loaded mucoadhesive films for oral dysplasia. J Pharm Sci.102(2):593–603.

85. Rahim Bahri N, Zahra R, Omar N.(2011). Formulation and Evaluation of Phenytoin Sodium Buccoadhesive Polymeric Film for Oral Wounds. IJPS 7(2): 69-77.

86. Obaidat RM, Bader A, Al-Rajab W, Abu Sheikha G, Obaidat AA (2011). Preparation of mucoadhesive oral patches containing tetracycline hydrochloride and carvacrol for treatment of local mouth bacterial infections and candidiasis. Sci Pharm 79(1):197–212.

87. Juliano C, Cossu M, Pigozzi P, Rassu G, Giunchedi P.(2008). Preparation, *in vitro* characterization and preliminary *in vivo* evaluation of buccal polymeric films containing chlorhexidine. AAPS Pharmscitech 9(4):1153–1158.

88. Abo Enin HA, El Nabarawy NA, Elmonem RA.(2016). Treatment of Radiation-Induced Oral Mucositis Using a Novel Accepted Taste of Prolonged Release Mucoadhesive Bi-medicated Double-Layer Buccal Films. AAPS PharmSciTech 18(2):563-575.

89. Natalie J Medlicott, Holborow DW, Rathbone MJ.(1999).Local delivery of chlorhexidine using a tooth-bonded delivery system. J Contr Rel 61(3), 337-43.

90. Fardal O, Turnbull RS. (1986). A review of the literature on use of chlorhexidine in dentistry. J Am Dent Assoc 112(6):863-9.

91. Schiøtt CR, Löe H. (1972). The sensitivity of oral streptococci to chlorhexidine. J Periodont Res 7:192-194.

92. Goodson JM, Tanner ACR, Haffajee AD.(1982) Patterns of progression and regression of advanced destructive periodontal disease. J. Clin. Periodontol 9:472–481.

93. Socransky SS, Haffajee AD, Goodson JM.(1984). New concepts of destructive periodontal disease. J Clin Peridontol 11:21–32.

94. Palem CR, Gannu R, Doodipala N, Yamasani VV, Yamasani MR.(2011). Transmucosal Delivery of Domperidone from Bilayered Buccal Patches: In Vitro, Ex Vivo and In Vivo Characterization. Arch Pharm Res 34(10):1701-1710.

95. Castán H, Ruiz MA, Clares B, Morales ME.(2015). Design, development and characterization of buccal bioadhesive films of Doxepin for treatment of odontalgia. Drug Deliv 22(6):869-876.

96. Chen D, Wu M, Chen J, Zhang C, Pan T, Zhang B, Tian H, Chen X, Sun J.(2014). Robust, Flexible, and Bioadhesive Free-Standing Films for the Co-Delivery of Antibiotics and Growth Factors. Langmuir 30(46):13898–13906**.**

97. Baldassari S, Solari A, Zuccari G, Drava G, Pastorino S, Fucile C, Marini V, Daga A, Pattarozzi A, Ratto A, Ferrari A, Mattioli F, Barbieri F, Caviglioli G, Florio T.(2018).Development of an injectable slow release metformin formulation and evaluation of Its potential antitumor Effects. Scientific reports 8:3929.

98. Morales, J.O., McConville, J.T.(2011). Manufacture and characterization of mucoadhesive buccal films. Eur. J. Pharm. Biopharm 77:187–199.

99. Parodi B, Russo E, Baldassari S, Zuccari G, Pastorino S, Yan M, Neduri K, Caviglioli G. (2017).Development and characterization of a mucoadhesive sublingual formulation for pain control: extemporaneous oxycodone films in personalized therapy.Drug Dev Ind Pharm 43(6):917-924.

100. Hafemann, B et al (1999). Use of a collagen/elastin-membrane for the tissue engineering of dermis.Burns 25:373-384.

101. Thomas S. (2000). Alginate dressings in surgery and wound management-Part 1.Journal of Wound Care 9 (2):56-60.

102. Saliba M.J. (2001). Heparin in the treatment of burns: a review.Burns 27:349-358.

103. Şenel S, Clure M.C. (2004). Potential applications of chitosan in veterinary medicine. Adv Drug Deliv Rev, 56:1467-1480.

104. Patankar MS, Oehninger S, Barnett T, Williams RL, Clark GF.(1993). A revised structure for fucoidan may explain some of its biological activities.J Biol Chem 268 (29):21770-21776.

105. Khan S, Trivedi V, Boateng J.(2016). Functional physico-chemical, ex vivo permeation and cell viability characterization of omeprazole loaded buccal films for paediatric drug delivery. Int J Pharm 500: 217–26.